THESIS FOR THE DEGREE OF DOCTOR OF PHILOSOPHY

ON POWER SYSTEM STABILIZERS: GENETIC ALGORITHM BASED TUNING AND ECONOMIC WORTH AS ANCILLARY SERVICES

by

ADRIAN ANDREOIU

Last revision: 2004-06-17

Department of Electric Power Engineering
Chalmers University of Technology
Göteborg, Sweden
2004

On Power System Stabilizers: Genetic Algorithm Based Tuning and Economic Worth as Ancillary Services

ADRIAN ANDREOIU

ISBN 91-7291-416-5 Doktorsavhandlingar vid Chalmers tekniska högskola
Ny serie nr. 2098
ISSN 1651-498x

Technical Report No. 477
ISSN 0346-718x

School of Electrical Engineering
Chalmers University of Technology
SE-412 96 Göteborg, Sweden

Telephone: +46 (0)31 772 1000
Fax: +46 (0)31 772 1633
http://www.elteknik.chalmers.se

Chalmers Bibliotek, Reproservice
Göteborg, Sweden 2004

ABSTRACT

The problem of power system stabilizer (PSS) parameter tuning is a complex exercise because of the presence of poorly damped modes of oscillation, and continuous variation in power system operating conditions. In recent years, as a result of the newly deregulated market environment, power systems tend to be operated at reduced security margins, thus making the system more vulnerable to disturbances. The role of PSS, among other power system control devices, becomes then even more critical, and subsequently, in light of the new operating paradigm, new methods of financial compensation for the generators providing this service to system would be needed.

The work presented in this thesis focuses on aspects related to PSSs tuning, on one hand, and evaluation of their contribution to system stability and security from an economic perspective in the context of ancillary services, on the other. Thus, a genetic algorithm (GA) based method to simultaneously tune PSSs is developed in the first part of this thesis, while the second is dedicated to developing a game theory based method to financially compensate the PSSs for the control effort they provide for the power system.

The simultaneous approach for tuning PSSs, as opposed to sequential approaches, usually involves exhaustive computational efforts, but, in turn, ensures the parameter setting optimality. The classical Lyapunov's parameter optimization method employing an Integral of Squared Error (ISE) criterion has been integrated within a GA framework to simultaneously tune PSSs. Within the genetic process, a potential solution – the PSS parameter setting – is coded as an *individual*, which is part of a *population* of such potential solutions randomly generated, and by applying the *survival of the fitness* principle based on each individual's *fitness* with respect to the objective, a sound basis to

finding the *best individual*, *i.e.* global optimum solution, is created. The method thus emerged has been used for tuning of lead-lag and derivative PSS. A similar GA based optimization process is implemented for tuning the proportional-integral-derivative (PID) PSS. Since the PID PSS acts in discrete mode, the power system model has been accordingly developed in discrete-time domain. An optimal sampling period has been determined considering the conflicting requirements of computation time vis-à-vis accuracy of information on system dynamics due to discretization. Tests for transient events, such as three-phase short circuits and transmission line outages, have also been performed with satisfactory results.

In the second part of this thesis, an attempt has been made to examine the role and performance of PSS in the context of deregulated power markets. It is proposed that the PSS control effort to enhance power system stability and security be regarded as an ancillary service – *PSS-control service* – and subsequently, the allocation of system savings/benefit, as accrued from a PSS, becomes an important issue. A game theory based approach, namely the Shapley value criterion, is used to develop a scheme for allocation of payments to generators equipped with PSS and providing this service. The PSSs contribution is evaluated in different ways: by assessing the transfer capability of the system due to PSS, or by employing various performance indices based on system dynamic behavior. A contingency analysis is also performed and the N-1 security criterion is taken into consideration as well, for evaluating the PSS-control payment.

Keywords: power systems, small-signal stability, power system stabilizers, Lyapunov equation, genetic algorithm, ancillary services, game theory, Shapley value, Integral of Squared Error.

PREFACE

The work presented in this thesis has been carried out at the Department of Electric Power Engineering of Chalmers University of Technology for the main part, and also at the Department of Electrical and Computer Engineering of the University of Waterloo, Ontario, Canada. This research project started in 1999 and has been funded through the Elektra program of Elforsk. The financial support is gratefully acknowledged.

I wish to express here my sincere gratitude to my supervisor, Associate Professor Kankar Bhattacharya, whose precious advice, unlimited patience and friendly encouragement, made this work go smoothly throughout this time. Many thanks go Professor Jaap Daalder, the examiner of this project, for the professional guidance and valuable help he offered in many and various ways.

I gratefully acknowledge the constructive criticism, and valuable input that Associate Professor Bo Eliasson of Malmö Högskola and Dr. Sture Torseng of ABB Power Systems have contributed with during the course of this work, as members of the Project Reference Group.

My stay as a Visiting Scholar at the University of Waterloo has been a fruitful working experience. I particularly appreciated the collaboration with Professor Claudio Cañizares, from whose knowledge and professionalism I have greatly benefited.

The colleagues at the department in Chalmers, particularly the Power Systems Group, created a stimulating working and social environment. Many thanks to Jan-Olov Lantto, who kept my computer up and running all this time. I would also like to acknowledge my colleagues at the University of Waterloo for support and friendly working atmosphere within the power systems laboratory.

I owe my deepest gratitude to my family, and to Corina especially, for their love, understanding and support, which gave me the comfort and motivation to pursue my research goals.

April 25, 2004
Göteborg

TABLE OF CONTENTS

1 INTRODUCTION

Power System Stabilizers (PSSs) are auxiliary control devices on synchronous generators, used in conjunction with their excitation systems to provide control signals toward enhancing the system damping and extending power transfer limits, thus maintaining reliable operation of the power system.

In this thesis, an attempt has been made to treat PSSs, their design and optimal tuning in multi-machine power systems, and evaluate their impact on the system welfare from an economic viewpoint. Since power systems of today are more and more being operated in a deregulated environment, and subsequently, often at reduced margins of security and reliability, the importance of accurate controls becomes more relevant than ever.

August 14, 2003 is a date that immediately comes to mind, alongside August 28 (London, UK), September 23 (Sweden and Denmark) and 28 (Italy), in the year 2003 alone, not to mention November 1965 (Northeast blackout), 1967 (Pennsylvania), 1977 (New York City), 1978 (France), 1983 (Sweden), December 1982 and July 1996 (West Coast, USA), 1988 (Canada), 1996 (Western USA) – major blackouts which illustrate the importance of power system stability.

1.1 Power System Stability – Small-Signal Stability

Power system stability problem has received a great deal of attention over the years. For convenience in analysis, gaining a better understanding of the nature of stability concerns, and developing solutions to problems, it has been the usual practice to classify power system stability problems into three categories as follows [1]:

a) *Angle stability* – ability of the system to maintain synchronism;
b) *Voltage stability* – the ability of the system to maintain steady acceptable voltage;
c) *Frequency stability* – ability of the system to maintain frequency within an acceptable variation range.

This classification is depicted below in a suggestive and more detailed block diagram, highlighting those blocks that are of interest and direct relevance to this thesis.

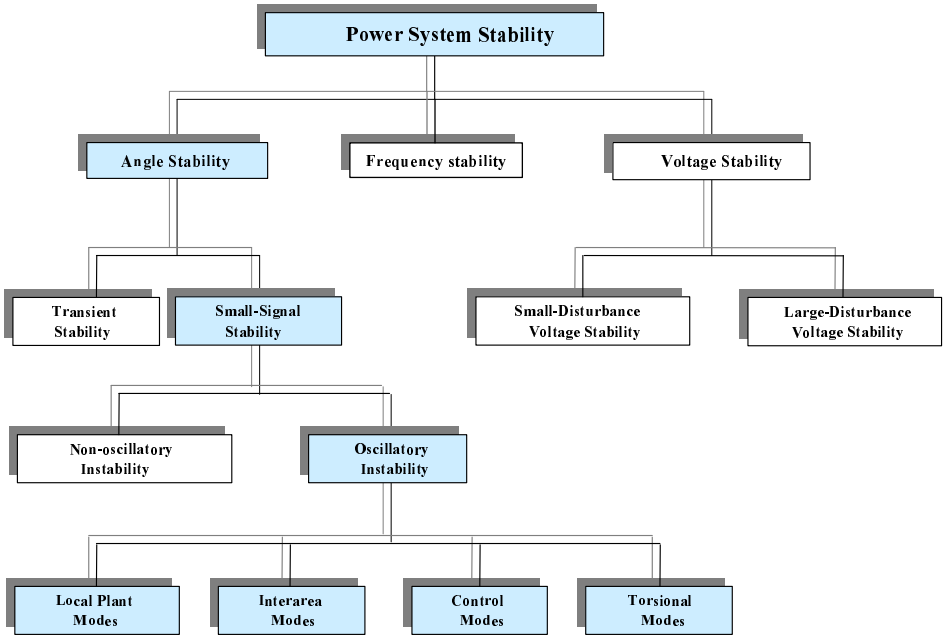

Figure 1.1 Power system stability classification [1]

This work focuses on the angle stability problem, with particular reference to the small-signal stability problem.

Amongst the different types of angular stability problems, the transient stability problem is related to the short term or transient period, which is usually limited to the first few seconds following a disturbance. It is concerned with the system response to a severe disturbance, such as transmission system fault. Much of the electric utility effort and interest related to system stability have been concentrated on the short-term response, and therefore the system is designed and operated so as to meet a set of reliability criteria concerning transient stability. Well-established analytical techniques and computer programs exist for the analysis of transient stability.

Small-signal stability on the other hand is concerned with the system response to small changes and is a fundamental requirement for the satisfactory operation of power systems. Usually, the problem is one of ensuring sufficient damping of system oscillations. Small-signal stability can be analyzed by linearizing the system about an equilibrium point represented by a steady state operating condition. This allows the use of powerful analytical tools of linear

systems to determine the stability characteristics, which aid in the design of corrective controls.

In the past, many utilities took small-signal stability for granted and carried out no studies at all to reveal problems related to small-signal performance. This was primarily because a system that remained stable for the first few seconds following a severe disturbance was very likely to remain stable for small perturbations about the post fault system condition. This is not true for present day systems. As power systems have been in continuous development, the need for small-signal studies and measures to ensure sufficient stability margins has been recognized.

More recently, due to restructuring of the utility industry, there has been a considerable increase of merchant generation activity. New generators are equipped with modern exciters that have a high gain and a fast response to enhance transient stability. However, these fast response exciters, if used without stabilizers, can lead to oscillatory instability affecting local or regional reliability. This problem is exacerbated particularly in areas where there is a large amount of generation with limited transmission available for exporting power.

Attention has been focused on the effect of excitation control on the damping of oscillations, characteristic for the phenomena pertaining to stability. It has been found particularly useful, and practical at the same time, to incorporate transient stabilizing signals derived from speed, terminal frequency or accelerating power superimposed on the normal voltage error signal to provide for additional damping to these oscillations, through PSSs.

Power system stabilizers have been extensively used as supplementary excitation controllers to damp out the low frequency oscillations, thus enhancing the overall system stability and extending its transfer capability limit, at the same time. The PSS extends the system stability limits by modulating generator excitation to provide damping to the oscillations of synchronous machine rotors relative to one another. They produce a component of torque in phase with rotor speed deviations, in order to enhance the system damping.

Some operating authorities have outlined rules on PSS installation requirements on synchronous generators. For example, the Western Electricity Coordinating Council (WECC) requires that PSS shall be installed on every existing synchronous generator, equipped with a suitable excitation system, that is larger than 75 MVA, or is larger than 30 MVA and is part of a generation complex that has an aggregate capacity larger than 75 MVA [2]. The ISO New England requires that, each new generating unit within New England Pool (NEPOOL) to have a PSS installed as part of its excitation system, which may be required to be put in place or reset at anytime in the future [3].

In the context of the NORDEL power system, Eliasson [4], using detailed model formulations, and Eliasson and Hill [5], using simplified versions of the previously developed models, have demonstrated how systematic siting of damping controllers can be achieved by constructing an overall damping matrix, also considering load characteristics and their impact on damping. This approach can be further used for coordinated tuning of damping device parameters in large-scale power systems.

1.2 Literature Review on PSS Tuning

Over the last four decades, a large number of research papers have appeared in the area of PSS. Research has been directed towards obtaining such a PSS that can provide an optimal performance for a wide range of machine and system parameters. However, as observed by DeMello and Concordia [6], a universally applicable stabilizing function is not practically feasible. Various control strategies and optimization techniques have found their applications in this area as also various degrees of system modeling have been attempted.

While it is difficult to bring out a detailed discussion of the historical development of PSS and its applications, a modest attempt has been made in this section to discuss the most significant works in the area.

Heffron and Phillips [7] analyzed the effect of modern amplidyne voltage regulators on under-excited operation of large turbine generators. They were the first to present the small perturbation model in terms of K_1-K_6 constants of a machine-infinite bus system. Their investigations revealed that the use of modern continuously acting regulators greatly increased the steady-state stability limit of turbine generators in the under-excited region. And that the trend towards lowering the short circuit ratio of large turbine generators was sound from steady state stability standpoint provided a modern continuously acting voltage regulator was used.

DeMello and Concordia [6] examined the case of a single machine connected to an infinite bus through external reactance. Their analysis developed insights into the effects of thyristor-type excitation systems and established understanding of the stabilizing requirements for such systems. These stabilizing requirements included the voltage regulator gain parameters as well as the PSS parameters. They explored the effect of a variety of machine loading, inertia and system external impedance (length of the transmission line) on damping characteristics of voltage or speed following a small perturbation in mechanical torque. They developed some unifying concepts that explained the stability phenomena of concern and predicted desirable phase and magnitude characteristics of stabilizing functions.

Larsen and Swann [8] presented application of PSS utilizing either speed, frequency or power input signals. Guidelines were presented for tuning PSS that enable the user to achieve desired dynamic performance with limited

effort. The need for torsional filters in the PSS path for speed input PSS was also discussed.

Kundur *et al.* [9] described the details of a *Delta-P-Omega* PSS design for generating units in Ontario Hydro. Two alternate excitation schemes were considered, one with and the other without Transient Gain Reduction (TGR). It was shown that with appropriate selection of PSS parameters, both schemes provide satisfactory performance. Appropriate choice of washout time-constant, PSS output limits and phase-lead compensation circuit parameters was demonstrated.

Yu and Siggers [10] presented the application of state-feedback optimal PSS, while Moussa and Yu [11] proposed an eigenvalue shifting technique for determining the weighing matrix in the performance index. The technique involved shifting of the dominant eigenvalue to the left, on the *s*-plane until a satisfactory shift is made or the controller's practical limit is reached. The optimal state-feedback controllers were also applied to a multi-machine system. However, in spite of the powerfulness of optimal control theory, the controllers so achieved failed to appeal to utilities because their realization was difficult, cumbersome and costly.

A lot of work has also been reported on coordinated tuning of PSS for multi-machine systems. DeMello *et al.* [12] presented an eigenvalue-eigenvector analysis to identify the most effective generating units to be equipped with PSS in multi-machine systems that exhibit dynamic instability and poor damping of several inter-area modes of oscillations.

Fleming *et al.* [13] proposed a sequential eigenvalue assignment algorithm for selecting the parameters of stabilizers in a multi-machine power system. In sequential tuning, the stabilizer parameters are computed using repeated application of single-input/single-output (SISO) analysis. The suggested approach enables the selection of parameters of stabilizers such that a specified improvement in the damping ratio of each poorly damped mode can be realized approximately. The stabilizers are applied sequentially at different locations as ascertained by modal analysis outlined by DeMello *et al.* [12]. However, it should be noted that the sequential addition of stabilizers disturbs the previously placed eigenvalues to some extent.

Abdalla *et al.* [14] also presented a procedure for the selection of the most effective machines for stabilization. They suggested the addition of a damping term to each machine's equation of motion, one at a time. An eigenvalue-based measure of relative improvement in the damping of oscillatory modes is implemented and used as a criterion to find the best candidate machine for stabilizer application.

The sequential tuning methods discussed in [12]-[14] are computationally simple compared to the simultaneous tuning methods, but they incur eigenvalue drift within the sequence. The eigenvalue drift problem does not

arise with simultaneous tuning methods, and thus they provide the true optimal solution, but, on the other hand, these methods are computationally expensive.

Doi and Abe [15] proposed the coordinated design/tuning of PSS in multi-machine system by combining eigenvalue sensitivity analysis and linear programming. The PSS parameters are determined by minimizing a performance index, which is the sum of all PSS gains. This method is simultaneously able to select generators where PSS can be effectively applied and to synthesize the adequate transfer function of the PSS for these generators.

Lim and Elangovan [16], [17] presented a method for designing decentralized stabilizers in a multi-machine system using complex frequency domain approach. Using this approach, the PSS parameters are obtained so that some or all of the system mechanical mode eigenvalues may be placed at the prescribed locations in the *s*-plane. The problem of exact eigenvalue assignment is transformed to that of solving iteratively a set of equivalent characteristic equations, whose final solution represents the desired stabilizer parameters. In [18], they have further proposed an efficient method for computing the set of characteristic equations to improve considerably the computation speed over that of the approach outlined in [16].

In all the above works, the PSS structure was considered to be fixed and the PSS parameters were tuned considering a set of nominal operating conditions and system parameters. Therefore, such a fixed structure optimum PSS would provide sub-optimum performance under variations in system parameters and operating conditions. Control strategies based on self-tuning control, variable-structure control (VSC), fuzzy-logic systems (FLS), artificial neural networks (ANN), genetic algorithms (GA), *etc.*, have been reported in the recent literature, aiming to develop robust PSS configurations.

The applicability, advantages and disadvantages of minimum variance, pole assigned, linear quadratic and pole shifting adaptive controllers for power systems were examined in detail by Ghosh *et al.* [19]. They presented a comparison of system dynamic performances obtained using three alternate PSS, *i.e.* adaptive pole-shifting, adaptive linear quadratic and a conventional PSS. Their studies show that the adaptive pole-shifting PSS provides the best performance.

Cheng *et al.* [20] presented an adaptive PSS using a self-searching pole-shifting control algorithm. The adaptive PSS so designed is effective in damping system oscillations under both small as well as large perturbations. Cheng *et al.* [21] further proposed a dual-rate adaptive PSS based on self-searching pole-shifting algorithm for damping multi-mode oscillations. In this algorithm the system parameters are identified every 80 msec while the control signal is updated every 20 msec.

Lim [22] proposed a method for designing a self-tuning PSS based on the minimization of a quadratic performance index. The effectiveness of the self-tuning PSS for either excitation or governor control under different

disturbances and over a wide range of operating conditions has been demonstrated.

As an alternative to self-tuning PSS, Variable Structure PSS (VSPSS) has been proposed in the literature in order to counteract the problem of variation of system parameters and operating condition. The VSC are insensitive to system parameter variations and can easily be realized using microcomputers. A systematic procedure for the selection of the proper switching vector is though very important for their design.

Chan and Hsu [27] proposed an optimal VSPSS for a machine-infinite bus system as well as for a multi-machine system. The proposed VSPSS is optimal in the sense that the switching hyperplane is obtained by minimizing a quadratic performance index, in the sliding mode operation. The resulting switching vector and hence the switching hyperplane depends on the weighing matrices associated with the performance index.

Kothari *et al.* [28] have presented the design of a VSPSS with desired eigenvalues in the sliding mode, where the switching hyperplane is obtained using a pole placement method. This has been further extended in [29] to apply a radial pole-shifting technique for design of VSPSS in the discrete-mode.

A fuzzy set theory based PSS was reported by Hsu and Cheng in [30]. The proposed stabilizer adopted a decentralized output feedback control law that required only local measurements within each generating unit, thus providing scope for further implementation.

In [31], Hoang and Tomsovic proposed a systematic approach to fuzzy logic control design, where the controller parameters are either calculated off-line or computed in real time in response to system changes. In this design approach, it was shown that the controller is insensitive to the precise dynamics of the system.

Artificial neural network is based on the concept of parallel processing and has great ability in realizing complicated non-linear mappings from the input space to the output space, thus providing an extremely fast processing facility for complicated non-linear problems.

Zhang *et al.* [32] presented a PSS design approach that employs the multi-layer perceptron with error back-propagation training method. The ANN was trained with the training data group generated by an adaptive power system stabilizer.

In [33], Segal *et al.* presented a new approach for real-time tuning of conventional PSS using a radial basis function network, which is trained using an orthogonal least squares (OLS) learning algorithm.

In [34] a PSS design was presented that combined numerical (ANN) and linguistic (FLS) information in a uniform fashion, thus providing a model-free description of the control system and overcoming the ANN and FLS weaknesses and facilitates on-line implementation.

Although recently various other controller devices (SVC, STATCOM, FACTS) designed to enhance system stability found applications in today's modern power systems, PSS remains still an attractive solution, as it is a very cost-effective means to ensure power system stability and security [35].

1.2.1 Genetic Algorithm in PSS Tuning

Although first proposed by Holland [36] in the seventies, only starting in the early nineties heuristic search algorithms, deeply rooted in the mechanisms of evolution and natural genetics, have emerged as practical, robust search methods – Genetic Algorithms (GAs). Among other fields of research, they found applicability and have been used extensively in solving various problems in power systems. Unit commitment, generation/transmission network expansion planning, optimal power flow, economic dispatch, reactive power planning, equipment optimal placement/selection, service restoration, control design in general, and last but not least PSS tuning and design, just to enumerate some of the problems tackled by researchers by employing GA based approaches.

Genetic algorithm based applications to tune the parameters of PSS have been reported in [37]-[41]. A GA based optimization method has been used in [37] to tune the parameters of a rule-based PSS; this way, the advantages of the rule-based PSS such as its robustness, less computational burden and ease of realization are maintained. Introduction of GAs helps obtain an optimal tuning for all PSS parameters simultaneously, which thereby takes care of interactions between different PSS.

In [38], simultaneous tuning for all the PSS in the system using a GA based approach has been developed. The GA seeks to shift all eigenvalues of the system within a region in the stable domain. In [39], a multiobjective design of PSSs in a multimachine power system operating at various loading conditions and system configurations is achieved using a GA search process. A multiobjective problem is formulated to optimize a composite set of objective functions comprising the damping factor, and the damping ratio of the lightly damped electromechanical modes, and the effectiveness of the suggested technique is confirmed through eigenvalue analysis and nonlinear simulation results.

Zhang and Coonick [40] proposed a GA based computational procedure to select PSS parameters simultaneously in multi-machine power systems, by solving a set of inequalities that represent the objectives of optimization problem.

In [41], a GA based tuning technique of fixed structure damping controllers over a prespecified set of operating conditions is proposed and demonstrated for large-scale realistic systems. It is emphasized here the importance of an accurate fitness function and the fact that a power system expert's input in the designing stage of the optimization process is very

important, and sometimes required to select the best solution out of a pool of solutions resulted from the algorithm.

1.3 Electric Power Ancillary Services – Role of PSS

In deregulated power systems, the Independent System Operator (ISO) is entrusted to ensure a required degree of quality, safety, reliability and stability, and perform several other functions. *Ancillary services* are all those activities that are necessary to support power transmission, while maintaining reliable and stable operation and ensuring the required degree of quality and safety. These services thus include regulation of frequency and tie-line power flow, voltage and reactive power control, ensuring system stability, maintenance of generation and transmission reserves, and many others.

According to the North American Electric Reliability Council (NERC) Operating Policy 10 [42], an ancillary service is defined as an *interconnected operation service* that is necessary to affect a transfer of electricity between purchasing and selling entities, and which a transmission provider must include in an open access transmission tariff.

In vertically integrated utility structures, where responsibility for generation, transmission and distribution is centralized at one organization, ancillary services are an integral part of the electricity supply and are *not* separated [43]. However with deregulation of the power industry, with generation and transmission becoming separate businesses, the ISO often has no direct control over individual power stations and has to *purchase ancillary services* from ancillary service providers. In such an environment, issues pertaining to payment mechanisms for such services are extremely important for the proper functioning of the system. There are several operator activities and services, which can come under the purview of ancillary services. The definitions of such services and distinctions between some of them are often unclear.

While the details and definitions of some ancillary services remain vague, the key concepts and purposes of these services are now widely understood and appreciated. However, much work remains in defining a set of services – mutually exclusive and exhaustive, in identifying which services can be provided competitively – which must be under the direct control of the ISO, and which can be obtained from outside the local control area.

In the deregulated environment, PSS tuning, coordination amongst participating generators and the entity responsible for the above, are some of the challenging questions that have not been properly addressed yet. As of now, no definite guidelines have been established by the ISO or equivalent authorities, with regard to this question.

In a system with several generators equipped with PSS, their parameters would have been optimally tuned in a coordinated manner by the ISO, or a similar entity. These PSSs render a service to the system by way of providing stabilization action to small disturbances that occur in the system continually. In the absence of this service, the system will in some cases become unstable due to sustained low frequency oscillations. Evidently, this directly affects the transmission system security and reliability and hence the service provided by such PSS control action can essentially be classified within the ancillary services definitions, as a service for bulk transmission system security.

1.4 Game Theory in Power Systems

Game theory is a branch of economics focused on behavior related to interactive decision problems. More than 50 years ago, when game theory first emerged, attempts were made to develop theories of bargaining that would predict outcomes. In a broad sense, game theory is a collection of mathematical models formulated to study situations of conflict and cooperation, and is concerned with finding the best actions for the individual decision makers in these situations and/or recognizing stable outcomes. Game theory does not cover games of chance, where the decision maker has no influence on the outcome and also excludes the descriptive, statistical approach [44].

Although there are many logical ways to distinguish between games, in accordance to the way in which the players interact with one another in a given game, and the extent to which they influence each other's decisions, the game can be classified into two major categories, namely *cooperative* or a *non-cooperative game*.

In a *noncooperative game*, strategies are chosen by the players independently, the rules would not allow players to join forces and coordinate actions for better outcomes.

On the other hand, in a *cooperative game*, the players have strictly identical interests or certain agreements and/or other commitments are enforceable on the players. Analysis in cooperative game theory is centered around two major issues: coalition formation and distribution of wealth gained through cooperation. Cooperation does not mean that any player would sacrifice its own interest for the sake of the other, but only that communication and coordination serve the purpose of better achieving their scopes.

In recent years, game theory has found applications in power systems research, in the context of their operation in deregulated environment, in which payment allocation, strategic bidding, and gaming are relevant issues. In particular, cooperative game theory arises as a very convenient tool to solve cost- or savings-allocation problems. The solution mechanisms of cooperative game theory behave well in terms of fairness, efficiency, and stability; implementations of such mechanisms were formulated in problems as:

wheeling transactions [45], in the allocation of expansion costs [46], [47], allocation of transmission losses costs [48], [49], demand management [49], bidding strategies [50], and trading mechanisms [52]. A Nash bargaining game has been used in [53] for power flow analysis in which each transaction and its optimal price are determined to optimize the interest of individual parties, while in [54], to simulate the decision making process for defining offered prices in an open market.

Nevertheless, to this date and to author's best knowledge, virtually no reported attempts to apply game theory principles to PSSs design or operation in a deregulated, decentralized environment have been made.

1.5 Thesis Outline

This thesis examines the application of Genetic Algorithms to PSS tuning in order to determine a globally optimum PSS parameter set that will ensure a stable and robust operation of a multi-machine power system, for each operating point within a wide range.

Chapter 1 introduces the topic of small-signal stability in power systems, with emphasis on the low frequency oscillation phenomena occurring due to small disturbances and its mitigation by means of PSS. *Genetic Algorithms* and *Game Theory* are also introduced and briefly discussed, since they have been used as tools to obtain optimum PSS parameters, and determine PSS-control payment allocation, respectively. A review of literature discusses the relevant work in this area of tuning of PSS and lays down the motivations and objectives of the present work.

Chapter 2 presents the small-signal stability models of single machine connected to an infinite bus (SMIB) and multi-machine power systems. The detailed mathematical formulations have been detailed in the Appendix. The models have been formulated in state-space form and their performances without PSS have been examined. The classical optimization method based on Lyapunov's parameter optimization to tune the parameters of the lead-lag PSS is presented in this chapter. Phase compensation characteristics of the lead-lag PSS have been examined and a method of PSS tuning using the exact phase compensation approach has been developed. Further, the Lyapunov's parameter optimization method has been extended to PSS tuning in multi-machine systems, and applied to a three-machine – nine-bus system.

Chapter 3 treats the same problem – the tuning of PSS – by means of a GA search on the classical Lyapunov's parameter optimization based method. This method ensures that for any operating condition within a pre-defined domain, the system remains stable when subjected to small perturbations. The optimization criterion employs a quadratic performance index that measures the quality of system dynamic response within the tuning process. The solution thus obtained is globally optimal and robust. The proposed method has been

tested on different PSS structures – the lead-lag and the derivative type – and in both cases was found that system dynamic performances are satisfactory for different load conditions and system configurations.

Chapter 4 discusses the optimum tuning of proportional-integral-derivative (PID) PSS for the SMIB and multi-machine power systems, in which a similar GA based tuning technique as the one introduced in the previous chapter is now developed. The tuning scheme proposed in this chapter uses a genetic GA based search that integrates a classical parameter optimization criterion based on Integral of Squared Error (ISE). This method succeeds in achieving a robust, simultaneously tuned and globally optimal PID-PSS parameter set, while maintaining the simplicity of the classical optimization method. The tuning method implicitly builds-in an increased robustness through an objective function that depends on the operating domain. The system is represented in a discrete-time state-space form and the influence of the sampling time on the PSS parameter tuning is also investigated.

Chapter 5 introduces in the concept of ancillary services with a specific emphasis on the contribution of PSSs, and proposes that the control action provided by PSSs to enhance system stability, be considered as one of the system ancillary services. To this effect, there is a need to formulate appropriate financial compensation mechanisms for the generators, in return for their service. A cooperative game theory based approach using the Shapley value criterion is developed in this chapter to identify the marginal contribution of each PSS to the total control effort. Accordingly, the method outlines appropriate allocation of payment to each generator involved in providing the PSS-control service. Enhancement in system performance due to PSS is measured through increased system transfer capability and the margin of stability thus achieved. Additionally, a set of contingencies is considered in order to examine whether and how the PSSs' payoffs are affected by a different system topology. Alternatively, the payment allocation method is applied, in conjunction with an N-1 security criterion, to determine the payoffs for a realistic case (*i.e.* over a 24-hour period, and for different load types), thus pinpointing how a given loading condition would affect the payment allocation.

Chapter 6 further dwells upon evaluating the contribution of each PSS to system stability and the system savings thus resulting. Therefore, it is of importance to appropriately choose a criterion to assess the performance of each PSS, so that a proper allocation of savings can eventually be attained. At the same time, it is also important to identify whether some PSSs would be critical for system stability, particularly if some could be even detrimental to overall system stability. Various performance criteria – extracting information from the system dynamic behavior – are implemented and, ultimately, a composite savings allocation function is constructed for a more accurate and comprehensive assessment of power system behavior. A similar cooperative game theory based method of payment allocation is employed in order to

identify the marginal contribution of each PSS to the total control effort. Accordingly, the method outlines appropriate allocation of payment to each generator involved in providing the PSS-control, and consequently, different designs investigated. The robustness of the allocation thus evolved is also tested against a set of contingencies.

Chapter 7 summarizes the work presented in this thesis, highlights its significant contributions and draws the scope for future work in this area.

2 SMALL-SIGNAL STABILITY MODELS AND CONVENTIONAL DESIGN OF LEAD-LAG PSS

In this chapter, small-signal stability models of power systems, formulated in state-space form, have been examined. Based on the phase characteristics of a SMIB system, a PSS tuning method using the exact phase compensation approach has been demonstrated for a lead-lag PSS. An optimization method based on Lyapunov's parameter optimization criterion to tune the PSS parameters has also been introduced, and then compared to the phase compensation method. Further, the Lyapunov's parameter optimization method has been extended to PSS tuning in multi-machine systems, and applied to tune a three-machine – nine-bus system, in a sequential approach.

Keywords: small-signal stability, lead-lag PSS, phase compensation, sequential tuning, Lyapunov's parameter optimization, Integral of Squared Error

2.1 General Approach

Small-signal stability is the ability of the power system to maintain synchronous operation when subjected to small disturbances. Since the disturbance is considered to be small, the equations that describe the resulting dynamics of the system may be linearized. Instability that may result can be of two types:

a) steady increase in generator rotor angle due to lack of synchronizing torque;

b) rotor oscillations of increasing amplitude due to lack of sufficient damping torque.

In today's practical power systems, the small-signal stability problem is usually one of insufficient damping of system oscillations.

For the analysis of small-signal stability, linearized models are generally considered to be adequate for representation of the power system and its various components.

The state-space representation is concerned not only with input and output properties, but also with its complete internal behavior. In contrast, the transfer function representation specifies only the input/output behavior. If state-space representation of a system is known, the transfer function is uniquely defined. In this sense, the state-space representation is a more complete description of the system, and it is ideally suited for the analysis of multi-variable MIMO systems.

In the development of a dynamic model for a multi-machine power system (classical stability model), the following assumptions are usually made [55]:

a) Mechanical power input is constant.
b) Damping or asynchronous power is negligible.
c) Constant-voltage-behind-transient-reactance model for the synchronous machines is valid.
d) The mechanical rotor angle of a machine coincides with the angle of the voltage behind the transient reactance.
e) Loads are represented by passive impedances.

To study the dynamic behavior of a system, the following data are needed:

- System data (lines, buses, transformers, machines);
- Load-flow data – the complex power and voltage at generator nodes.

Each machine model is first expressed in its own *d-q* frame, which rotates with its rotor. For the solution of interconnecting network equations, all voltages and currents must be expressed in a common reference frame. The real-axis of one machine, rotating at synchronous speed, is used as the common reference. Axis transformation equations are used to transform between the individual machine (*d-q*) reference frames and the common (*D-Q*) reference frame. The real-axis of the common reference frame is used as the reference for measuring the machine rotor angle. For a machine represented in detail, including dynamics of rotor circuit(s), the rotor angle is defined as the angle by which the machine *q*-axis leads/lags the real axis. Under dynamic conditions, the angle δ changes with rotor speed [56].

The following calculations are essential in order to prepare the system for a stability study:

a) All system data are converted to a common base.
b) The loads are converted to equivalent admittances. The needed data is taken from a load-flow study. The equivalent shunt admittance at the bus is given by:

$$\overline{Y}_L = \frac{\overline{I}_L}{\overline{V}_L} = \frac{\overline{S}_L^*}{V_L^2} = \frac{P_L}{V_L^2} - j\frac{Q_L}{V_L^2} \tag{2.1}$$

where $\overline{V}_L$, P_L, Q_L, and $\bar{I}_L$ are the voltage, active power, reactive power and current, respectively, corresponding to $\overline{Y}_L = G_L + jB_L$ load admittance.

c) The internal voltages of a generator $E_i\angle\delta_{i0}$ are calculated from a load-flow run. The internal angle of the generator during transients (δ') is computed from the pre-transient terminal voltages $V\angle\alpha$.

d) The network admittance matrix $\overline{\mathbf{Y}}$ is calculated. $\overline{\mathbf{Y}}$ is a $n \times n$ matrix, where n is the total number of buses.

e) Obtain the admittance matrix for the reduced network ($\overline{\mathbf{Y}}_\mathbf{m}$) by eliminating all the nodes that are not internal generator nodes. All nodes except for the internal generator nodes should have zero injection currents, and this property is used to obtain the network reduction [55].

Note that $\overline{\mathbf{Y}}_\mathbf{m}$ is a $n_g \times n_g$ dimension matrix, where n_g is the number of generators. In Appendix I, Section 9.1.1 provides details of the above.

2.1.1 Systems Investigated

The systems considered for analysis in this thesis are the single machine connected to infinite bus through a double circuit transmission line (Figure 3.1), and the well-known nine-bus power system [55], which has three generators and three loads (Figure 2.2).

For all generators, IEEE Type ST-1 excitation systems have been considered. System parameters and operating data for both systems investigated have been provided in Appendix II.

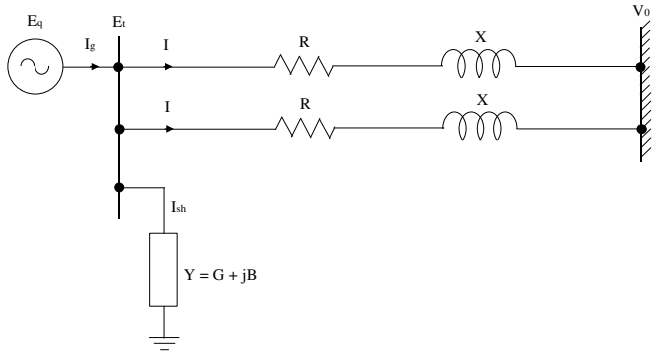

Figure 2.1 Single machine connected to an infinite bus system

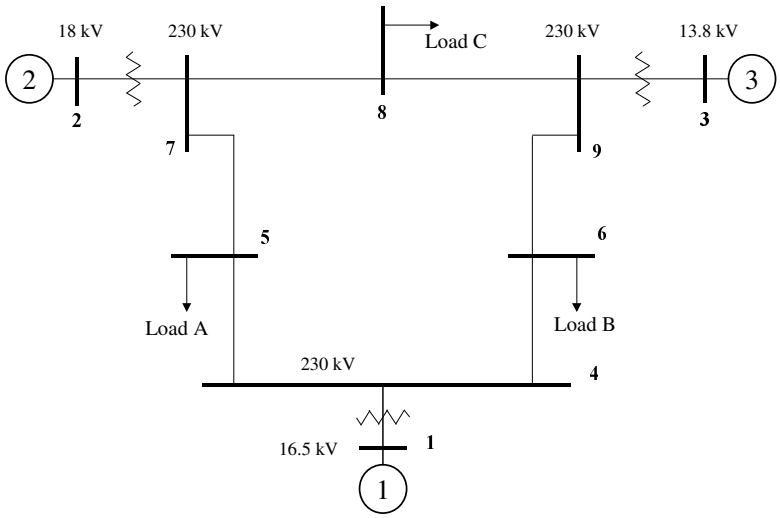

Figure 2.2 Three-machine nine-bus system [55]

2.1.2 Small Perturbation Dynamic Model of the Power Systems

The phenomena of stability and damping of synchronous machines for the mode of small perturbations can be examined with the aid of block diagrams relating pertinent variables of the system (such as, electrical torque, speed, angle, terminal voltage, field voltage, flux linkages). The small-perturbation transfer-function block diagrams of the systems investigated are shown in Figure 2.3 and Figure 2.4. For convenience, the SMIB system will be treated first and then the three-machine nine-bus system will be discussed in a general manner applicable to any multi-machine power system for the purpose of small-signal stability studies.

The state-space model of the SMIB system can be expressed as follows:

$$\frac{d}{dt}\underline{X}(t) = \mathbf{A}\cdot\underline{X}(t) + \underline{b}\cdot u(t) + \underline{\Gamma}\cdot p(t) \tag{2.2}$$

where **A** is the state matrix
$\underline{X}$ is the state vector
$\underline{b}$ is the control vector
u is the control signal
$\underline{\Gamma}$ is the perturbation vector
p is the perturbation

and are expressed as follows:

$$\mathbf{A} = \begin{bmatrix} -\frac{D}{M} & -\frac{K_1}{M} & -\frac{K_2}{M} & 0 \\ 2\pi f & 0 & 0 & 0 \\ 0 & -\frac{K_4}{T_{do}'} & -\frac{1}{T_{do}'K_3} & \frac{1}{T_{do}'} \\ 0 & -\frac{K_A K_5}{T_A} & -\frac{K_A K_6}{T_A} & -\frac{1}{T_A} \end{bmatrix}$$

$$\underline{X} = [\Delta\omega \quad \Delta\delta \quad \Delta E_q' \quad \Delta E_{fd}]^T$$

$$\underline{b} = \begin{bmatrix} 0 & 0 & 0 & \frac{K_A}{T_A} \end{bmatrix}^T$$

$$\underline{\Gamma} = \begin{bmatrix} \frac{1}{M} & 0 & 0 & 0 \end{bmatrix}^T$$

Note that the control signal *u*, which is actually the PSS output, would act on the summing junction of the terminal voltage reference of the AVR-excitation system (Figure 2.3). Also note that, since we deal with a SISO system, *u* is a scalar.

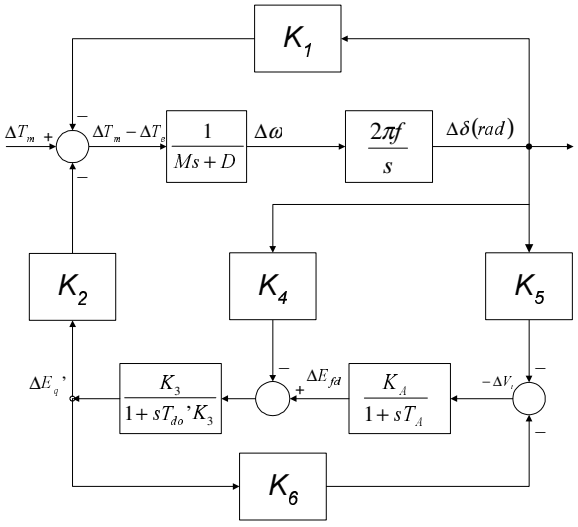

Figure 2.3 Small-perturbation transfer function block diagram of SMIB system

The perturbation is a step increase of 1% in mechanical torque T_m of the synchronous generator.

The state matrix of the system contains the so called K constants of the system, which in turn are derived from the electric torque expression (K_1, K_2), field winding circuit equation (K_3, K_4), and from the terminal voltage magnitude (K_5, K_6).

The transfer function block diagram in Figure 2.4 describes the dynamics of the i^{th} machine in a multi-machine power system [57]. This is a generalization of the extensively used single machine connected to infinite bus transfer function block diagram [6] and takes into account the interaction between machines via **K** matrices, which are square matrices of order n_g. The diagonal elements of the $\mathbf{K_1}$, … , $\mathbf{K_6}$ matrices determine the machine's dynamics, while the off-diagonal elements model the dynamic interactions between machines. Observe that in this block diagram the PSS is not represented, for convenience. The number of state variables is $n_v \times n_g$, where n_v is the number of state variables used to model one machine and its excitation system.

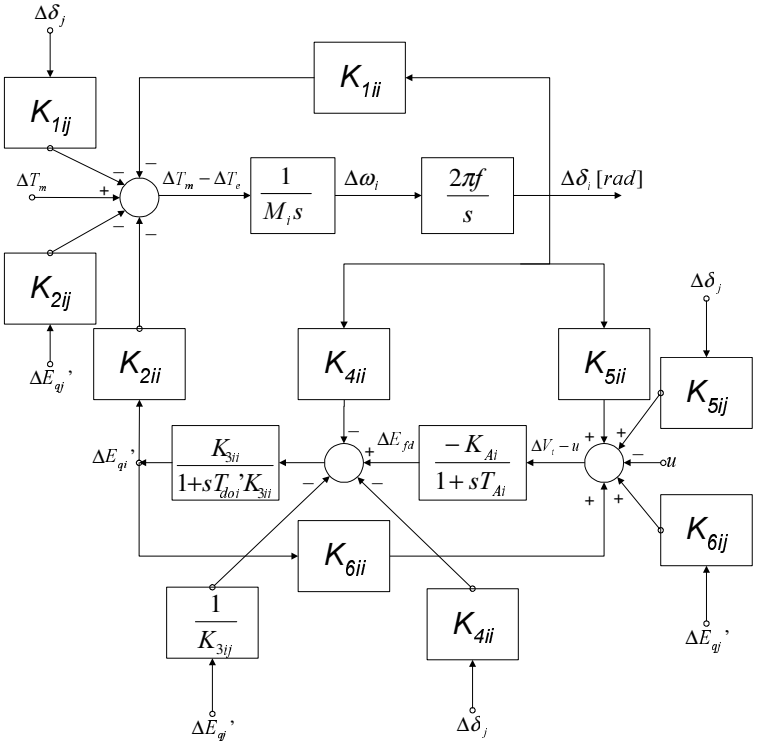

Figure 2.4 Transfer function block diagram representation of a multi-machine system for small-signal stability analysis

For the calculation of $\mathbf{K}_1$, $\mathbf{K}_2$, … $\mathbf{K}_6$ matrices, the armature current components I_d and I_q, and the terminal voltage components V_d and V_q of each machine are expressed with respect to the common frame of reference. It is to be noted that the scalar parameters K_1, … K_6 used to represent the SMIB system can be obtained from the general $\mathbf{K}_1$, … $\mathbf{K}_6$ matrices from the general multi-machine mode representation.

During low-frequency oscillations, the current induced in a damper winding is negligibly small; hence the damper windings are completely ignored in the system model. As for the *d*- and *q*-axes armature windings of the synchronous machine, their natural oscillating frequency being extremely high, their eigenmodes will not affect the low-frequency oscillations, and hence can be described simply by algebraic equations [57]. What is left is the field winding circuit of the machine, which is described by a differential equation, not only because of its low eigenmode frequency, but also because it is connected directly to the excitation system to which the supplementary excitation control is applied. The excitation system itself must be described by differential equations. Finally, the torque differential equation of the synchronous machine is included in the model.

The complete mathematical formulation of the multi-machine dynamics, as well as the subsequent small perturbation model have been discussed in Appendix I. Based on the transfer function block diagram (Figure 2.4), the system dynamics can be expressed by a set of linear differential equations in the small-perturbation variables $\Delta\omega_i$, $\Delta\delta_i$, $\Delta E_{qi}'$, ΔE_{fdi} as follows:

$$
\begin{aligned}
&\frac{d}{dt}(\Delta\omega_i) = -\frac{D_i}{M_i}\Delta\omega_i - \frac{K_{1_i}}{M_i}\Delta\delta_i - \frac{K_{2_i}}{M_i}\Delta E_{q_i}^{'} + \frac{1}{M_i}\Delta T_{m_i} \\
&\frac{d}{dt}(\Delta\delta_i) = 2\pi f \cdot \Delta\omega_i \\
&\frac{d}{dt}(\Delta E_{q_i}^{'}) = -\frac{K_{4_i}}{T_{do_i}^{'}}\Delta\delta_i - \frac{1}{T_{doi}^{'} \cdot K_{3i}} \cdot \Delta E_{q_i}^{'} + \frac{1}{T_{do_i}^{'}}\Delta E_{fd_i} \\
&\frac{d}{dt}(\Delta E_{fd_i}) = \frac{K_{A_i}K_{5_i}}{T_{A_i}}\Delta\delta - \frac{K_{A_i}K_{6i}}{T_{A_i}}\Delta E_{q_i}^{'} - \frac{1}{T_{A_i}}\Delta E_{fd_i} + \frac{K_{A_i}}{T_{A_i}}u_{E_i} \\
&\qquad\qquad \forall\ i = 1, \ldots, n_g
\end{aligned}
\tag{2.3}
$$

It is to be noted here that when $n_g = 1$, the above set of equations reduce to the well-known SMIB system representation.

Using vector-matrix notation, the set of equations (2.3) can be represented in state-space form as follows:

$$\dot{\underline{X}}(t) = \mathbf{A} \cdot \underline{X}(t) + \mathbf{B} \cdot \underline{U}(t) + \mathbf{\Gamma} \cdot \underline{p}(t) \tag{2.4}$$

In equation (2.4), **A, B** and Γ are the state, control and perturbation matrices respectively, and $\underline{X}(t)$, $\underline{U}(t)$ and $\underline{p}(t)$ are state, control and perturbation vectors, respectively.

State matrix **A** is a function of the system parameters and operating conditions, while the control matrix **B** and perturbation matrix Γ depend on system parameters only.

For the system operating conditions and parameters considered (see Appendix II), the system eigenvalues are obtained by solving the *characteristic equation* of the system.

The stability characteristic of the system is dependent on the eigenvalues of the state matrix as follows:

a) A *real eigenvalue* corresponds to a non-oscillatory mode. A negative real eigenvalue represents a decaying mode, while a positive real eigenvalue represents aperiodic instability.

b) A pair of *complex eigenvalues* represents an oscillatory mode. The real component of the eigenvalue gives *the damping*, and the imaginary component gives *the frequency of oscillation*. A negative real part represents a damped oscillation whereas a positive real part represents oscillation of increasing amplitude.

2.1.3 No PSS Operation

Table 2.1 shows the eigenvalues of the SMIB system for the nominal operating point and system parameters considered. The corresponding system dynamics (rotor angle and speed deviations with respect to their corresponding steady-state values) are shown in Figure 2.5 and Figure 2.6. Evidently, the system is unstable under small perturbations, and would require a stabilizing signal from the PSS.

Table 2.1 Eigenvalues of SMIB system without PSS

Operating point [p.u.]	**Eigenvalues**	**Damping factor**	**Natural frequency** [Hz]
$P = 0.8$ $Q = 0.6$	$0.1028 \pm j5.5022$ -6.3710 -14.2975	-0.0187 1.0 1.0	0.875 – –

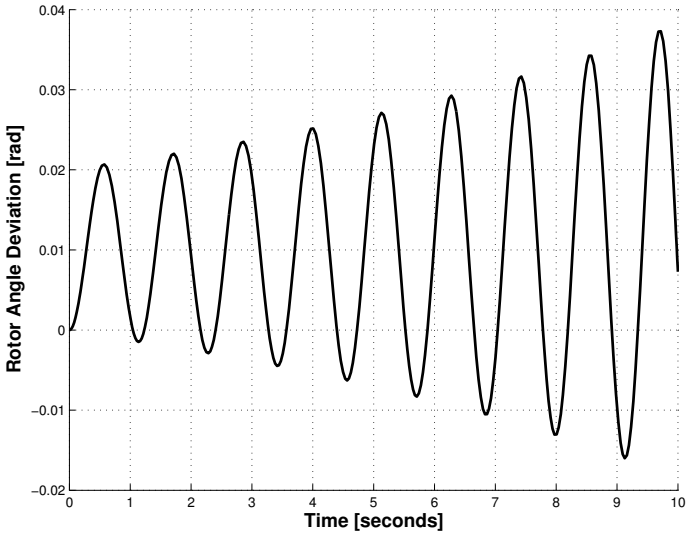

Figure 2.5 Rotor angle deviation for SMIB system under small perturbation

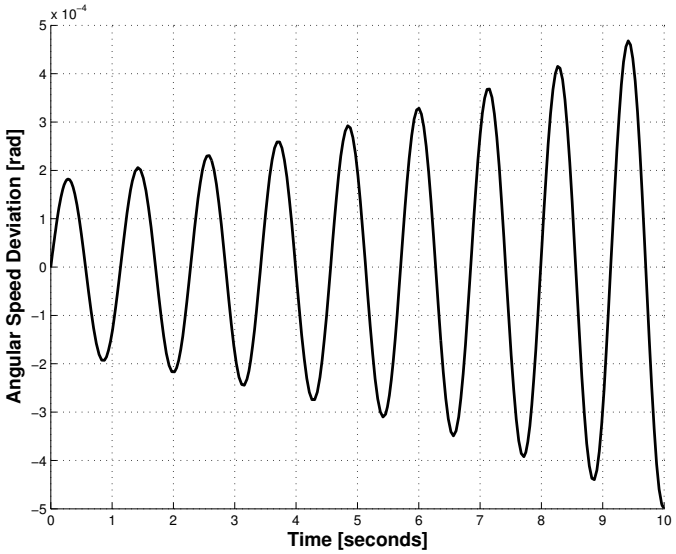

Figure 2.6 Rotor speed deviation for SMIB system under small-perturbation

As discussed in Section 2.1.1, the three-generator, nine-bus system [55] has been considered for our analysis of multi-machine systems. The same set of state variables as that used for SMIB system has been used to describe each machine of the multi-machine system behavior through state-space modeling approach.

The state-space model for the three-machine system is expressed as follows:

$$\frac{d}{dt}\underline{\mathrm{X}}(t) = \mathbf{A}\cdot\underline{\mathrm{X}}(t) + \mathbf{B}\cdot\underline{\mathrm{u}}(t) + \mathbf{\Gamma}\cdot\underline{\mathrm{p}}(t) \tag{2.5}$$

where $\underline{\mathrm{X}}(t)$, $\underline{\mathrm{u}}(t)$ and $\underline{\mathrm{p}}(t)$ are state, control and perturbation vectors, respectively and they are expressed as follows:

$$\begin{aligned}\underline{\mathrm{x}}(t) = [&\Delta\omega_1(t) \quad \Delta\delta_1(t) \quad \Delta E_{q1}(t) \quad \Delta E_{fd1}(t)\ldots \\ &\Delta\omega_2(t) \quad \Delta\delta_2(t) \quad \Delta E_{q2}(t) \quad \Delta E_{fd2}(t)\ldots \\ &\Delta\omega_3(t) \quad \Delta\delta_3(t) \quad \Delta E_{q3}(t) \quad \Delta E_{fd3}(t)]^T\end{aligned}$$

$$\underline{\mathrm{u}}(t) = [\Delta u_1(t) \quad \Delta u_2(t) \quad \Delta u_3(t)]^T$$

$$\underline{\mathrm{p}}(t) = [\Delta T_{m_1} \quad \Delta T_{m_2} \quad \Delta T_{m_3}]^T$$

A, B and Γ are the state, control and perturbation matrices, respectively. They are constructed by generalizing the SMIB model to multi-machine model and are given in Appendix III, Section 9.3.1.

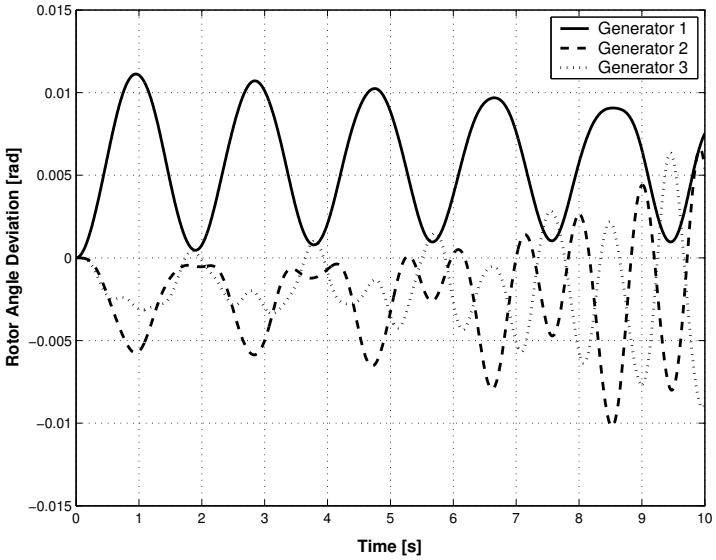

Figure 2.7 Angular speed deviations of all machines when Gen-1 is perturbed

This system is analyzed in a similar manner as the SMIB system. Figure 2.7 and Figure 2.8 show the time response of angular speed and rotor angle

deviations of all the machines of the system without PSS, when a 1% step perturbation in mechanical input of occurs at the shaft of Generator 1.

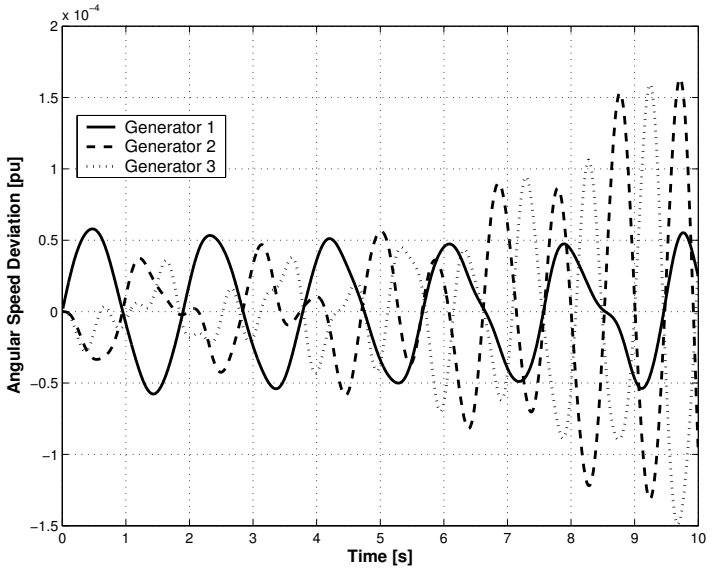

Figure 2.8 Rotor angle deviations for 3-machine system without PSS

Table 2.2 presents the eigenvalues and corresponding damping factors and natural frequencies of oscillations. As also suggested by the figures is now evident that the system is unstable under small perturbations on Generator 1.

Table 2.2 Eigenvalues of 3-machine system without PSS

Operating point [p.u.]	**Eigenvalues**	**Damping factor**	**Natural frequency** [Hz]
P_1 = 0.7160	0.0303 ± *j* 6.62	- 0.00457	1.050
P_2 = 1.6300	0.0895 ± *j*12.4	- 0.0072	1.970
P_3 = 0.8500	- 0.004 ± *j* 3.32	0.0120	0.528
	-10.50 ± *j*6.75	0.8410	1.989
Q_1 = 0.2700	- 3.92	1.0000	–
Q_2 = 0.0670	- 6.21	1.0000	–
Q_3 = -0.1090	-14.80	1.0000	–
	-16.30	1.0000	–

2.2 Conventional Design of Lead-Lag PSS

Two distinct types of system oscillations are usually recognized in interconnected power systems [9]. One is associated with units at a generating station swinging with respect to rest of the power system. Such oscillations are referred to as *local mode* oscillations and have a frequency in the range of 0.8 to 2.0 Hz. The term local is used because the oscillations are localized at one power plant. The second is associated with swinging of many machines in one part of the system against machines in another part. These are *inter-area mode* oscillations, and have frequencies in the range of 0.2 to 0.7 Hz.

The basic function of PSS is to add damping to the generator rotor oscillations by controlling its excitation using auxiliary stabilizing signal(s). To provide damping, the PSS must produce a component of electrical torque in phase with the rotor speed deviations.

PSS typically works on phase compensation and adjusting it is the main task in PSS tuning. Phase compensation is accomplished by adjusting the PSS to compensate for phase lags through the generator, excitation system, and power system, such that PSS provides torque changes in phase with speed changes. Tuning should be performed when system configurations and operating conditions result in the least damping, and verification should demonstrate that no instability is introduced within normal operating ranges as well as expected faults.

2.2.1 Performance Objectives of PSS

The overall excitation control system (including PSS) is designed to [9]:

a) Maximize the damping of the local plant mode as well as inter-area mode oscillations without compromising the stability of other modes;

b) Enhance system transient stability;

c) Not adversely affect system performance during major system upsets which cause large frequency excursions;

d) Minimize the consequences of excitation system malfunction due to component failures.

Since the purpose of a PSS is to introduce a damping torque component, the speed deviation represents an appropriate signal to be used as input for the PSS. In practice, both generator and its exciter exhibit frequency dependent gain and phase characteristics, *GEP(s)*. Hence, the PSS transfer function should have appropriate phase-lead circuits to compensate for the phase lag between the exciter input and the electrical torque.

For large values of K_A and the usual range of constants, the composite transfer-function for $GEP(s)$ and the corresponding phase-lag characteristic can be written as follows [6]:

$$GEP(s) = \frac{K_2}{K_6 \cdot \left(1 + s\frac{T_{do}^{'}}{K_6 K_A}\right) \cdot (1 + sT_A)}$$

$$\angle GEP = \tan^{-1}\left(\frac{\omega T_{do}^{'}}{K_6 K_A}\right) + \tan^{-1}(\omega T_A) \tag{2.6}$$

The transfer function of the lead-lag PSS on the i^{th} machine is shown in equation (2.7) and the corresponding block diagram is shown in Figure 2.9.

$$G_{PSS}(s) = \frac{\Delta u_i(s)}{\Delta \omega_i(s)} = K_{C_i} \cdot \left[\frac{sT_{W_i}}{1 + sT_{W_i}}\right] \cdot \left[\frac{1 + sT_{1_i}}{1 + sT_{2_i}}\right] \cdot \left[\frac{1 + sT_{3_i}}{1 + sT_{4_i}}\right] \tag{2.7}$$

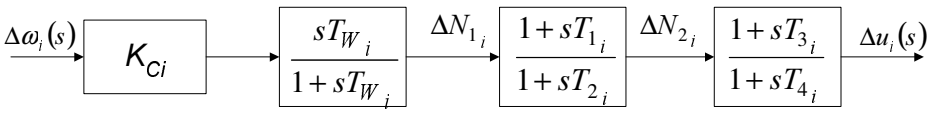

Figure 2.9 Transfer function block diagram for lead-lag PSS

The corresponding phase-lead characteristic of the lead-lag PSS is given by:

$$\angle G_{PSS} = \frac{\pi}{2} - \tan^{-1}\omega T_W + 2\left[\tan^{-1}(\omega T_1) - \tan^{-1}(\omega T_2)\right] \tag{2.8}$$

Note that, for the purpose of simplification, the phase angle of PSS signal in (2.8) was expressed under the assumption that $T_1 = T_3$ and $T_2 = T_4$.

Figure 2.10 shows the phase-lead characteristics of the PSS for several values of T_1. For the frequency range considered, the lead-lag PSS can provide up to about 90° phase compensation, with $T_1 = 0.3$ seconds.

The parameters of the lead-lag PSS are required to be tuned optimally, in order to obtain the best performance of the system.

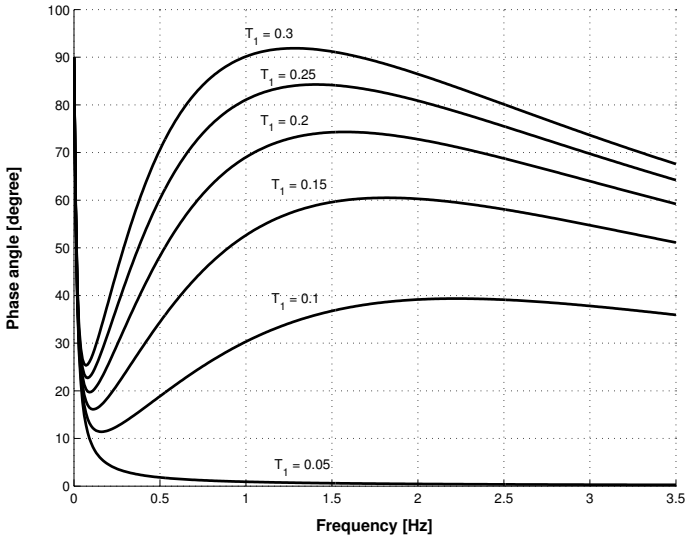

Figure 2.10 PSS phase lead characteristics for different time constants, $T_1 = T_3$ and $T_2 = T_4 = 0.05$ sec

2.2.2 Primary Considerations for the Selection of Lead-lag PSS Parameters

In principle, the lead-lag PSS (also regarded as the *conventional* PSS) consists of three blocks: a phase compensation block, a signal washout block and a gain block (refer Figure 2.9).

The *phase compensation* block provides the appropriate phase-lead characteristic to compensate for the phase lag between the exciter input and the generator electrical torque *GEP(s)*. The phase characteristic to be compensated changes with the system conditions, therefore a characteristic acceptable for a range of frequencies (normally 0.1 to 2.0 Hz) is sought. This may result in less than optimum damping at any one frequency. The required phase lead can be obtained by choosing appropriate values of time constants T_1, ... , T_4.

The signal *washout* block functions as a high-pass filter, which allows the dc signals to pass unchanged, thus avoiding terminal voltage variation due to steady changes in speed. The washout time constant T_W should be long enough to pass stabilizing signals at the frequencies of interest unchanged, but not so long that it leads to undesirable generator voltage excursions during system-island conditions.

The stabilizing gain K_C determines the amount of damping introduced by the PSS, and, ideally, it should be set to a value corresponding to maximum damping. However, in practice the gain is set to a value that results in satisfactory damping of the critical system modes without compromising the

stability of other modes, or transient stability, and that does not cause excessive amplification of PSS input signal noise.

In order to restrict the level of generator terminal voltage fluctuation during transient conditions, limits are imposed on PSS outputs.

The PSS parameters to be optimized are the time constants, T_{1i}, T_{2i}, T_{3i}, T_{4i} and gain K_{Ci}. A washout time constant T_{Wi} = 10 seconds is chosen at all machines in order to ensure that the phase-lead and gain contributed by the washout block for the range of oscillation frequencies normally encountered is negligible [9]. The number of PSS parameters to be optimized is reduced by considering the PSS to comprise two identical cascaded lead-lag networks. Therefore, $T_{1i} = T_{3i}$ and $T_{2i} = T_{4i}$. Also, $T_{2i} = T_{4i} = 0.05$ seconds is assumed fixed from physical realization considerations [6]. Thus, the optimization problem reduces to determining T_{1i} and K_{Ci} (i = 1, ... , n) only.

2.3 Analysis of a Single-Machine Infinite Bus System with a Lead-lag PSS

2.3.1 Composite Model

Figure 2.11 shows the composite transfer-function block-diagram of the SMIB system equipped with a lead-lag PSS.

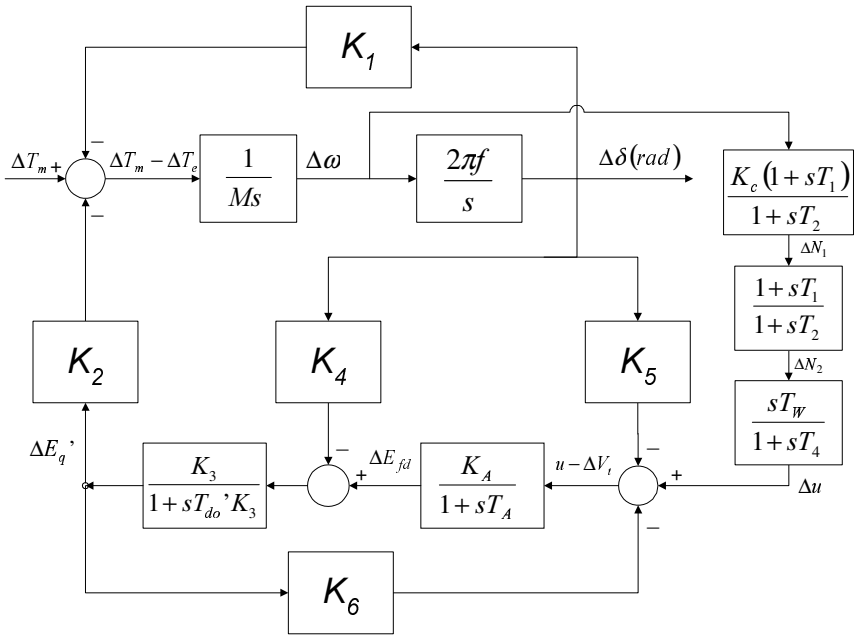

Figure 2.11 Small perturbation block diagram of a single machine to infinite bus system equipped with a lead-lag PSS

The linear dynamic model of the power system without PSS was discussed in detail in Section 2.1.3. Following the same convention, the representation of the above composite system inclusive of the PSS can be described by:

$$\frac{d}{dt}\underline{X}(t) = \mathbf{A} \cdot \underline{X}(t) + \mathbf{\Gamma} \cdot \underline{p}(t) \tag{2.9}$$

A and Γ are the state and perturbation matrices, respectively, $\underline{X}(t)$ the state vector, and $\underline{p}(t)$ is the perturbation. The state vector $\underline{X}(t)$ is given as follows:

$$\underline{X}(t) = \left[\Delta\omega \quad \Delta\delta \quad \Delta E_q^{'} \quad \Delta E_{fd} \quad \Delta N_1 \quad \Delta N_2 \quad \Delta u\right]^T \tag{2.10}$$

Note that the two additional intermediate variables of the PSS, namely ΔN_1 and ΔN_2 appear in (2.9) as state variables, as does the PSS output signal Δu.

The state matrix **A** of this system is given by:

$$\mathbf{A} = \begin{bmatrix} 0 & -\frac{K_1}{M} & -\frac{K_2}{M} & 0 & 0 & 0 & 0 \\ 2\pi f & 0 & 0 & 0 & 0 & 0 & 0 \\ 0 & -\frac{K_4}{T_{do}^{'}} & -\frac{1}{K_3 \cdot T_{do}^{'}} & \frac{1}{T_{do}^{'}} & 0 & 0 & 0 \\ 0 & -\frac{K_A \cdot K_5}{T_A} & -\frac{K_A \cdot K_6}{T_A} & -\frac{1}{T_A} & 0 & 0 & \frac{K_A}{T_A} \\ \frac{K_C}{T_2} & -\frac{K_C K_1 T_1}{T_2 M} & -\frac{K_C K_2 T_1}{T_2 M} & 0 & -\frac{1}{T_2} & 0 & 0 \\ \frac{K_C T_3}{T_2 T_4} & -\frac{K_C K_1 T_1 T_3}{T_2 T_4 M} & -\frac{K_C K_2 T_1 T_3}{T_2 T_4 M} & 0 & \frac{1}{T_4} - \frac{T_3}{T_2 T_4} & -\frac{1}{T_4} & 0 \\ \frac{K_C T_3}{T_2 T_4} & -\frac{K_C K_1 T_1 T_3}{T_2 T_4 M} & -\frac{K_C K_2 T_1 T_3}{T_2 T_4 M} & 0 & \frac{1}{T_4} - \frac{T_3}{T_2 T_4} & -\frac{1}{T_4} & -\frac{1}{T_W} \end{bmatrix}$$

2.3.2 Optimization of PSS Parameters Using Phase Compensation Technique

The phase compensation technique is based on the objective of tuning the PSS parameters to fully compensate for the phase lag introduced through the exciter and generator characteristics $GEP(s)$, such that the torque changes provided by the PSS are in phase with the rotor speed deviations. The following step-by-step approach is used:

a) Find the natural frequency of oscillation ω_n of the electromechanical mode. Neglecting the damping, the characteristic equation of the mechanical loop may be written as:

$$Ms^2 + 2\pi f \cdot K_1 = 0 \tag{2.11}$$

and the solutions are:

$$s = \pm j\omega_n, \qquad \omega_n = \sqrt{2\pi f \cdot K_1 / M} \tag{2.12}$$

where M is the inertia constant in seconds
f is the system frequency in Hz
K_1 is the synchronizing torque coefficient

For the system investigated and the operating conditions described in Section 9.2, K_1 = 0.9538, and the electromechanical mode natural frequency of oscillation is ω_n = 5.474 rad/s.

b) Find the phase lag between Δu and $\Delta E_q'$ of the electrical loop using the relationship established in (2.6). For ω_n = 5.474 rad/s the phase-lag introduced by $GEP(s)$ equals 69.87°.

c) Using (2.8), obtain the PSS phase-lead time constants that exactly compensate for the system phase-lag. In the given system, to exactly compensate for the phase-lag of 69.87°, it was found that the phase-lead time constant required is $T_1 = T_3$ = 0.216 s. Figure 2.12 shows the phase-lag characteristic of *GEP(s)* vis-à-vis the phase-lead characteristic of the lead-lag PSS for $T_1 = T_3$ = 0.216 s. It can be seen that the so tuned PSS closely compensates for the phase-lag in a frequency range up to 1 Hz and compensates accurately for the electromechanical mode.

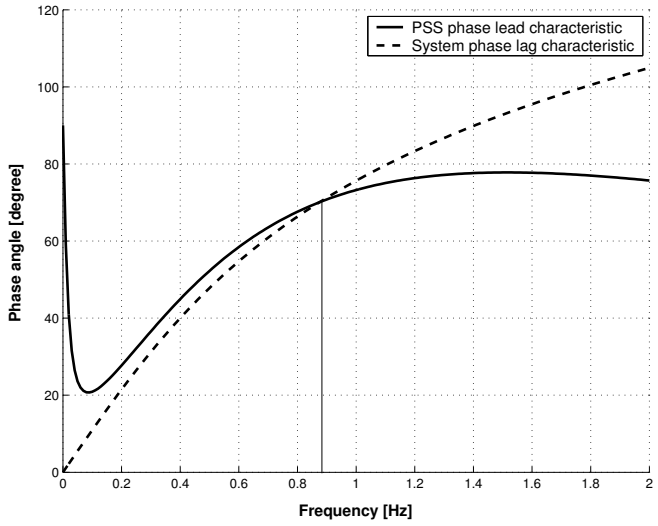

Figure 2.12 Phase characteristics for a SMIB system without controller and a lead-lag PSS

d) Tune the gain K_C of the PSS using any suitable criterion. In this work, the Lyapunov's parameter optimization method, which will be discussed in detail in the next section, was used. The optimum K_C thus found was equal to 26.0.

2.3.3 Lyapunov Method Based Optimization of PSS Parameters

2.3.3.1 *The Performance Index*

The choice of a suitable performance index is extremely important for the design of PSS. In this work, a performance index as given in (2.13), where $\underline{X}$ is the state vector, and **Q** – the weighing matrix – is positive semi-definite and comprises the importance attached to different state-variables in the optimization process, has been used.

$$J = \int_0^\infty (\underline{X}^T \cdot \mathbf{Q} \cdot \underline{X})\, dt \tag{2.13}$$

The performance index J can be evaluated using the relation:

$$J = \underline{X}^T(0) \cdot \mathbf{P} \cdot \underline{X}(0) \tag{2.14}$$

where $\underline{X}(0)$ is the initial state of the state-vector, and **P** is a positive definite symmetric matrix obtained by solving Lyapunov equation:

$$\mathbf{A}^T \cdot \mathbf{P} + \mathbf{P} \cdot \mathbf{A} = -\mathbf{Q} \tag{2.15}$$

where **A** is the state matrix of the system.

By appropriate choice of **Q** matrix elements, various penalization weights can be assigned to state variables (which in this case are deviations from steady-state conditions) and a desirable dynamic performance for the system can be achieved.

2.3.3.2 *Determining the PSS Parameters*

As described in the previous section, by an appropriate choice of **Q** the performance criterion, and hence the optimal PSS parameters, can be manipulated according to design engineer's requirements. In this work, an *Integral of Squared Error* (ISE) criterion that seeks to minimize the square of the power angle deviation from its steady-state value ($\Delta\delta$) is chosen. Subsequently, the state variable $\Delta\delta$ is penalized for deviations by being assigned a high weight in the **Q** matrix, and the PSS parameters are obtained accordingly. Mathematically, this can be written as:

$$J = \int_0^\infty (\Delta\delta - \Delta\delta_{ss})^2 \, dt \tag{2.16}$$

It can be seen that in this case, **Q** = *diag* [0 1 0 0 0 0 0].

In order to obtain the optimal values of K_C and T_1, the following procedure has been used:

1. Choose a set of PSS parameters for which the state matrix of the composite system (including the PSS) is nonsingular.
2. Fix the value of T_1 and vary K_C over a wide range of values and determine the performance index, using (2.16). It is observed that for a fixed T_1, when K_C increases, the performance index J decreases continuously attaining a minimum J_{min} and then start increasing again as K_C increases further.
3. Carry out Step-2 for various values of T_1 and determine the *minimum* J_{min}

Figure 2.13 shows the plot of variation of J as a function of K_C for different values of T_1. Notice that J attains the overall minimum for K_C = 38.65 and T_1 = 0.11 seconds, which are then the optimal settings of the lead-lag PSS.

Table 2.3 Performance indices corresponding to different PSS settings

	Phase compensation method	**Lyapunov method**
PSS settings, T_1, K_C	0.216 26.0	0.11 38.65
Performance Index, J	1.791×10^{-5}	1.445×10^{-5}

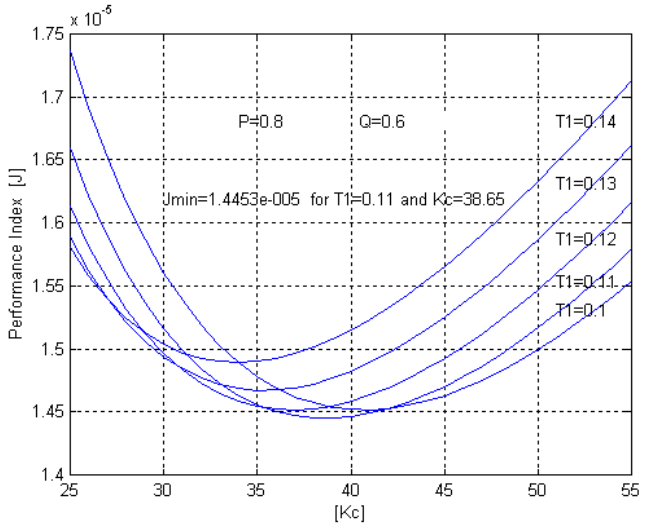

Figure 2.13 Performance index as a function of PSS gain K_C, for different T_1

Figure 2.14 shows a comparison of the system dynamic performances with the optimal lead-lag PSS, but designed using two different techniques: the full phase-compensation approach and the Lyapunov's method. It can be seen that both the design approaches provide satisfactory performances, though the phase compensation approach requires somewhat more settling time, which is evident from a comparison of the values of performance indices J also (Table 2.3).

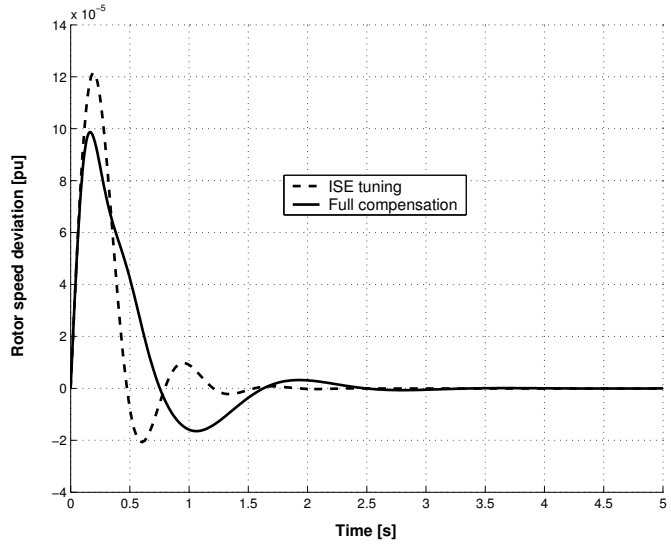

Figure 2.14 Performance of SMIB system with optimal lead-lag PSS

Further, the phase compensation characteristics (Figure 2.15) drawn from the two optimal PSS settings previously obtained are examined.

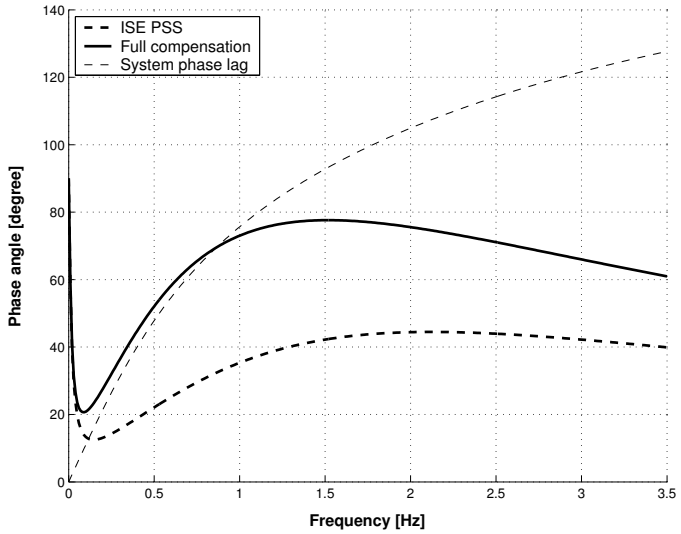

Figure 2.15 Phase characteristics for systems and different PSS designs

While the phase compensation technique closely compensates for the *GEP*(*s*) phase lag up to a frequency of 1 Hz, the system phase-lag is considerably under-compensated when the optimal parameters from Lyapunov's method PSS are used.

2.4 Analysis of a Multi-Machine Power System with Lead-Lag PSS

2.4.1 Composite Model

The representation of the multi-machine system without PSS has been discussed earlier, and a state-space model was developed. In this section, the state-space model for the same system considering that all generators are equipped with a lead-lag type PSS is developed.

For the sake of clarity, the state-space model of the multi-machine system without PSS is re-stated below:

$$\frac{d}{dt}\underline{\mathrm{X}}(t) = \mathbf{A}\cdot\underline{\mathrm{X}}(t) + \mathbf{B}\cdot\underline{\mathrm{U}}(t) + \mathbf{\Gamma}\cdot\underline{\mathrm{p}}(t) \tag{2.17}$$

A, **B** and Γ are the state, control and perturbation matrices and have been described in Section 9.3.1. The associated state, control and perturbation vectors are given below:

$$\underline{X}(t) = [\Delta\omega_1(t) \quad \Delta\delta_1(t) \quad \Delta E'_{q1}(t) \quad \Delta E_{fd1}(t) \ldots$$
$$\Delta\omega_2(t) \quad \Delta\delta_2(t) \quad \Delta E'_{q2}(t) \quad \Delta E_{fd2}(t) \ldots$$
$$\Delta\omega_3(t) \quad \Delta\delta_3(t) \quad \Delta E'_{q3}(t) \quad \Delta E_{fd3}(t)]^T$$

$$\underline{U}(t) = [\Delta u_1(t) \quad \Delta u_2(t) \quad \Delta u_3(t)]^T \qquad \underline{p}(t) = [\Delta T_{m1} \quad \Delta T_{m2} \quad \Delta T_{m3}]^T$$

The control vector $\underline{U}(t)$ is a vector of stabilizing signals that represents the PSS output at different machines.

The dynamic equations of the PSS in state-space form, as obtained from the transfer function block-diagram, are given below:

$$\frac{d}{dt}(\Delta N_{1i}(t)) = K_C \frac{d}{dt}(\Delta\omega_i) - \frac{\Delta N_{1i}(t)}{T_{W_i}}$$
$$\frac{d}{dt}(\Delta N_{2i}(t)) = \left[\Delta N_{1i}(t) - \Delta N_{2i}(t) + T_1 \frac{d}{dt}(\Delta N_{1i}(t))\right] \cdot \frac{1}{T_{2i}} \qquad (2.18)$$
$$\frac{d}{dt}(\Delta u_i(t)) = \left[\Delta N_{2i}(t) + T_{3i} \frac{d}{dt}(\Delta N_{2i}(t)) - \Delta u_i(t)\right] \cdot \frac{1}{T_{4i}}$$
$$\forall\ i = 1,2,3$$

where ΔN_{1i} and ΔN_{2i} are the state-variables associated with each PSS, T_W is the *washout* time constant, $T_1, \ldots, T_4$ are the *phase-lead* time constants and K_C is the stabilizer *gain*. Equations (2.18) above may be arranged in standard vector-matrix form as shown in (2.19), which represents the state-space model of the system with PSSs at all machines:

$$\frac{d}{dt}\underline{X}_{PSS}(t) = \mathbf{C} \cdot \underline{X}(t) + \mathbf{D} \cdot \underline{X}_{PSS}(t) + \mathbf{\Gamma}_1 \cdot \underline{p} \qquad (2.19)$$

where

$$\underline{X}_{PSS}(t) = [\Delta N_{11}(t) \quad \Delta N_{21}(t) \quad \Delta u_1(t) \ldots$$
$$\Delta N_{12}(t) \quad \Delta N_{22}(t) \quad \Delta u_2(t) \ldots$$
$$\Delta N_{13}(t) \quad \Delta N_{23}(t) \quad \Delta u_3(t)]^T$$

C, **D** and Γ_1 are the matrices associated with the PSS model with appropriate dimensions, and are given in the Section 9.3.2.

By defining the following augmented state-vector

$$\underline{X}_C(t) = [\underline{X}(t) \quad \underline{X}_{PSS}(t)]^T$$

the state-space model of the closed-loop system becomes:

$$\dot{\underline{X}}_C(t) = \mathbf{A}_C \cdot \underline{X}_C(t) + \mathbf{\Gamma}_C \cdot \underline{p} \tag{2.20}$$

where $\mathbf{A}_C = \begin{bmatrix} \mathbf{A} & \mathbf{B}_1 \\ \mathbf{C} & \mathbf{D} \end{bmatrix}$ and $\mathbf{\Gamma}_C = \begin{bmatrix} \mathbf{\Gamma} \\ \mathbf{\Gamma}_1 \end{bmatrix}$

$\mathbf{B}_1$ in $\mathbf{A}_C$ is a re-defined control matrix, with $\underline{b}_1$, $\underline{b}_2$, $\underline{b}_3$ the column vectors of **B**.

$$\mathbf{B}_1 = [\ \underline{0}\ \ \underline{0}\ \ \underline{b}_1\ \ \underline{0}\ \ \underline{0}\ \ \underline{b}_2\ \ \underline{0}\ \ \underline{0}\ \ \underline{b}_3\ ]$$

By applying the coordinate transformation in the state-space given in (2.21), the perturbation term in (2.20) can be eliminated.

$$\underline{X}'(t) = \underline{X}_C(t) - \underline{X}_C(\infty) \tag{2.21}$$

Hence, (2.20) reduces to the standard state-variable form:

$$\dot{\underline{X}}'(t) = \mathbf{A}_C \cdot \underline{X}'(t) \tag{2.22}$$

where $\underline{X}'(0) = -\underline{X}(\infty) = -\mathbf{A}_C^{-1} \cdot \mathbf{\Gamma}_C \cdot \underline{p}$ is the initial state of $\underline{X}'(t)$, which is also the steady-state value of $\underline{X}(t)$.

2.4.2 Lyapunov Method Based Optimization of Lead-Lag PSS for Multi-Machine Power Systems

Section 2.3.3 provides the details of the method of PSS parameter optimization using Lyapunov's method. In this section, the analysis is extended in a similar manner, to find the optimal parameters of PSS in a multi-machine system. In this case also, the perturbation of 1% step increase in the mechanical torque is applied at shaft of Generator 1.

One important aspect associated with PSS tuning in multi-machine systems is the problem of siting of PSS on appropriate machines. This is required in order to find those critical machines where a PSS optimally tuned would damp out specific modes. This helps reduce the computational burden, particularly in case of large systems. A lot of work addressing the siting problem has been already reported in literature [12], [14], [15], [58]. In this chapter, and in the thesis as well, this issue has not been addressed.

Conventionally, the PSS tuning methods used for multi-machine systems have either used a sequential approach or a simultaneous approach. The sequential tuning approach is computationally simple, but introduces an undesired phenomenon – termed as *eigenvalue drift*, which will be pinpointed later – while the simultaneous tuning approach though being very complex to handle, particularly for large systems, does provide the optimal solution.

In the following analysis, the Lyapunov method was applied to multi-machine PSS tuning using the sequential approach.

The weighing matrix **Q** is now the sum of the squares of each machine's power angle deviation from their respective steady-state value.

Thus

$$\mathbf{Q} = diag[0\ \ 1\ \ 0\ \ 0\quad 0\ \ 1\ \ 0\ \ 0\quad 0\ \ 1\ \ 0\ \ 0]$$

and

$$J = \int_0^{\infty} \sum_{i=1}^{3} (\Delta\delta_i - \Delta\delta_{i_{SS}})^2 dt \tag{2.23}$$

Using the approach described in Section 2.3.3, the parameters of each PSS can be obtained through a sequential optimization approach. Various combinations of tuning sequences were tried out and the best system performance was obtained with Gen-1–Gen-2–Gen-3 sequence. Table 2.4 provides a detailed report of the behavior of the PSS parameters tuned using the above sequence, and shows the corresponding system eigenvalues during the sequential tuning process. It can be observed how the system eigenvalues keep changing as the tuning sequence progresses – the eigenvalue drift phenomenon. Thus, there is a need to determine the PSS parameters simultaneously while also looking for ways of how to address the problem of increased computational burden arising from such an approach.

Table 2.4 Sequential tuning of multi-machine power systems

Machine	**PSS settings**							
	Step 1: sub-optimal PSS		Step 2: Gen-1 tuned		Step 3: Gen-1 and 2 tuned		Step 4: Gen-1, 2 and 3 tuned	
	T_1 [s]	K_C	T_1 [s]	K_C	T_1 [s]	K_C	T_1 [s]	K_C
1	0.10	3	0.11	73	0.11	73	0.11	73
2	0.10	3	0.10	3	0.16	15	0.16	15
3	0.10	3	0.10	3	0.10	3	0.29	12.5
	Eigenvalues and damping ratios							
	Eigenvalues	Damping	Eigenvalues	Damping	Eigenvalues	Damping	Eigenvalues	Damping
	-0.0555 ± j15.6009	0.0036	-0.1357 ± j15.4128	0.0088	-0.0555 ± j15.6009	0.0036	-1.8970 ± j5.0133	0.3539
	-0.1674 ± j0.4693	0.0259	-0.3618 ± j7.5701	0.0477	-0.1674 ± j6.4693	0.0259	-2.1724 ± j13.218	0.1622
	-0.1908 ± j8.2613	0.0231	-2.2198 ± j11.1289	0.1956	-0.1908 ± j8.2613	0.0231	-3.3237 ± j23.4719	0.1402
	-10.1813 ± j3.3373	0.9503	-10.2190 ± j3.3341	0.9507	-10.1813 ± j3.3373	0.9503	-5.1392 ± j8.9380	0.4985
	-10.3332 ± j7.6062	0.8053	-10.4467 ± j7.3496	0.8179	-10.3332 ± j7.6062	0.8053	-5.4933 ± j12.1247	0.4127
	-16.2746 ± j1.6007	0.9952	-10.5846 ± j4.2205	0.9289	-16.2746 ± j1.6007	0.9952	-10.1550 ± j4.0160	0.9299
	-17.9045	1.0000	- 0.1000	1.0000	- 0.1000	1.0000	- 0.1001	1.0000
	-22.1960	1.0000	- 0.1002	1.0000	- 0.1001	1.0000	- 0.1007	1.0000
	-23.0825	1.0000	- 0.1023	1.0000	- 0.1002	1.0000	- 0.1025	1.0000
	-23.9450	1.0000	- 2.7481	1.0000	- 4.6823	1.0000	- 2.7223	1.0000
	- 0.1000	1.0000	-15.7679	1.0000	-15.7824	1.0000	- 6.5977	1.0000
	- 0.1001	1.0000	-17.6073	1.0000	-17.9045	1.0000	-11.4036	1.0000
	- 0.1002	1.0000	-22.7811	1.0000	-22.1960	1.0000	-31.0425	1.0000
	- 4.6823	1.0000	-23.9223	1.0000	-23.0825	1.0000	-32.0547	1.0000
	-15.7824	1.0000	-31.2342	1.0000	-23.9450	1.0000	-41.8136	1.0000

2.4.3 Minimum PSS

Since the system without PSS is not stable when subjected to a small perturbation, a *Minimum PSS* (MPSS) is first determined. MPSS shall be referred to as being that set of PSS parameters for which the system is stable with a minimum control action from PSS. Evidently, the MPSS is a sub-optimal solution, and hence any optimal PSS would provide a better performance. Figure 2.16 shows the three generators' rotor angle deviations for the MPSS (K_{Ci} = 3.0, T_{1i} = 0.1 s).

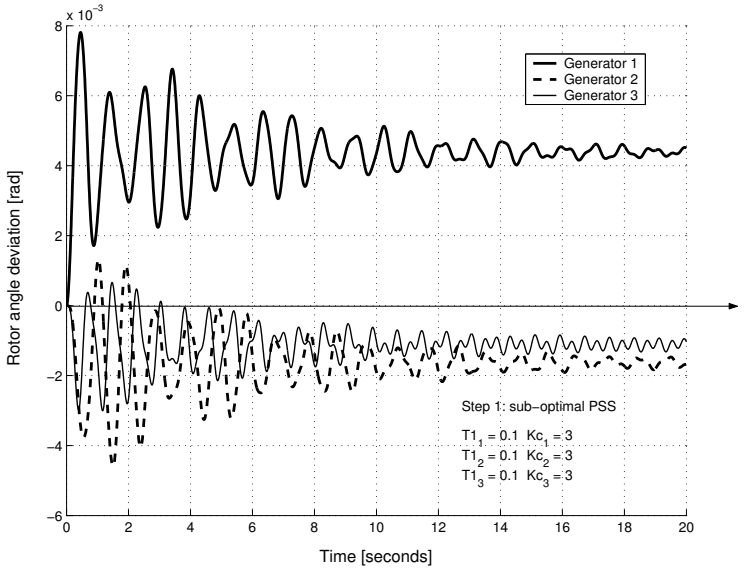

Figure 2.16 System dynamic performance with the minimum PSS

Alternatively, the rotor angle deviations of the generators with the sequentially tuned PSS (as given in Table 2.4) are shown in Figure 2.17, and reveal a superior performance, reaching a quasi-steady state in about 2 seconds, as opposed to MPSS, for which, even after 20 seconds, the system has not attained a steady-state.

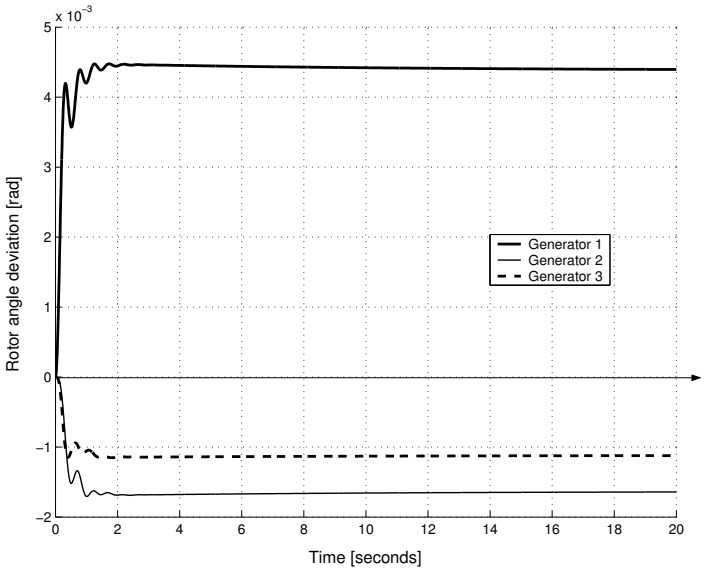

Figure 2.17 System dynamic performance with the optimal PSS

2.5 Concluding Remarks

This chapter presents the details of mathematical models required for the analysis of small-signal stability for both single machine connected to infinite bus and multi-machine systems. The mathematical models are in the state-space form, thereby making the application of linear analysis possible. As has been demonstrated, both systems are unstable under small perturbations and require additional stabilizing control from the power system stabilizer, the design of which will be treated in the following chapters.

This chapter presents the development of a composite state-space model of the system including the lead-lag power system stabilizer (PSS). Phase characteristics of the system as well as the PSS have been investigated and a method for tuning of PSS parameters based on exact phase compensation has been presented. It is found that for desirable system performance, a full phase compensation may not be necessary.

Subsequently, a method based on Lyapunov's parameter optimization has been presented for tuning of lead-lag PSS. This method makes use of the ISE criterion with an objective of minimizing the power angle deviation from its steady-state value. System dynamic performance for single-machine to infinite bus, as well as a multi-machine system, show that this method provides superior responses as compared to the phase-compensation technique based PSS.

Due to the eigenvalue drift phenomenon and the high computational burden required for simultaneous type of tuning approach, genetic algorithm based simultaneous tuning methods have a promising research scope and could address many of the concerns raised in large scale PSS parameter tuning.

3 GENETIC ALGORITHM BASED TUNING OF PSS

This chapter proposes a genetic algorithm (GA) based method to tune the parameters of a power system stabilizer (PSS). The proposed method integrates the classical parameter optimization approach, involving the solution of Lyapunov equation, within a genetic search process. The method ensures that for any operating condition within a pre-defined domain, the system remains stable when subjected to small perturbations. The optimization criterion employs a quadratic performance index that measures the quality of system dynamic response within the tuning process. The solution thus obtained is globally optimal and robust. The proposed method has been tested on two different PSS structures, namely the lead-lag and the derivative type. System dynamic performances with PSS tuned using the proposed technique are satisfactory for different load conditions and system configurations.

Keywords: small-signal stability, GA, PSS, Lyapunov method, ISE technique

3.1 General Aspects

Genetic Algorithms are global search techniques providing a powerful tool for optimization problems by miming the mechanisms of natural selection and genetics. These operate on a population of potential solutions applying the principle of *survival of the fittest* to produce better and better approximations to a solution. In each generation, a new set of approximations is created by selecting the individuals according to their level of fitness in the problem domain and breeding them together using operators borrowed from natural genetics [59]. Thus, the population of solutions is successively improved with respect to the search objective by replacing least fit individuals with new ones (offspring of individuals from the previous generation), better suited to the environment, just as in natural evolution.

According to Goldberg [59], GAs are different from other optimization and search procedures in four ways:

a) GA work with a coding of the parameter set, not the parameters themselves.
b) GA search from a population of points, not a single point.
c) GA use payoff information, not derivatives or other auxiliary knowledge.
d) GA use probabilistic transition rules, not deterministic rules.

Figure 3.1 shows a schematic diagram of a genetic algorithm. The process commences with random generation of a pool of possible solutions, *i.e.* the population and the individuals that form it. Each individual in the population, also called *chromosome* is represented by a string, which is formed by a number of sub-strings equal to the number of the problem's variables. Each variable is coded in a suitable coding system (binary, integer, real-valued, *etc*). The population size and the chromosome size are kept constant during the whole search process.

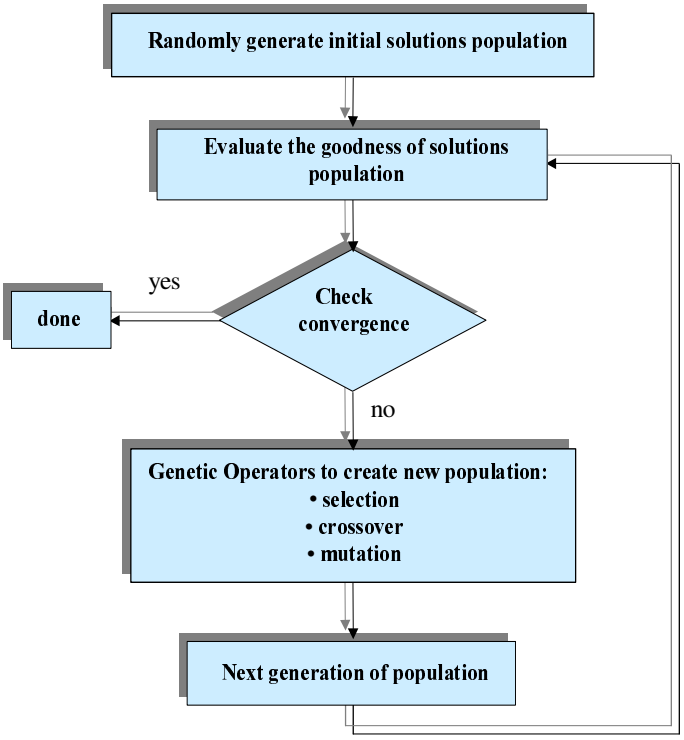

Figure 3.1 Genetic Algorithm flowchart

The performance of each individual in the population is evaluated through an objective function, which models the dynamic problem and has as output a *fitness value.* The fitness value is a measure of how good the respective individual is with respect to the problem objective.

Individuals will be selected in accordance with their fitness value to take part in the genetic process. The purpose of *selection* is to keep the best well-fit individuals and increase the number of their offspring in the next generation, on the account of the least fit individuals.

The *recombination* process consists in the grouping of the selected individuals in pairs (parents) in which they exchange genetic information forming two new individuals (children or offspring). This process helps the optimization search to escape from possible local optima and search different zones of the search space. A *mutation* genetic operator that replaces allele of genes is implemented to increase the probability of complete search, by allowing the investigations in vicinity of local optima.

Reinsertion is the process in which children will populate the next generation by replacing parents. Reinsertion can be made partially or completely, uniformly (offspring replace parents uniformly at random) or fitness-based.

All genetic operators are implemented with a certain predefined probability.

Power System Stabilizers designed using the GA based search and optimization are more likely to converge to a global optima than a conventional optimization based PSS, since they search from a population of possible solutions, and are based on probabilistic transition rules.

Fixed-structure lead-lag type of power system stabilizers discussed in Chapter 2 have found practical applications and these generally provide acceptable dynamic performances [9]. There have been arguments that these controllers, being tuned for one nominal operating condition, provide sub-optimal performance when there are variations in system operating load or system configuration. To address this issue, PSS parameter tuning methods that incorporate robustness within the optimization scheme and are applicable to fixed structure stabilizers are desirable. To ensure a sufficiently robust behavior, a wide operating domain need be considered in the tuning process.

The present chapter proposes an application of the Lyapunov parameter optimization criterion within a GA search framework, in which each individual in the population represents a possible solution to the problem, *i.e.* a coding of PSS parameter setting. In order to evaluate the degree of *goodness* of an individual within the population, a quadratic performance index that measures the quality of system dynamic performance, is employed within the objective function of the tuning process. Thus, the performance of each individual in the population is assessed, and a *fitness value* comprising a dynamic evaluation of the system is assigned. The selected individuals are then modified through the application of *genetic operators*, in order to obtain the next generation. The proposed method ensures that for any operating condition within a pre-defined domain, the system with the optimally tuned PSS remains stable when subjected to small perturbations. The solution obtained is globally optimal and

robust. The proposed method has been tested on two different PSS structures: the lead-lag and derivative types.

3.1.1 Genetic Algorithm Specifications and the Proposed Method

The proposed Lyapunov method based genetic algorithm is initiated by generating randomly an initial population of binary coded individuals, where each individual represents a possible solution for the PSS parameters.

A basic requirement for obtaining a feasible solution to the Lyapunov equation is that the state-matrix **A** should be stable. Fulfillment of this condition is ensured by *stability screening*. The entire population of individuals in each generation is screened (Figure 3.2) in order to ensure that only those individuals (each of them representing a PSS parameter set) that provide a stable system over the whole operating domain *D*, are allowed to proceed further in the optimization process. This also brings about significant reduction in the computational burden. Individuals resulting in unstable systems for an operating point within the domain *D* ("bad individuals") are assigned a very high value of J_{AVG}, where J_{AVG} is the mean value of performance indices over the N_{op} points of the operating domain *D*, and given by (3.1). The bad individuals are gradually phased out from the population within a few generations.

$$J_{AVG} = \frac{1}{N_{op}} \cdot \sum_{P,Q} \left(\int_0^{\infty} (\underline{X}^T \cdot \mathbf{Q} \cdot \underline{X})\, dt \right) \qquad \forall\, P,\, Q \in D \tag{3.1}$$

Every individual (*chromosome*) of the current population is evaluated for J_{AVG} and a basis for the biased selection process is then established. To avoid premature convergence and speeding up of the search when the convergence is approached, the objective values obtained for each individual are mapped into *fitness values* through a ranking process. The rank-based fitness assignment overcomes the scaling problems of the proportional fitness assignment. The individuals will be ranked in the population in descending order of their fitness with respect to the problem domain. The higher the individual's fitness is, the higher is its chance to pass-on genetic information to successive generations.

The next generation will be populated with offspring, obtained from selected parents. The *selection* is a process used to determine the number of trials for one particular individual used in reproduction. The selection process uses the *stochastic universal sampling* method, a single-phase sampling algorithm with minimum *spread*, zero *bias* and time complexity in the order of the number of individuals (N_{IND}).

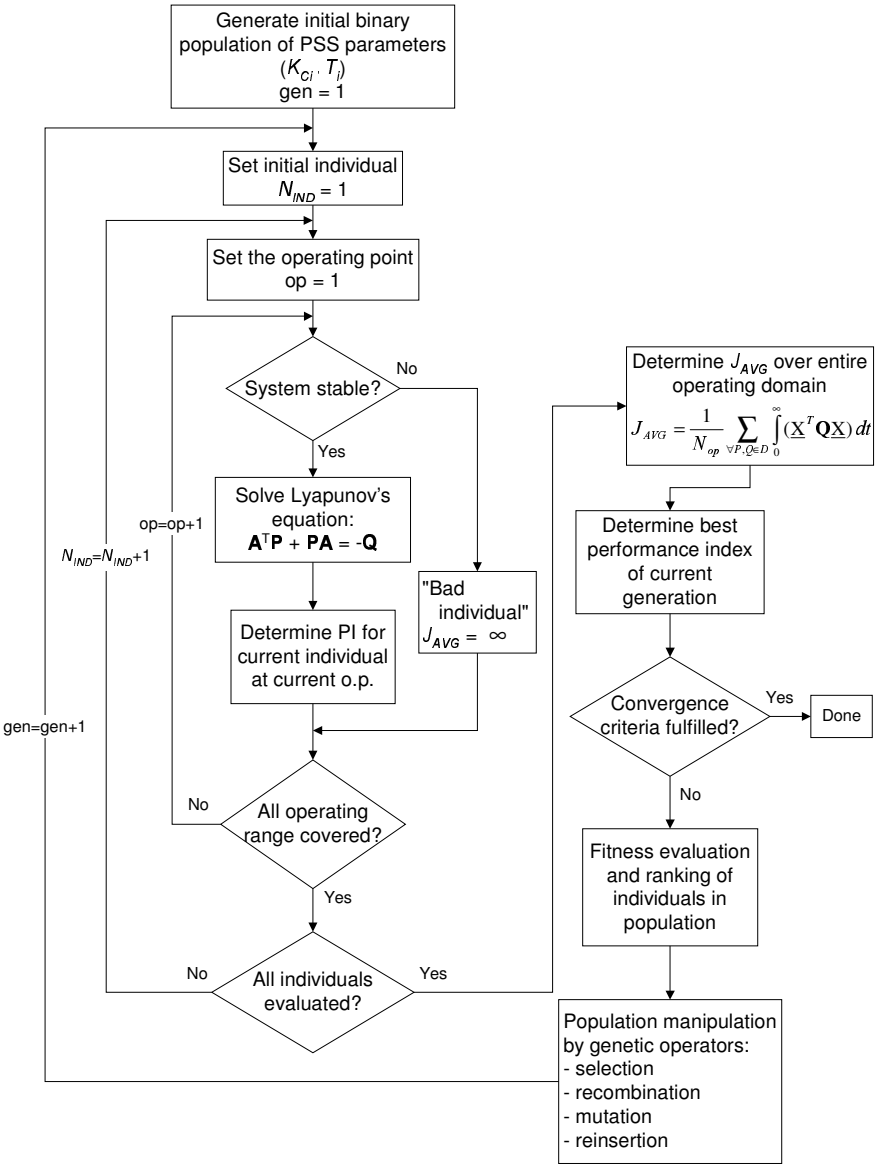

Figure 3.2 Lyapunov Method Based Genetic Algorithm for PSS Tuning

Recombination of the selected individuals is carried out with pairs of individuals from the current population using a *multi-point crossover* process having a certain probability. The individuals in the pairs will exchange genetic information with each other, thereby creating two new individuals, the offspring. After that, each individual in the population will be *mutated* with a given probability, through a random process of replacing one allele of a gene with another to produce a new genetic structure.

The GA employed in this study uses an *elitist strategy,* in which the offspring is created with a *generation gap* of 80% and reinserted in the old population by replacing the least fit predecessors. Most fit individuals are allowed to propagate through successive generations and only a better individual may replace them.

The GA stops when a pre-defined maximum number of generations is achieved or when the value returned by the objective function, being below a threshold, remains constant for a number of iterations.

3.2 Mathematical Model of the System

Two types of PSS have been considered for analysis: (a) the lead-lag PSS (3.2) with gain K_C, time-constants T_1 and T_2, and wash-out filter time-constant T_W, and (b) the derivative PSS (3.3) with gain K_d and time constant T.

$$u(s) = K_c \cdot \frac{sT_W}{1+sT_W} \cdot \left(\frac{1+sT_1}{1+sT_2}\right) \cdot \left(\frac{1+sT_1}{1+sT_2}\right) \cdot \Delta\omega(s) \tag{3.2}$$

$$u(s) = K_d \cdot \frac{sT}{(1+sT)} \cdot \frac{T}{(1+sT)} \cdot \Delta T_e(s) \tag{3.3}$$

As discussed in Chapter 2, T_W is the washout time-constant, which is used to washout dc signals and without it, steady changes in speed would modify the terminal voltage. To guarantee the lead characteristic of the control signal, T_2 is kept at a minimum physically achievable (T_2 = 0.05 seconds). Thus, the lead-lag PSS parameters to be optimized are K_C and T_1.

It is important to note here the difference in input signals to the two PSS. The phase-lead PSS is based on the commonly used rotor speed deviation input signal as shown in (3.2). On the other hand, the derivative PSS given in (3.3) is based on electrical torque deviation signal ΔT_e. The parameters to be tuned in the later case are the derivative gain K_d and the time constant T.

The linear dynamic model of the composite system inclusive of excitation system and PSS on all generators can be obtained in a similar manner to the one outlined in Chapter 2, and its state-space representation is given below:

$$\frac{d\underline{X}(t)}{dt} = \mathbf{A} \cdot \underline{X}(t) + \mathbf{\Gamma} \cdot \underline{p} \tag{3.4}$$

A and Γ are the state and perturbation matrices and depend on the system configuration and operating conditions, while $\underline{X}$ and $\underline{p}$ are state and perturbation vectors, respectively.

In order to eliminate the perturbation term in (3.4) and reduce the system model to the standard closed-loop state-space form, a coordinate transformation in the state-space is applied as given by:

$$\underline{X}' = \underline{X} - \underline{X}(\infty) \tag{3.5}$$

The resulting state-transformed system model thus obtained is given by:

$$\frac{d}{dt}\underline{X}' = \mathbf{A} \cdot \underline{X}' \tag{3.6}$$

where $\underline{X}'(0) = -\underline{X}(\infty) = -\mathbf{A}^{-1}\,\mathbf{\Gamma} \cdot \underline{p}$ is the steady state value of $\underline{X}'(t)$.

3.3 Single Machine Connected to Infinite Bus

The proposed genetic algorithm based approach applying the classical Lyapunov stability and parameter optimization technique is now used to determine the optimal parameters of a PSS that is robust over a wide operating domain. For the purpose of these study cases, an operating domain D (P = [0.3, 1.3] and Q = [-0.3, 1.0], in per unit) shall be considered with a step-size of 0.1 p.u. in each case (*i.e.* N_{op} = 154).

Figure 3.3 shows the small perturbation transfer function model of the SMIB system with lead-lag PSS. The state vector $\underline{X}$ and state matrix **A** for the SMIB system equipped with the lead-lag PSS of (3.2) have been provided in Section 2.3.1.

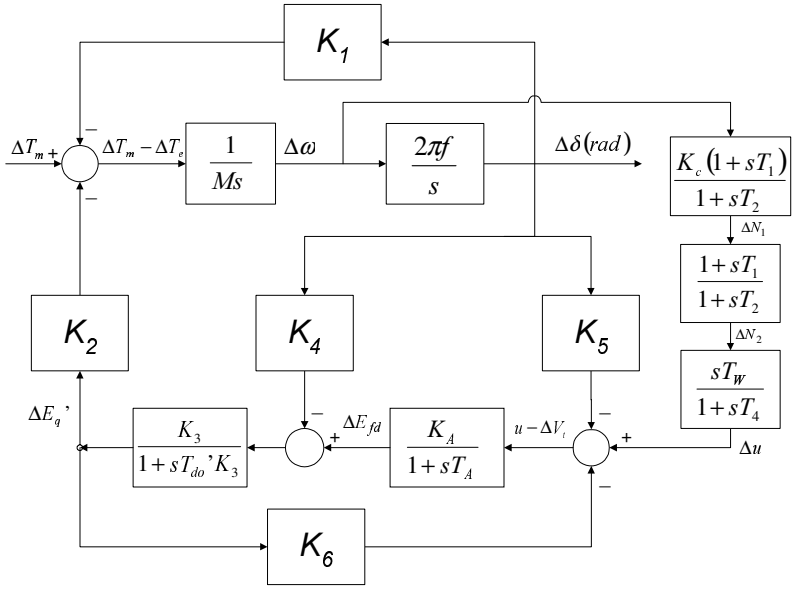

Figure 3.3 Small perturbation transfer function model of SMIB system equipped with lead-lag PSS

Figure 3.4 shows the small perturbation transfer function model of the SMIB system equipped with a derivative PSS.

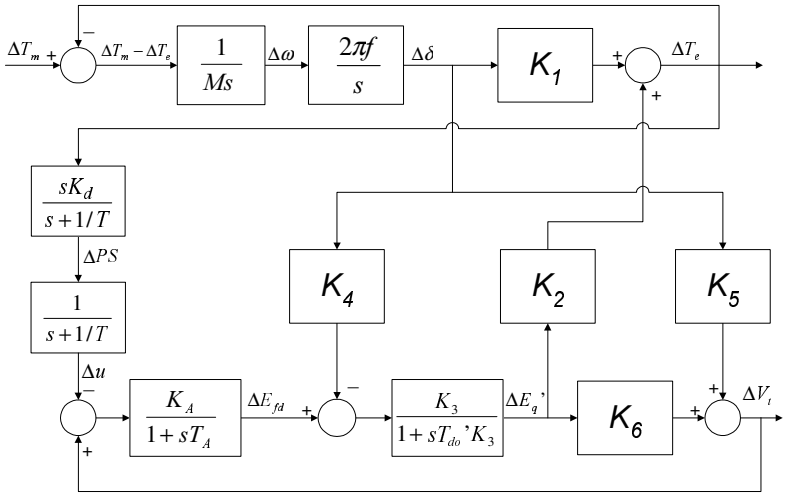

Figure 3.4 Small perturbation transfer function block-diagram of SMIB system equipped with derivative PSS

The state vector of the system can be defined as:

$$\underline{X}(t) = [\Delta\omega \quad \Delta\delta \quad \Delta E_q^{'} \quad \Delta E_{fd} \quad \Delta u]^T \tag{3.7}$$

The system matrix **A** with the derivative type PSS of (3.3) is described by:

$$\mathbf{A} = \begin{bmatrix} 0 & -\frac{K_1}{M} & -\frac{K_2}{M} & 0 & 0 & 0 \\ 2\pi f & 0 & 0 & 0 & 0 & 0 \\ 0 & -\frac{K_4}{T_{do}^{'}} & -\frac{1}{K_3 \cdot T_{do}^{'}} & \frac{1}{T_{do}^{'}} & 0 & 0 \\ 0 & -\frac{K_A \cdot K_5}{T_A} & -\frac{K_A \cdot K_6}{T_A} & -\frac{1}{T_A} & 0 & -\frac{K_A}{T_A} \\ 0 & \frac{K_d}{K_1} & \frac{K_d}{K_2} & 0 & -\frac{1}{T} & 0 \\ 0 & \frac{K_d}{K_1} & \frac{K_d}{K_2} & 0 & -\frac{1}{T} & -\frac{1}{T} \end{bmatrix} \tag{3.8}$$

3.3.1 Analysis

The optimal parameters for both lead-lag and derivative PSSs obtained with the proposed GA based method are compared with the optimal parameters setting obtained by applying the ISE Technique earlier reported in [60], that was obtained considering one nominal operating condition.

Additionally, for the derivative PSS, the set of optimal parameters obtained with the proposed GA based method is also compared with an earlier reported eigenvalue shift based GA method [61].

Figure 3.5 depicts the tuning process of a derivative PSS in a SMIB system performed using a sequential method, in a similar manner as described in Section 2.3.3.2 for the lead-lag PSS.

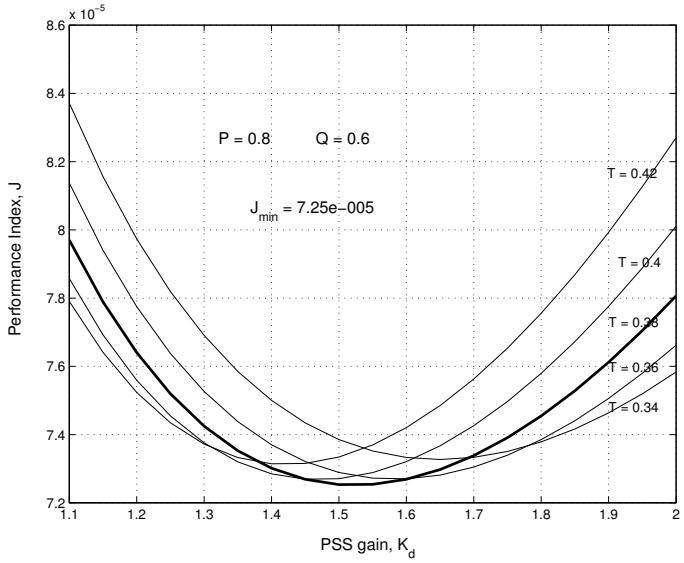

Figure 3.5 Performance index as function of PSS gain K_d, for different time constants T

Table 3.1 provides a summary of the PSS parameters for the lead-lag PSS, along with the corresponding system eigenvalues, and for the oscillatory modes the damping factors ζ and natural frequencies f_n. The ISE technique based PSS [60] achieves a fairly robust optimum parameter set that is very close to the global optimal set obtained using the GA based method. J_N and $J_{AVG,N}$ are the corresponding values of J and J_{AVG}, respectively, *normalized* with respect to the best, and provide a quantitative measure of the quality of dynamic performance with a particular type of PSS and PSS settings.

Table 3.1 Optimal parameter setting for lead-lag PSS obtained with two different methods

	No PSS	**Proposed GA based method**			**ISE technique [60]**		
Gain and Time constant	–	33.98 0.12			38.65 0.11		
Eigenvalues at nominal operating point, ξ, f_n [Hz]	-14.298, - 6.371 0.103 ± j 5.5	-30.964 -3.888 ± j7.773 -8.472 ± j5.003 -4.777 -0.102	– 0.43 0.86 – –	– 1.380 1.566 – –	-30.461 -3.196 ± j8.471 -9.901 ± j3.928 - 3.806 - 0.102	– 0.35 0.93 – –	– 1.441 1.695 – –
J_N **at nominal operating point**	–	1.008			**1.0**		
$J_{AVG,N}$	–	**1.0**			1.01		

Table 3.2 shows the optimal settings for derivative PSS, and the corresponding-eigenvalues and performance indices. For convenience, the performance indices are normalized with respect to the best (see Table 3.1). The proposed GA based method, though with $J_{AVG,N}$ of 4.72, does provide a fairly satisfactory dynamic performance, while the eigenvalue shifting method based PSS with $J_{AVG,N}$ of 24 provides a much inferior response. Note that although ISE Technique based PSS performs better at the nominal operating point than the genetically tuned systems, the system thus tuned will not be stable for the entire operating domain *D*.

Table 3.2 Optimal parameter setting for derivative PSS obtained with three different methods

	No PSS	**Proposed GA based method**	**GA based Eigenval. shift. techn. [61]**	**ISE Technique [60]**
Gain and Time constant	–	2.03 0.30	6.47 0.34	1.55 0.38
Eigenvalues at nominal operating point	-14.298 - 6.371 0.103 ± j 5.50	-16.823 -1.357 ± j5.33 -2.756 ± j4.62 -2.081	-19.417 -1.959 ± j9.210 -0.726 ± j2.892 -1.56	-16.225 -0.877 ± j5.759 -2.981 ± j3.248 -1.7857
J_N at nominal operating point	–	4.97	21.33	4.69
$J_{AVG,N}$	–	4.72	24.0	–

Figure 3.6 and Figure 3.7 show the distribution of J_{AVG} for individuals in the population and their convergence to the global optimum during the search process, for two different PSS types – the lead-lag and the derivative PSS, respectively. It is evident that the best individual from a generation progresses towards convergence, corresponding to the minimum of J_{AVG} and thereby providing the optimal values of PSS parameters. The figures provide an image of the distribution of possible solutions cumulatively obtained during the genetic search, thus emphasizing the algorithm's convergence towards the global optimum and intuitively pinpointing the same.

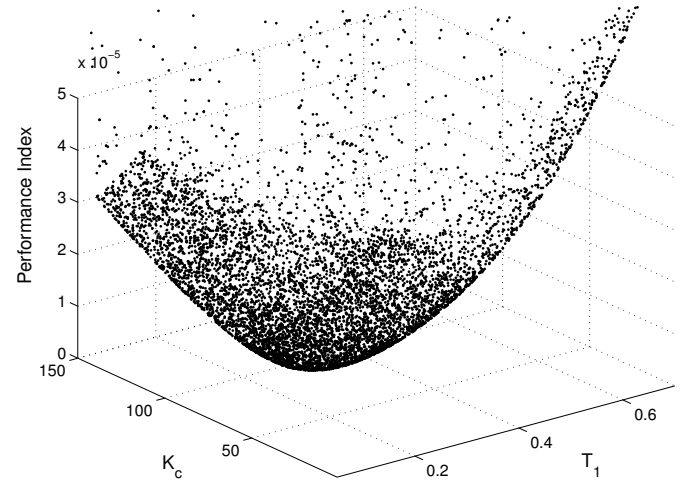

Figure 3.6 Distribution of the solution during the search process for lead-lag PSS

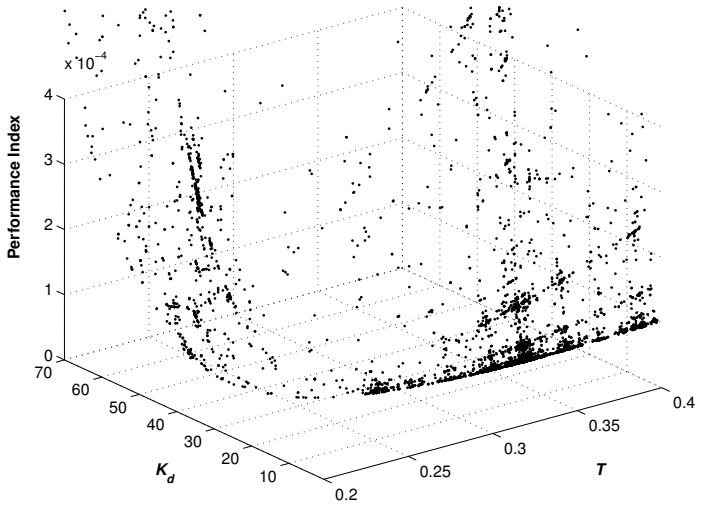

Figure 3.7 Distribution of the solution during the search process for derivative PSS

It should be noted that, the vertical axis denoting the performance J_{AVG}, appears with a different scale for the two PSS cases- the derivative PSS scale being of the order of 10^{-4}, while the lead-lag PSS is of the order of 10^{-5}.

Figure 3.8 shows that J_{AVG} decreases monotonously with the number of generations, and in approximately 50 generations, the optimization process finds a solution that remains unchanged thereafter, and J_{AVG} reaches a steady

minimum value. These results were obtained with a genetic process over 160 generations and having a population of 50 individuals.

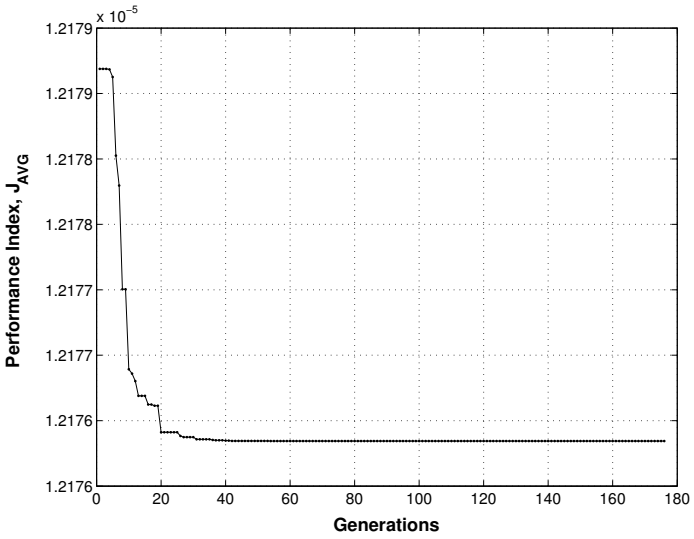

Figure 3.8 J_{AVG} of best individual for each generation

Figure 3.9 shows the corresponding PSS parameters variation during the genetic process, and indicates their convergence to the optimal value.

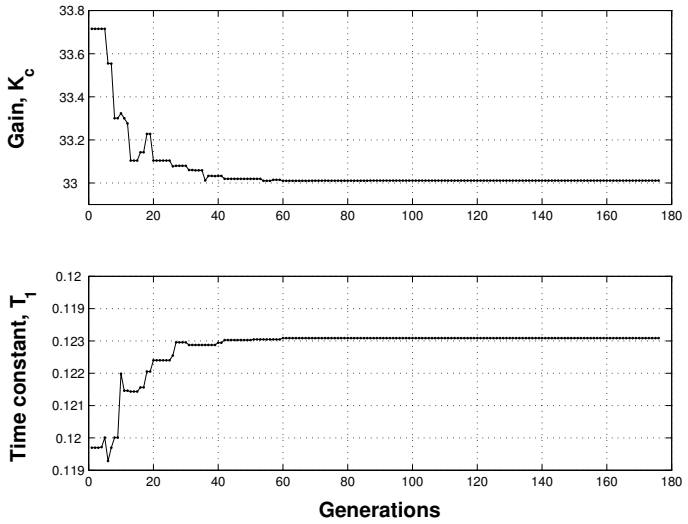

Figure 3.9 PSS parameter variation during genetic process, for each generation

Figure 3.10 and Figure 3.11 show the distribution of the positive imaginary part of system eigenvalues over the entire operating domain *D*, for optimum parameter settings of lead-lag PSS and derivative PSS, respectively. It can be seen that the lead-lag PSS provides a more stable system since its eigenvalues are further away from the imaginary axis vis-à-vis the derivative PSS.

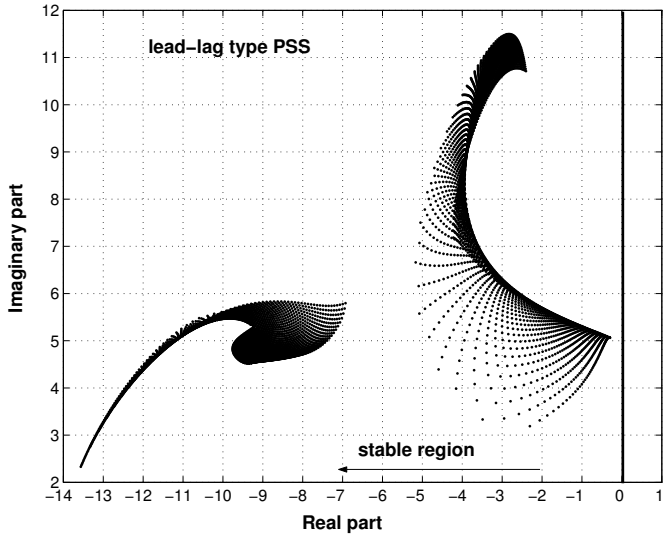

Figure 3.10 Distribution of system eigenvalues with optimal lead-lag PSS over the operating domain

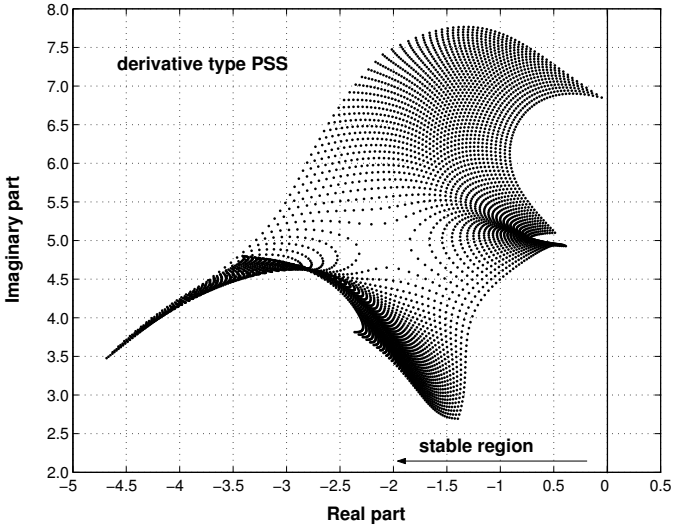

Figure 3.11 Distribution of system eigenvalues for optimal derivative PSS over the operating domain

The optimum parameters obtained using the proposed method, which is based on measurement of system dynamic performance in time-domain, is now compared with an earlier reported GA based PSS [61], in which a frequency-domain approach that applies eigenvalue shifting technique is used. Understandably, the addition of an optimally tuned PSS enlarges the stability region on the *P*-*Q* plane considerably. The lead-lag PSS tuned using the proposed GA based method provides the largest stability region (the entire dot-marked region in Figure 3.12). It is to be noted that this stability region is considerably larger than the domain actually considered for the GA based optimization (shown by the rectangular box).

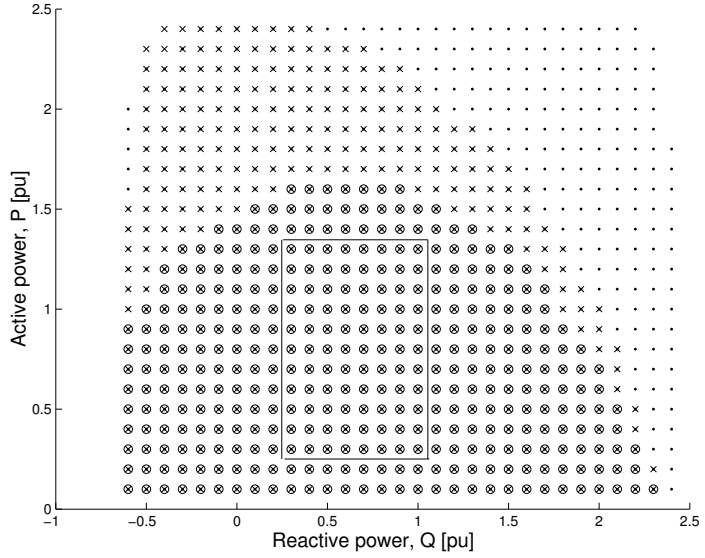

Figure 3.12 Stability regions on the *P*-*Q* plane with different PSS designs

Also shown in Figure 3.12 are the corresponding stability regions with the derivative PSS tuned using the proposed GA based method (shown by o-marks), and when tuned using the eigenvalue shifting method of [61], [58] (shown by x-marks).

3.3.2 System Dynamic Performances

Performance of the PSS with optimum parameters obtained using the proposed method was examined through dynamic analysis for various system loading conditions (heavy, nominal and light), small perturbations, as well as large faults. Figure 3.13 and Figure 3.14 show the comparative performances of lead-lag and derivative PSS, respectively, for different load conditions when subjected to one per cent change in mechanical torque. The system behaved

satisfactorily with both PSS for light and nominal load conditions. However, during heavy load, the settling time of the oscillations is considerably shorter and the overall performance is better with the lead-lag PSS.

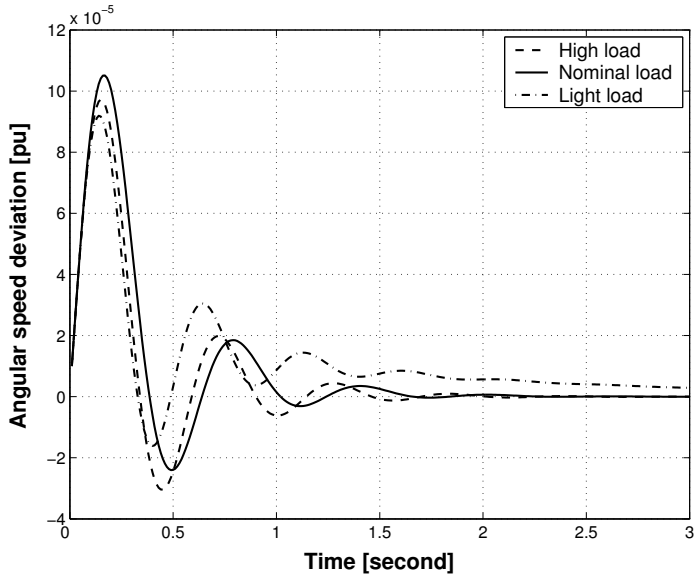

Figure 3.13 System performance under small perturbation for lead-lag PSS tuned using the proposed GA based method

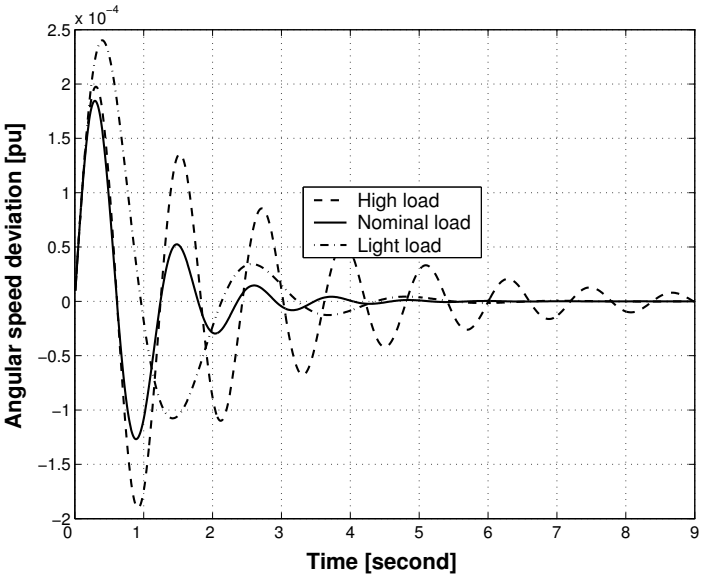

Figure 3.14 System performance under small perturbation for derivative PSS tuned using the proposed GA based method

Further, comparing dynamic performance of the lead-lag PSS obtained using the proposed GA based method with two different PSS parameter sets of derivative type PSS, one obtained using our proposed method (deriv PSS 1 in Figure 3.15) and the other obtained in [61] (deriv. PSS-2 in Figure 3.15), it can be noted that the proposed GA based lead-lag PSS provides considerably superior responses. This behavior was also explained through the comparison of $J_{AVG,N}$ values in Table 3.2.

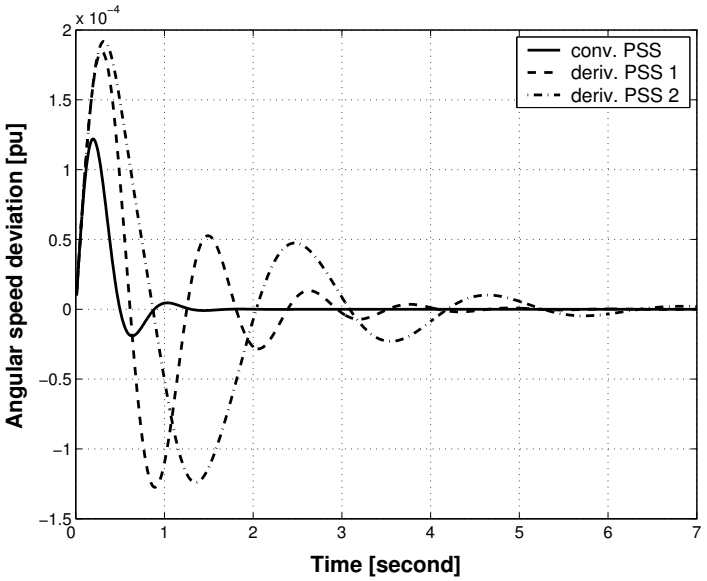

Figure 3.15 Dynamic behavior of lead-lag and derivative type PSS at nominal operating point

Subsequent studies on dynamic performance analysis reported in this chapter are carried out considering the lead-lag PSS only. The system is now tested for a combination of events, commencing with a small perturbation at time t = 0 s, followed by a three-phase short circuit on one of the two parallel lines, very close to the generator bus, at time t = 3 seconds. The short circuit is cleared by the protection system after 0.1 seconds, *i.e.* at time t = 3.1 seconds, by disconnecting the faulted line.

The system dynamic response and the associated PSS output signal with the lead-lag PSS tuned using the proposed GA based method are shown in Figure 3.16, Figure 3.17 and Figure 3.18. It is seen that following the disturbance, the system recovers very satisfactorily, while reaching a new steady state in approximately 6 seconds. It is also to be noted that in order to avoid large excursions in terminal voltages, a signal limiter has now been applied to restrict the PSS output within certain prespecified limits, [-0.1 p.u., 0.2 p.u.], in the present case.

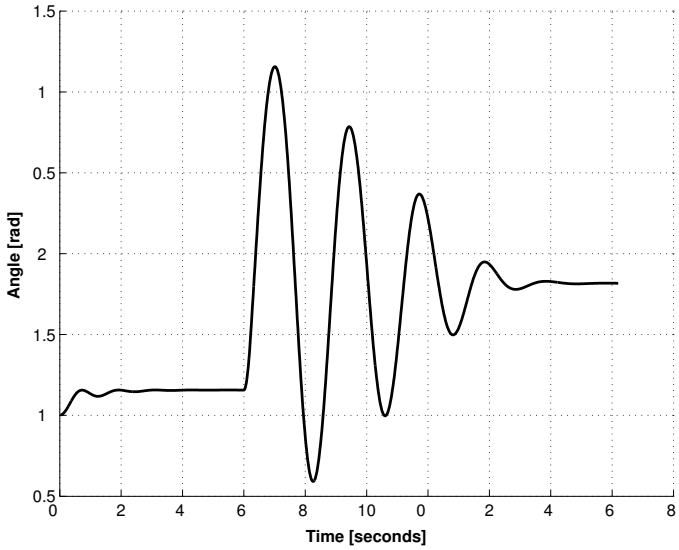

Figure 3.16 Rotor angle deviation for the system with optimal GA based lead-lag PSS during a small perturbation, followed by a three-phase short-circuit and removal of fault

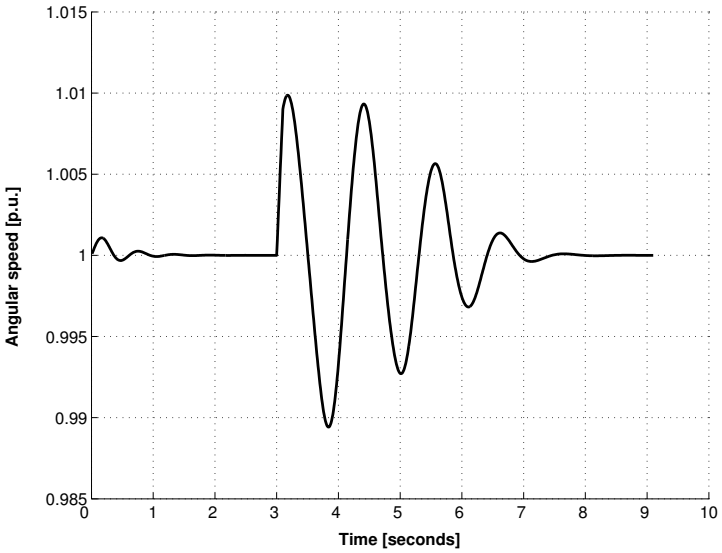

Figure 3.17 Angular speed deviation for the system with optimal GA based lead-lag PSS during a small perturbation, followed by a three-phase short-circuit and removal of fault

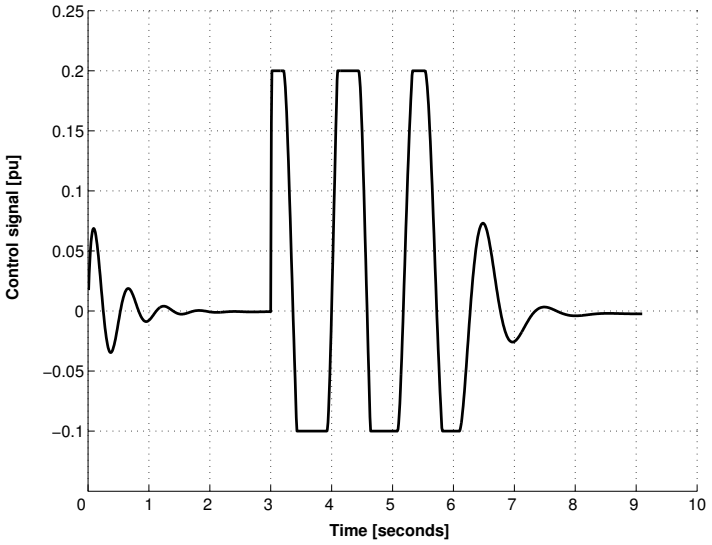

Figure 3.18 Optimal GA based lead-lag PSS output signal during a small perturbation, followed by a three-phase short-circuit and removal of fault

3.4 Multi-Machine Power System

The proposed GA based technique incorporating Lyapunov's parameter optimization criterion is now used to determine the optimal parameters of PSS on the three-machine system described in Section 2.1.1. In order to bring about robustness, a set of six operating points (OP-1 to OP-6) is considered by varying the system loads, Load-A, Load-B and Load-C (see Figure 2.2) in steps. The set of system load conditions considered for the GA based method is presented in Table 3.3.

Table 3.3 The set of six load conditions (in p.u.)

	LC-1	**LC-2**	**LC-3**	**LC-4**	**LC-5**	**LC-6**
Load-A	0.83+j0.55	0.91+j0.61	0.99+j0.67	1.1+j0.73	1.21+j0.81	1.33+j0.97
Load-B	0.44+j0.33	0.48+j0.36	0.53+j0.40	0.59+j0.44	0.64+j0.48	0.71+j0.59
Load-C	0.55+j0.39	0.61+j0.42	0.67+j0.47	0.73+j0.51	0.81+j0.56	0.89+j0.68

Based on the above load conditions, an *optimal power flow (OPF)* with "minimization of losses" as the optimization criterion, is run for each load configuration. The optimal generation schedule so obtained for each unit for each load configuration considered is shown in Table 3.4. This OPF solution is

used as the initial operating condition for the multi-machine system for PSS tuning using the proposed GA based method.

Table 3.4 The OPF solution providing the initial operating conditions

	OP-1	OP-2	OP-3	OP-4	OP-5	OP-6
Gen-1	0.93+j0.16	1.02+j0.24	1.12+j0.33	1.23+j0.43	1.36+j0.54	1.49+j0.67
Gen-2	0.51-j0.04	0.56+j0.02	0.62+j0.08	0.68+j0.14	0.76+j0.22	0.84+j0.31
Gen-3	0.38-j0.14	0.42 -j0.10	0.47-j0.05	0.52+j0.01	0.57+j0.07	0.63+j0.15
V_1	1.04 ∠0°	1.04 ∠0°	1.04 ∠0°	1.04 ∠0°	1.04 ∠0°	1.04 ∠0°
V_2	1.025∠-0°	1.025∠ 0°	1.025∠ 0°	1.025∠ 0°	1.025∠0°	1.025∠ 0°
V_3	1.025∠ 0°	1.025∠ 0°	1.025∠ 0°	1.025∠ 0°	1.025∠0°	1.025∠ 0°
V_5	1.07 ∠-5.6°	0.99 ∠-6.2°	0.99 ∠-6.8°	0.98 ∠-7.6°	0.97 ∠-8.4°	0.95 ∠-9.3°
V_6	1.02 ∠-4.5°	1.02 ∠-4.9°	1.01 ∠-5.4°	1.0 ∠-5.96°	0.99 ∠-6.6°	0.98 ∠-7.3°
V_8	1.02 ∠-4.8°	1.01 ∠-5.3°	1.01 ∠-5.9°	1.0 ∠-6.5°	0.99 ∠-7.2°	0.99 ∠-7.9°

Table 3.5 shows the optimal PSS parameters obtained using the proposed GA based method. For the sake of comparison, the optimal parameters obtained using the ISE technique described in [62] are also presented. The eigenvalues of the closed-loop matrix **A**, for the optimal PSS parameter settings, are also provided. It should be noted that the ISE technique uses a sequential approach to tune the parameters while in the present GA based approach, all PSSs have been tuned simultaneously.

Table 3.5 Optimal PSS parameters using the proposed GA based technique as compared to those obtained using ISE Technique

GA-PSS		**ISE-PSS**	
PSS Parameters (K_C, T_1)	**Eigenvalues**	**PSS Parameters (K_C, T_1)**	**Eigenvalues**
Generator-1: (45.06, 0.17)	-5.93 ± j16.37 -1.54 ± j15.14 -5.78 ± j12.63 -2.19 ± j8.753	Generator-1: (73.0, 0.11)	-3.33 ± j23.48 -1.42 ± j13.11 -2.85 ± j10.41 -9.085 ± j6.63
Generator-2: (45.52, 0.06)	-10.72 ± j2.78 -4.52 ± j5.215 -35.834 -34.191	Generator-2: (15.0, 0.10)	-10.53 ± 4.055 -1.983 ± j5.48 -41.7615 -31.12
Generator-3: (2.13, 0.44)	-24.167 -18.238 -5.0434 -3.1556 -0.1024 -0.1000 -0.1009	Generator-3: (12.5, 0.29)	-26.75 -14.866 -2.69 -6.4069 -0.1025 -0.1001 -0.1007

The average performance index, J_{AVG} (given by (3.1)), of the "best" individual in each generation is selected and plotted over generations to show its convergence rate. Figure 3.19 is an accurate representation of all GA based optimization processes performed during this study, and presents the convergence rate evolution of a population of 40 individuals, during a genetic process of 460 generations. The values of the solution and performance index are presented in Table 3.6, Case 7.

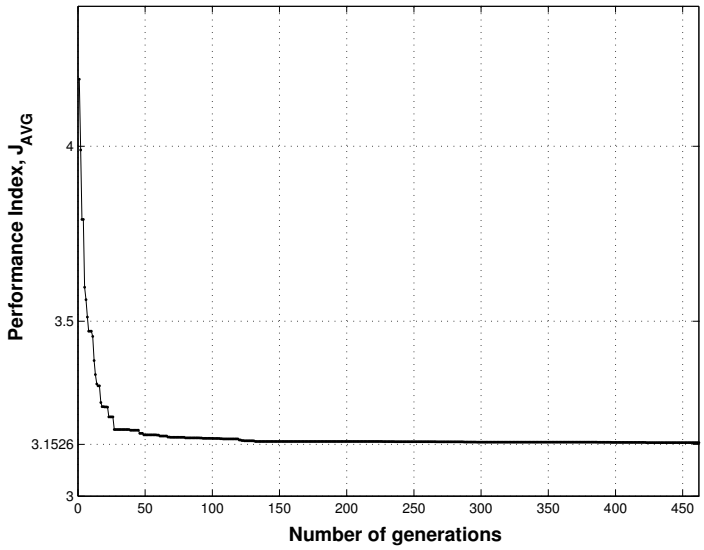

Figure 3.19 Plot of J_{AVG} for the "best" individual in each generation, for a population of 40 individuals

The corresponding PSS (a) time constants and (b) gains' variations during the genetic process are depicted in Figure 3.20, for 460 generations.

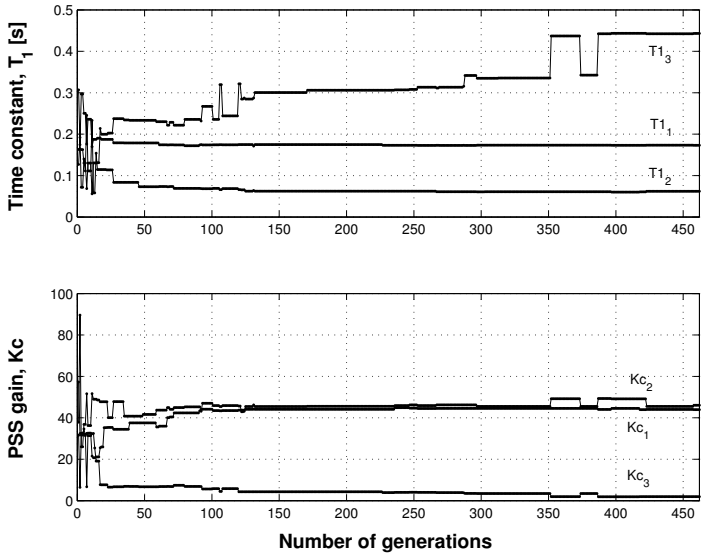

Figure 3.20 Parameters (T_{1i} and K_{Ci} for i =1,2,3) of best individual, for each generation

The convergence rate of the performance index is also reflected in the variation of the best individual of each generation during the entire genetic process.

Table 3.6 shows the performance indexes J_{AVG} of the Lyapunov optimization method based GA search solutions for different configurations and in different stages of the genetic search process. It can be seen that the GA search provides the best solution in Case 8, for N_{IND} = 50 over 500 generations.

Table 3.6 Performance of the proposed GA based PSS tuning method for different genetic configurations

Case	N_G	N_{IND}	PSS Parameters (K_C, T_1)			Performance Index J_{AVG} $\times 10^{-6}$
			Gen-1	Gen-2	Gen-3	
1.	50	50	(44.63, 0.18)	(40.7, 0.06)	(2.32, 0.45)	3.1606
2.	100	30	(44.29, 0.18)	(49.38, 0.06)	(2.48, 0.39)	3.1546
3.	100	50	(45.20, 0.17)	(42.66, 0.06)	(2.64, 0.37)	3.1546
4.	150	30	(44.84, 0.17)	(46.15, 0.06)	(3.16, 0.35)	3.1538
5.	200	30	(43.21, 0.17)	(49.89, 0.06)	(3.61, 0.35)	3.1545
6.	200	50	(42.03, 0.18)	(43.94, 0.07)	(3.42, 0.297)	3.1639
7.	460	40	(44.56, 0.17)	(46.24, 0.06)	(1.96, 0.46)	3.1526
8.	500	50	(45.06, 0.17)	(45.52, 0.06)	(2.13, 0.44)	3.1524

Usually, a viable solution is not reached in 50 generations, for reliable result, approximately 100 generations are required. A higher number of individuals in population will increase the probability of finding the optimum solution in a smaller number of generations, but will also increase the computational time to complete the evaluation of one generation. The simulations performed show that often a population with 30 individuals would suffice to find an optimum within 150 generations (*e.g.* Table 3.6, case 4).

A significant issue in the GA based optimization process, is the convergence criterion, whose inadequate setting may cause premature termination of the process, far away from the global optimum.

3.4.1.1 *Various Loading Conditions and System Configurations*

In order to test the robustness of the GA based PSS, three different operating conditions and five contingencies were considered. The different operating conditions (represented by light, nominal and heavy loading) are given in Table 3.7. It might be noted that these load conditions at buses #5, #6 and #8, are same as those used in [38], except that the corresponding generation levels are obtained here using an OPF simulation with "minimizing losses" as objective.

Table 3.7 Three different loading conditions for examining the performance of the GA based PSS

Operating conditions, p.u.						
Loading	Gen-1		Gen-2		Gen-3	
	P	*Q*	*P*	*Q*	*P*	*Q*
Nominal	0.71	0.28	1.63	0.07	0.85	-0.11
Heavy	2.77	1.20	1.38	0.50	1.26	0.36
Light	0.81	0.14	0.44	-0.11	0.36	-0.20

The dynamic responses are plotted for rotor speed deviation of Generator-1 following a 1% step change in mechanical torque on the same generator. The responses are plotted for both the GA based PSS and the ISE technique based PSS.

Figure 3.21 shows the plot for the nominal operating condition. The GA based PSS has a lower peak off-shoot and smaller oscillations and an overall better damped response.

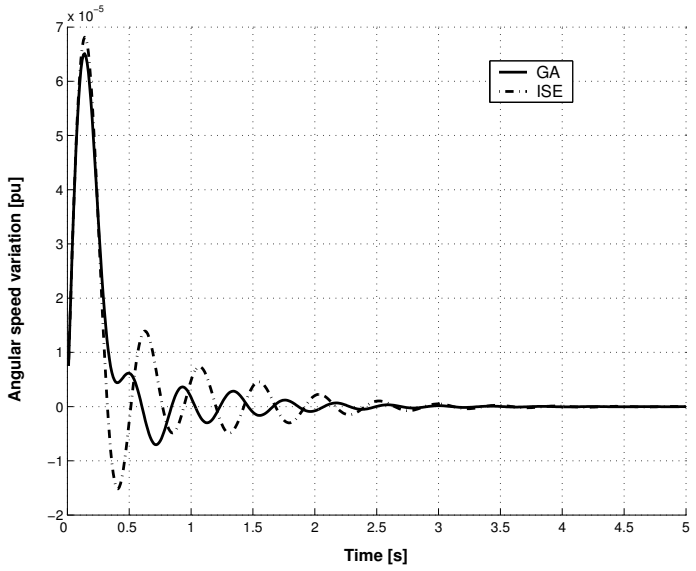

Figure 3.21 Rotor speed deviation of Generator 1 with GA based PSS and ISE technique based PSS for nominal load condition

Figure 3.22 shows the plot of rotor speed deviations for the heavy operating load condition. It is evident that the GA based PSS performs distinctly better compared to the ISE technique based PSS.

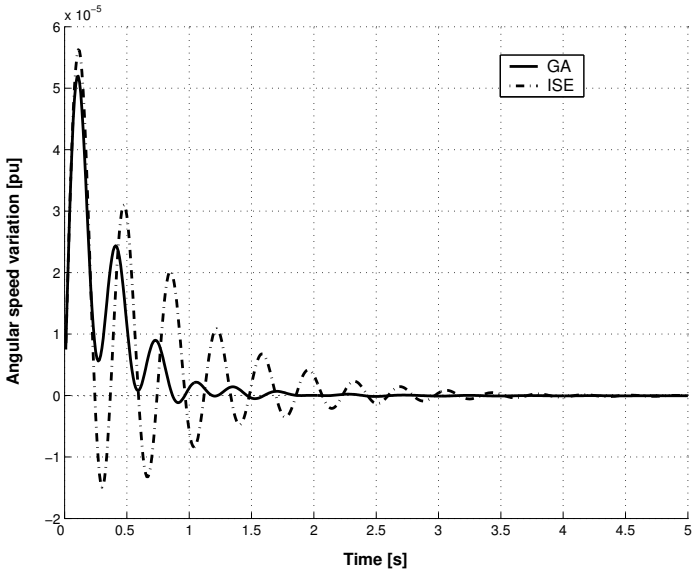

Figure 3.22 Rotor speed deviations of Generator 1 with GA based PSS and ISE technique based PSS for heavy load condition

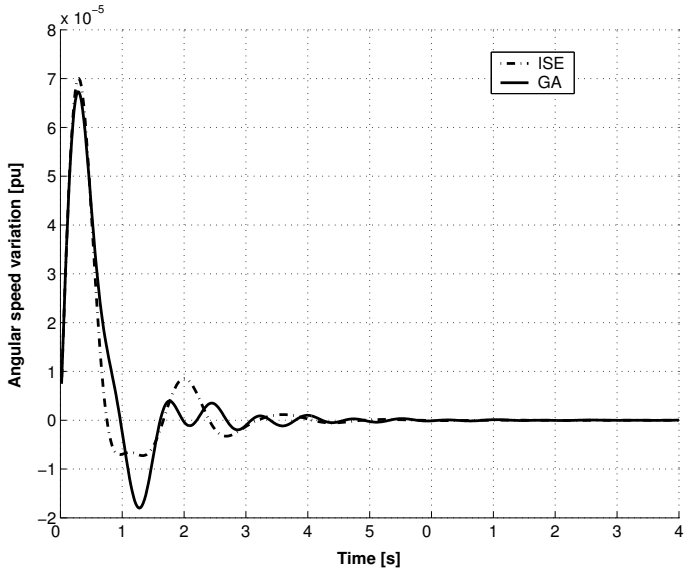

Figure 3.23 Rotor speed deviations of Generator 1 with GA based PSS and ISE technique based PSS for light load condition.

Figure 3.23 shows the comparison of dynamic performances under a light load operating condition. In this case, the GA based PSS and the ISE technique based PSS both do provide satisfactory responses. Evidently, it can be said that the conventionally tuned PSS provides satisfactory performance at light loads and up to the nominal operating point, at which it is tuned. However, when the system load increases beyond the nominal point, the performance deteriorates. The GA based PSS, on the other hand, continues to perform well for all operating loads and hence has a higher level of robustness.

Further, in order to test the solution for different system topologies, a set of contingencies represented by outages of transmission lines, one at a time, has been considered. The dynamic responses of Gen-1 rotor speed deviation when subjected to the same disturbance are plotted in Figures 3.24 to 3.28, for all the contingencies considered, each being plotted against the similar dynamic response for normal operation conditions. In all cases, the grand coalition of PSSs is employed.

Note that for outage of line 4-5, there is no feasible set of PSS parameters that can stabilize the system; hence this contingency was not considered.

As expected, for all the contingencies considered, the dynamic performance worsens; however, the PSS manages to maintain the system stable, while exhibiting a reasonably well-damped dynamic behavior. The plots below show the rotor speed deviation up to the point when the total squared

deviation from steady-state becomes less than 3% with respect to the steady-state.

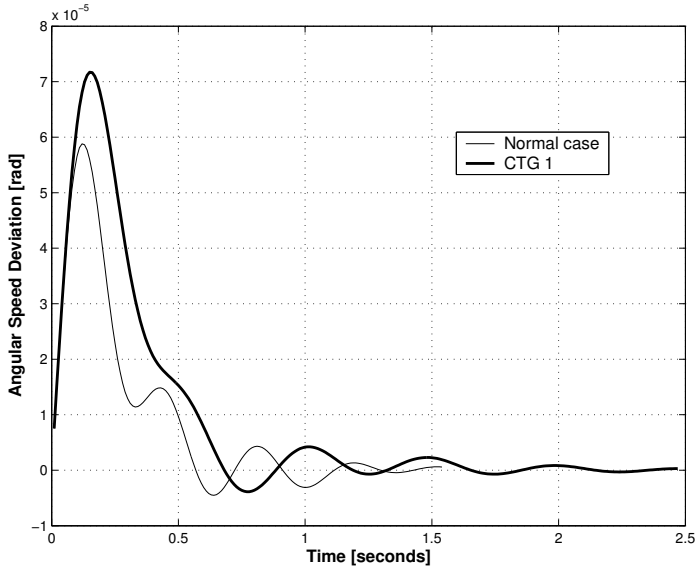

Figure 3.24 Angular speed deviation for normal and under contingency condition (outage of line 4-6)

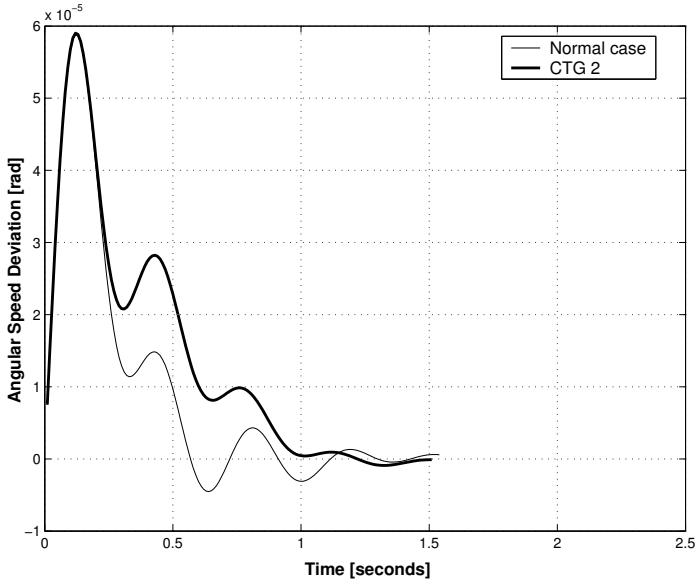

Figure 3.25 Angular speed deviation for normal and under contingency condition (outage of line 5-7)

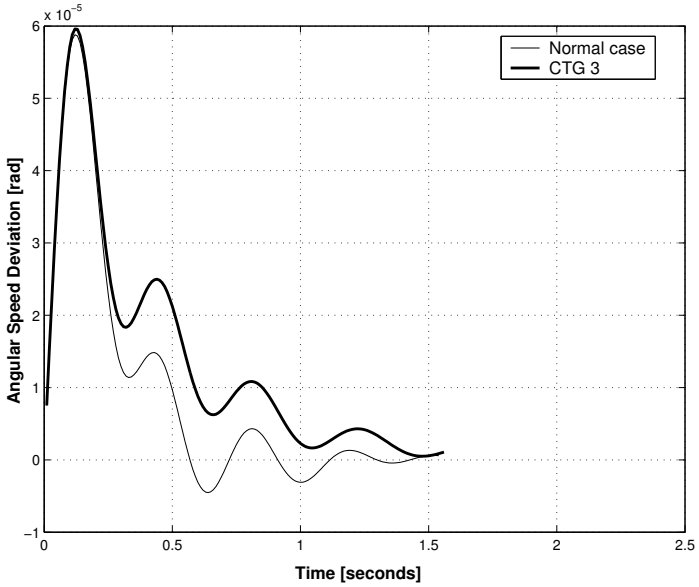

Figure 3.26 Angular speed deviation for normal and under contingency condition (outage of line 6-9)

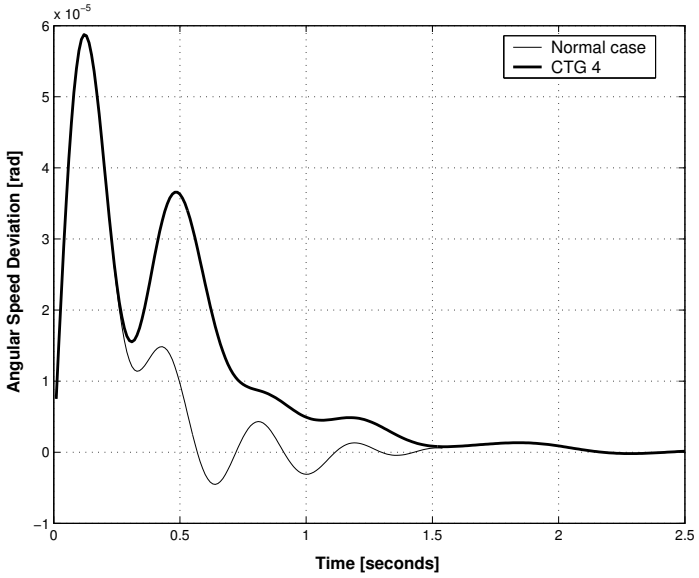

Figure 3.27 Angular speed deviation for normal and under contingency condition (outage of line 7-8)

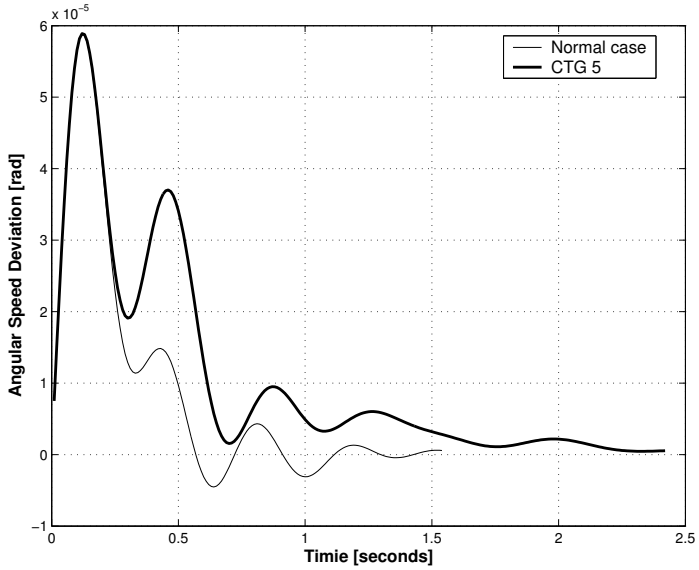

Figure 3.28 Angular speed deviation for normal and under contingency condition (outage of line 8-9)

It can be seen from the figures above that, even for the worst contingencies among the ones considered, a reasonable damping is achieved within 2.5 seconds.

3.5 Concluding Remarks

This chapter presents a novel approach to tuning of Power System Stabilizers (PSS) using Genetic Algorithms (GA) based search process that incorporates the classical Lyapunov optimization criterion. The advantage of using a GA based search is that within these global search techniques a wide operating range can be taken into consideration in the tuning process. In contrast, the conventional tuning approaches are based on one nominal operating condition. Furthermore, the problems associated with eigenvalue drift arising from sequential tuning in multi-machine PSS are avoided in the GA based search, since it search the set of optimal parameters for all PSSs simultaneously.

The advantage of the proposed Lyapunov method based GA over other earlier reported GA methods is that the proposed method takes into consideration the dynamics of the system in the time-domain and is hence much more convenient to understand. The Integral of Squared Error criterion also provides an exact quantification of the system performance as against other methods, which primarily use the eigenvalue shift approach and measuring of the damping factors. The optimal PSS obtained using the

proposed method provides considerably superior dynamic performances under a wide range of operating conditions. The computational burden of the proposed method is within practical limits.

Genetic algorithms represent a useful tool for large-scale optimization problems, but inappropriate selection of genetic search parameters may lead to premature termination, or even to the divergence of genetic process. However, during the investigations reported here, the final solution was always found to be in vicinity of the same location within the search space, depending on the desired accuracy (pre-specified in the convergence criterion).

The proposed method has been tested on two different PSS structures- the lead-lag and the derivative type, and two different system models- the SMIB and a multi-machine model. Investigations reveal that the lead-lag PSS provides performances superior to the derivative PSS.

The simulations and tests performed showed that the operating range for which the proposed GA based PSS withstands small perturbations is much bigger than the range considered within the objective function.

The dynamic responses were satisfactory for large variations in system load conditions, for different system topologies (contingencies) and even for transient phenomena occurred due to severe faults in the system.

4 GENETIC ALGORITHM BASED TUNING OF PID PSS

In a similar manner as in the previous chapter, a genetic algorithm based method to tune the parameters of a proportional-integral-derivative (PID) power system stabilizer (PSS) is proposed here. To enhance the overall performance of the system under small perturbations, a set of operating points is considered within the objective function. The solution thus obtained is globally optimal and robust. Realization of the genetic algorithm based PID-PSS is carried out in discrete-time domain and the effect of sampling period on PSS parameter tuning has been examined. Dynamic performances with PID-PSS tuned using the proposed method have been compared with the lead-lag PSS previously designed. The designed PSSs were tested for different load conditions and found to be satisfactory.

Keywords: genetic algorithm, PID PSS controller design, small-signal stability

4.1 Introduction

In this chapter, the tuning of fixed structure proportional-integral-derivative (PID) PSS for the SMIB and multi-machine power systems has been considered. PID controllers have found applications in power system control problems for their simplicity and ease of realization. In [63] a pole-shifting self-tuning PID controller has been designed for damping of low frequency oscillations in multi-machine systems. The PID controller gains are adapted in real-time to track the system conditions in order to provide robustness to the system. In [64], a fuzzy rule-base is used to tune the gain settings of a PID stabilizer. The introduction of fuzzy logic to tune the PID gains makes the PID control structure inherently non-linear. On-line tracking of the error signal and their time derivative (difference) is used to evaluate the gains. Genetic algorithm based PID controllers have been proposed in [65] for controller design to improve the transient stability of ac-dc lines after faults. The PID controller is applied to the HVDC control system, both on the rectifier side as

well as the inverter side and the gains are tuned such that the disturbance from a fault is minimum.

The tuning scheme proposed in this chapter uses a GA based search that integrates a classical ISE based parameter optimization criterion. This method succeeds in achieving a robust, simultaneously tuned and globally optimal PID-PSS parameter set, while maintaining the simplicity of the classical optimization method. The tuning method implicitly builds-in an increased robustness through an objective function which depends on the operating domain.

PID controllers have been used for power system stabilization for their simplicity and ease of realization. They are feedback controllers whose output is generally based on the error between a user-defined set point, ω_o and the measured variable ω_i. Each element of the PID controller refers to a particular action taken on the error for example, the *proportional gain* K_P is an adjustable amplifier that is usually responsible for system stability. The *integral gain* K_I is responsible for driving the error to zero, while the derivative gain K_D is responsible for system damping.

In all practical implementations of PSS, the input signals are available in discrete form since digital instruments are used to measure the system variables such as speed, voltages, terminal power, current, *etc.* Therefore, it is important to capture the effect of discrete inputs on PSS parameter settings, which understandably will be affected. A proper selection of the sampling time is important because, though a small sampling time would be desirable, it would nevertheless increase the computational burden significantly. On the other hand, a large sampling time will miss significant system information on the dynamics while achieving fast computation. A proper selection of T_S is thus critical, and shall be discussed later in this chapter.

Tuning of a PID controller involves the adjustment of its gains K_P, K_I, and K_D to achieve some user-defined "optimal" character of system response. The structure of a PID PSS with rotor speed deviation as input can be represented as

$$u(t) = K_P \Delta\omega(t) + K_D \frac{d}{dt}\Delta\omega(t) + K_I \int \Delta\omega\, dt \tag{4.1}$$

The above control logic can be expressed in discrete-mode as follows:

$$u_k = K_P \Delta\omega_k + K_D\left(\Delta\omega_k - \Delta\omega_{k-1}\right) + K_I \sum_{p=1}^{N} \Delta\omega_k T_S \tag{4.2}$$

In equation (4.2), the PSS parameters to be optimized are K_P, K_D and K_I.

The small perturbation dynamic model of the multi-machine system without PSS was discussed in detail in Chapter 2, and the transfer function

block diagram representation is given in Figure 2.4. The PSS output signal *u(t)* shall be acting on the voltage regulator summing junction of each machine.

The general structure of the PID-PSS is shown in Figure 4.1 where K_P, K_D and K_I are the *proportional*, *derivative* and *integral* gains respectively. Note that the input to the PSS comprises discrete samples of the speed deviation signal $\Delta\omega$ obtained with a sampling time T_S.

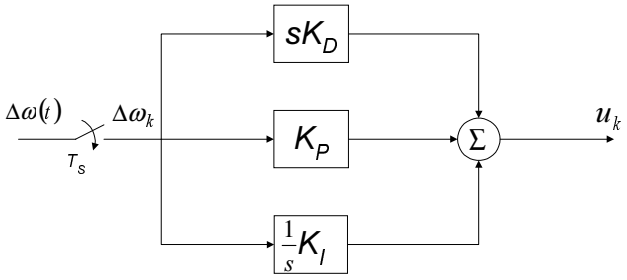

Figure 4.1 The general structure of a PID-PSS with discrete input signal

The small perturbation transfer function model for the above system can be expressed in state-space form as follows:

$$\frac{d}{dt}\mathrm{X}(t) = \mathbf{A}\cdot\underline{\mathrm{X}}(t) + \mathbf{B}\cdot\underline{\mathrm{u}} + \mathbf{\Gamma}\cdot\underline{\mathrm{p}} \tag{4.3}$$

In (4.3), **A** is the state matrix, **B** is the control matrix and Γ is the perturbation matrix and depend on the system parameters and operating conditions, $\underline{\mathrm{X}}$(t) is the state-vector defined in (4.4) and $\underline{\mathrm{p}}$ is the perturbation vector. N_G is the number of generators.

$$\underline{\mathrm{X}} = [\Delta\omega_i \quad \Delta\delta_i \quad \Delta E'_{q_i} \quad \Delta E_{fd_i}] \quad \forall\ i \in N_G \tag{4.4}$$

The linear dynamic model of the composite system inclusive of excitation system and the PID-PSS can be represented in state-space form as in (4.5). $\mathbf{A_C}$ is the corresponding composite system matrix.

$$\frac{d}{dt}\underline{\mathrm{X}}(t) = \mathbf{A_C}\cdot\underline{\mathrm{X}}(t) + \Gamma\cdot\underline{\mathrm{p}} \tag{4.5}$$

The discrete mode equivalent of (4.3) can be expressed as:

$$\underline{\mathrm{X}}_{\mathrm{k+1}} = \mathbf{G}\cdot\underline{\mathrm{X}}_{\mathrm{k}} + \mathbf{H}\cdot\underline{\mathrm{u}}_{\mathrm{k}} + \mathbf{\Gamma}_{\mathrm{D}}\cdot\underline{\mathrm{p}} \tag{4.6}$$

G, **H** and Γ_D are discrete-mode equivalents of **A**, **B** and Γ respectively and are defined as follows:

$$\mathbf{G} = e^{\mathbf{A}T_S}$$
$$\mathbf{H} = (e^{\mathbf{A}T_S} - \mathbf{I}) \cdot \mathbf{A}^{-1} \cdot \mathbf{B} \tag{4.7}$$
$$\mathbf{\Gamma}_{\mathrm{D}} = (e^{\mathbf{A}T_S} - \mathbf{I}) \cdot \mathbf{A}^{-1} \cdot \mathbf{\Gamma}$$

4.1.1 Genetic Algorithm Specifications

The GA employed in this study uses an *elitist strategy,* in which the offspring is created with a *generation gap* of 90% and reinserted in the old population by replacing the least fit predecessors. Most fit individuals are allowed to propagate through successive generations and only a better individual may replace them.

Each individual of a generation is a Gray coded binary string of search variables, each variable using a 30-bit representation. The selection process uses the *stochastic universal sampling* method, a single-phase sampling algorithm with minimum *spread*, zero *bias* and time complexity in the order of the number of individuals N_{IND}. Recombination is performed using a *multi-point crossover* process with a probability of 0.7 and mutation is applied with a low probability of 0.03.

Within the genetic search, the evaluation process is performed by an objective function, which is a measure of the system's behavior under a small perturbation. The average performance index J_{AVG} is calculated as follows:

$$J_{AVG} = \frac{1}{N_{op}} \cdot \sum_{P,Q} \left(\sum_{k=1}^{N} \Delta\delta_k^2 \cdot T_S \right) \qquad \forall\, P, Q \in D \tag{4.8}$$

where N_{op} is the number of operating points in domain D
T_S is the sampling time
$\Delta\delta$ is the rotor angle deviation

Simulations with population sizes ranging between 30 to 200 individuals have been performed. Very often, a population of 30 individuals would suffice to reach an optimum, and the number of generations required being proportional to the number of variables. As the population size increases, the probability of finding the global optimum increases, while also increasing the simulation time required for each generation. The results presented in this chapter have been obtained with population sizes of 40 and 60 individuals for single- and multi-machine systems respectively.

The convergence criterion is of critical importance and it determines the required number of generations to complete the genetic process. Improper choice of the criterion may lead to premature termination of the process, far away from the global optimum.

Figure 4.2 shows the working scheme of the proposed GA based method for tuning of PID PSS using the ISE criterion.

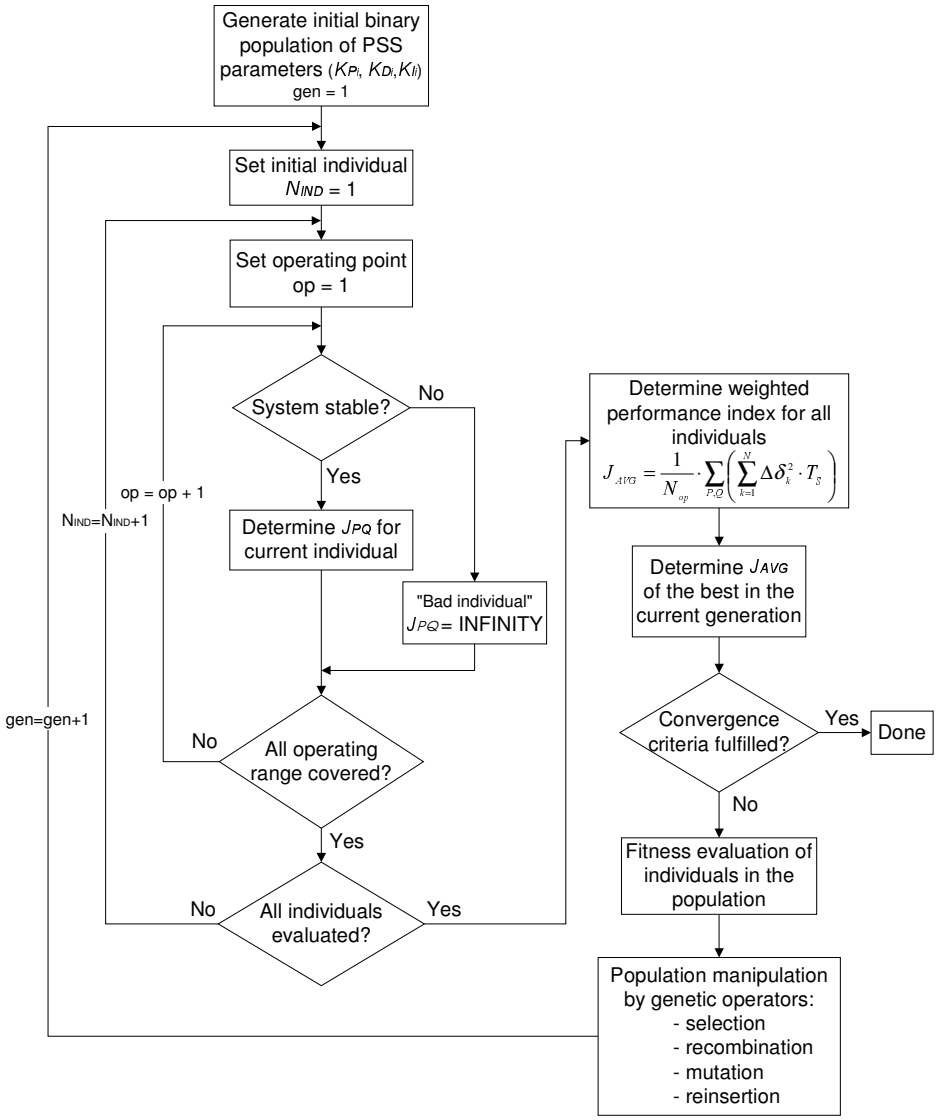

Figure 4.2 Proposed GA based tuning scheme for PID-PSS

4.2 Single-Machine Infinite Bus System Analysis

The proposed GA based tuning scheme is applied to a single-machine infinite bus system operating over a wide operating domain. For this study case an operating domain D ($D \in P$ = [0.3, 1.3] and Q = [-0.3, 1.0] p.u.) comprising 154 operating points was considered. Figure 4.3 shows the variation of the performance index of the best individual in current generation of the GA based search process and Figure 4.4 shows the variation of the corresponding PID controller gains over the generations and their convergence towards the optimal solution.

It can be noted that the process reaches the optimum solution in about 25 generations, after which the performance index reaches a value that remains steady over the remaining search process, and genetic operators do not affect the best individual in consequent generations.

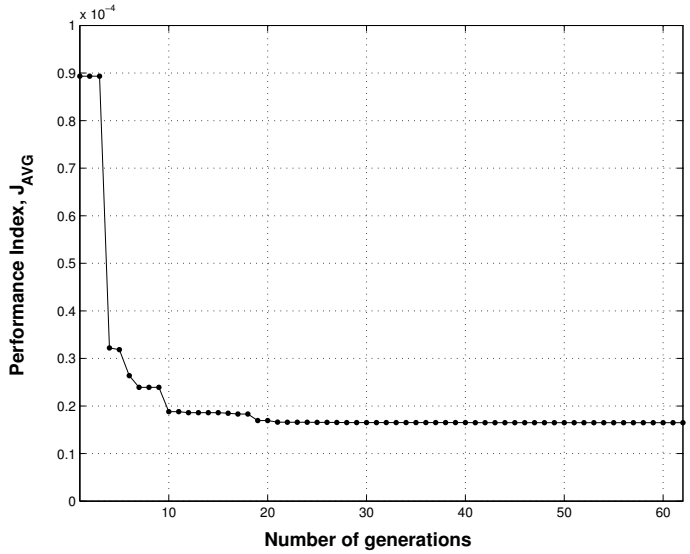

Figure 4.3 Genetic search performance for SMIB PID-PSS tuning

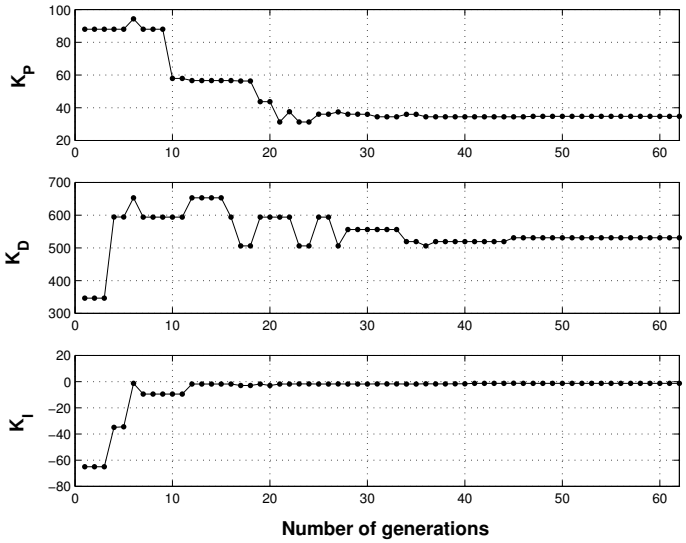

Figure 4.4 PID-PSS parameter variation and convergence during genetic process for SMIB

The optimal gains of the PID-PSS are shown in Table 4.1. Also shown in the table, are the corresponding optimum parameters of a lead-lag PSS (Table 3.1) tuned using the GA based scheme discussed in Chapter 3. The values of J_{AVG} for PID-PSS and lead-lag PSS are very close, indicating that both provide very good performance for the single-machine system considered.

Table 4.1 Optimum PSS parameters and performance index for GA based PID and lead-lag PSS

GA based PID-PSS				**GA based lead-lag PSS**		
K_P	K_D	K_I	J_{AVG} $\times 10^{-5}$	K_C	T_1	J_{AVG} $\times 10^{-5}$
38.28	529.39	-0.30	1.649x 10^{-5}	33.98	0.12	1.598x 10^{-5}

A comparison of the dynamic behavior of the SMIB system equipped with optimally tuned PID and lead-lag PSS is shown in Figure 4.5. The system is subjected to a 1% step change in mechanical torque under heavy load operating conditions (P = 1.5 p.u., Q = 1.1 p.u.). It can be seen that both the PSS show good dynamic performance even for a load condition that is outside the operating domain D that was considered for the PSS tuning.

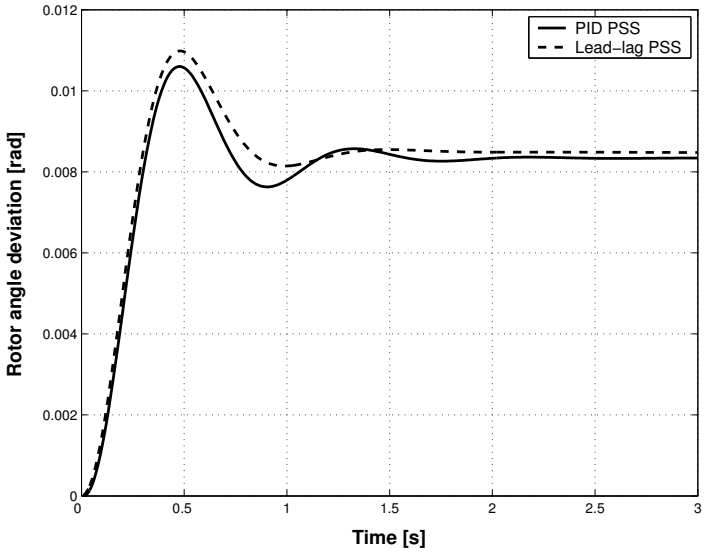

Figure 4.5 Rotor angle deviation of SMIB equipped with PID and Lead-lag PSS

4.2.1 Effect of Sampling Time on PID-PSS Tuning and System Dynamic Performance

For the design of the PID-PSS, the sampling time T_S plays an important role and Table 4.2 shows the dependence of optimum PSS setting and corresponding performance index on T_S. One can observe from Table 4.2 that a gradual deterioration in performance takes place as T_S increases. In order to achieve a high degree of accuracy, a very small sampling time is desirable, which however increases the computational burden. The performance index is lowest for T_S = 0.001 seconds, which will have a very high computing burden. As T_S is progressively increased, the performance index deteriorates gradually while reducing the computational burden. In this analysis, it was considered that the best trade-off between accuracy and computational burden is achieved at T_S = 0.01 seconds.

Now, let us examine if the chosen sampling period of T_S = 0.01 sec is the optimal choice. The last column of Table 4.2 shows the performance index for different T_S with *nominal PSS*[1]. The *nominal PSS* works well up to T_S = 0.05 sec while beyond this, the performance index is very high, thus implying that re-tuning is required.

[1] *Nominal PSS* is the optimum PSS obtained with T_S = 0.01 sec (*i.e.* K_P = 38.28, K_D = 473.84, K_I = -0.30)

Table 4.2 Effect of TS on GA based PID-PSS design

T_S sec	Optimum GA based PID-PSS at nominal operating point			J_{nom} ($\times 10^{-5}$)	J_{nom} ($\times 10^{-5}$) with *nominal PSS*
	K_P	K_D	K_I		
0.001	**38.00**	**4592.00**	**-0.60**	1.529	3.841
0.005	40.60	957.00	-1.02	1.542	1.672
0.010	38.28	473.84	-0.30	1.557	1.557
0.050	34.28	126.36	0.06	1.692	2.458
0.100	23.26	76.64	0.35	2.033	*very high*

In all further investigations in this paper, a sampling time of T_S = 0.01 seconds was considered.

4.3 Multi-machine Power System Analysis

The proposed GA based technique is now used to determine the optimal parameters of the PSS on the three-machine system (see Figure 2.2*)*. In order to bring about robustness, a set of six operating points, as discussed in Section 3.4 is considered by varying the system loads, Load-A, Load-B and Load-C, in steps. Based on these load conditions, an *optimal power flow (OPF)* with minimizing losses as the criterion is run for each load configuration. Thus, the generation level for each unit in each load configuration considered is obtained and represents the initial operating point for the system.

As in the case of SMIB system, Figure 4.6 shows the current generation best individual's performance index and Figure 4.7 shows the convergence of PID-PSS parameters.

Note that the optimum solution is achieved in approximately 115 generations when J_{AVG} attains a steady value. However, the derivative and integral gains change slightly even afterwards, while on the other hand, K_P remains unchanged. This indicates a strong relationship between K_P and J_{AVG} and a weak dependence between the other two gains (K_D and K_I) and J_{AVG}.

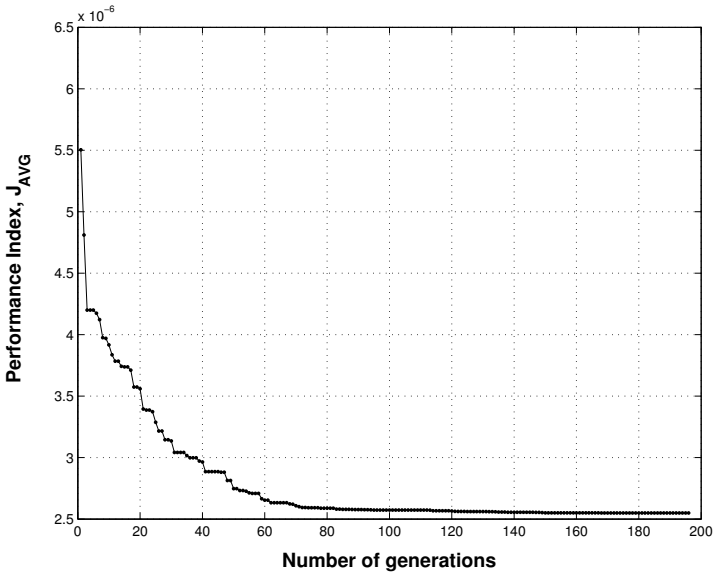

Figure 4.6 Genetic search performance for multi-machine PID PSS tuning

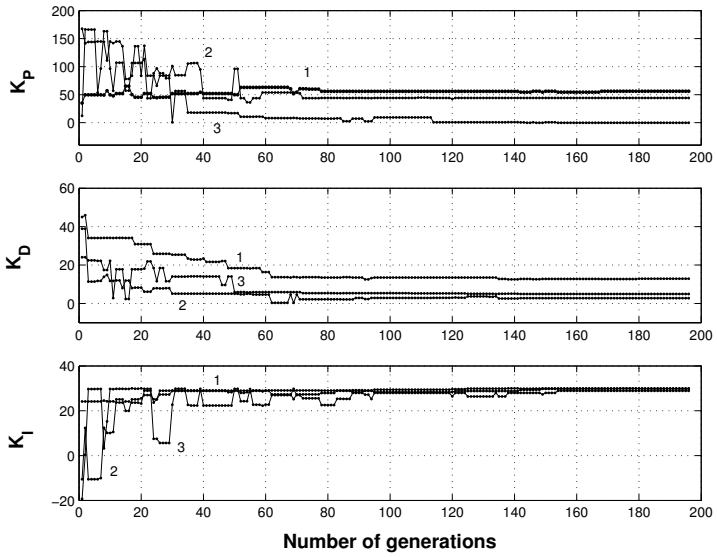

Figure 4.7 Solution variation during genetic search for multi-machine PID-PSS tuning

Table 4.3 shows the optimal solutions obtained with the proposed technique for PID and lead-lag types of PSS (3.1). In this case, just by comparing the values

of the corresponding performance indices it can be concluded that the PID-PSS performs better.

Table 4.3 Optimum PSS solution and performance indices for GA based PID and lead-lag types of stabilizer

Machine	PID PSS			J_{AVG} $\times 10^{-6}$	Lead-lag PSS		J_{AVG} $\times 10^{-6}$
	K_P	K_D	K_I		K_C	T_1	
1	56.11	12.92	29.93	2.55	45.06	0.17	3.15
2	44.01	2.75	29.81		45.52	0.06	
3	-0.24	4.91	28.92		2.13	0.44	

In order to test the robustness of the GA based PSS, three different operating conditions corresponding to, apart from the nominal load, a light and a heavy load, as given in Table 4.4. It might be noted that these load conditions at buses #5, #6 and #8, are same as those used in [38], except that the corresponding generation levels are obtained here using an OPF simulation with minimizing losses as objective.

Table 4.4 Loading conditions used to test the robustness of GA based PID-PSS

Operating conditions (in per unit)						
Loading	Gen-1		Gen-2		Gen-3	
	P	*Q*	*P*	*Q*	*P*	*Q*
Nominal	0.71	0.28	1.63	0.07	0.85	-0.11
Heavy	2.77	1.2	1.38	0.5	1.26	0.36
Light	0.81	0.14	0.44	-0.11	0.36	-0.2

Figure 4.8, Figure 4.9 and Figure 4.10 show the dynamic responses corresponding to PID and lead-lag PSS plotted for rotor speed deviation of generator-1 following a 1% step change in mechanical torque on the same generator for nominal, light and heavy load conditions, respectively. The PID-PSS has a lower peak off-shoot and a well-damped response for all cases investigated.

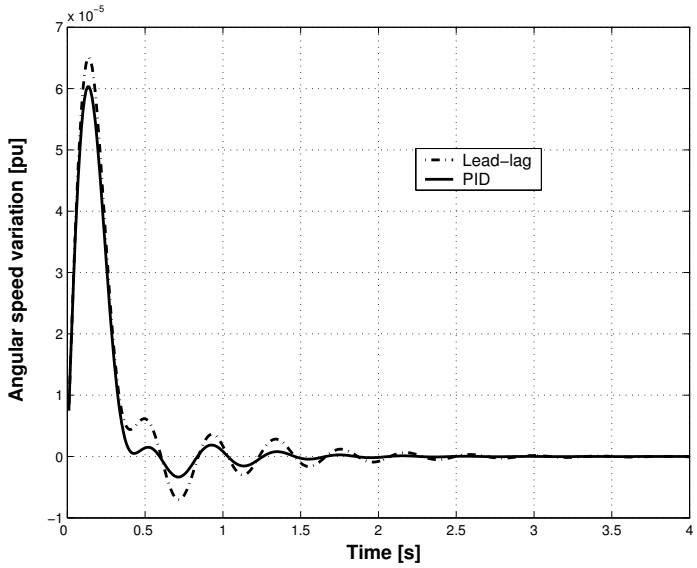

Figure 4.8 Rotor speed deviation on generator 1 for multi-machine system with PID or lead-lag stabilizer under nominal load conditions

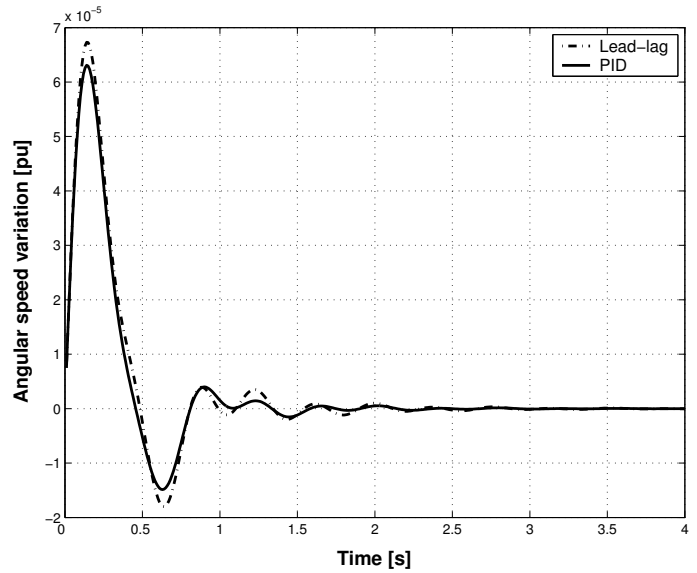

Figure 4.9 Rotor speed deviation on generator 1 for multi-machine system with PID and lead-lag stabilizer under light load conditions

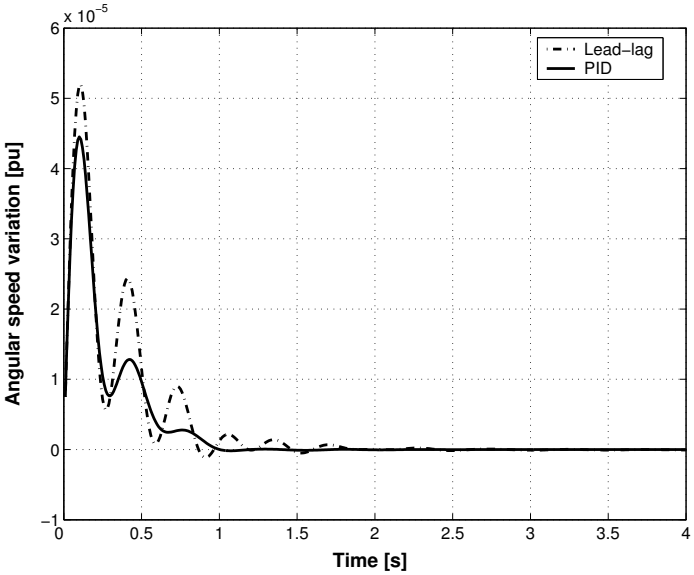

Figure 4.10 Rotor speed deviation on Generator 1 for multi-machine system with PID and lead-lag stabilizer under heavy load condition

4.4 Concluding Remarks

The paper presents the design of a genetic algorithm based tuning method to obtain optimum parameters of a proportional-integral-derivative (PID) power system stabilizer (PSS) in power systems. The classical integral of squared error based parameter optimization approach is integrated within the genetic process and the parameters of the PID-PSS that evolve, can be said, to be globally optimal. The PID-PSS works in discrete-time domain and thus implementation of the controller would be simple. Investigations have been carried out regarding the optimal sampling period for such PSS. A sampling period of 10 ms is found to be appropriate for the design and the so-designed PSS is seen to work well up to a sampling period of 50 ms in the simulation phase. The PID-PSS compares well with a lead-lag type PSS and its robustness to system load variations proved better.

The method proposed here is designed as an off-line method, therefore the computation time was not considered as a priority. However, depending on the size of both population and operating domain, computational times ranging from 30 minutes to 3 hours have been recorded.

The advantage of using PID-PSS is that these are easy to realize and being in discrete mode, their associated computations are lesser. Genetic algorithms applications to such PID-PSS provide an increased benefit, that of robustness.

Analytical studies show that the proposed GA based method for tuning PID-PSS provides very satisfactory dynamic performances over a wide operating domain and that their performances are comparable with the lead-lag PSS.

5 PSS-CONTROL – SHAPLEY VALUE BASED ECONOMIC WORTH ALLOCATION

This chapter proposes a method to quantify the individual contributions of power system stabilizers (PSSs) to enhance system performance. Enhancement in system performance due to PSS is measured through increased system transfer capability and the margin of stability thus achieved. The proposed method is based on cooperative game theory and makes use of the Shapley value concept, thus pinpointing the importance of a particular PSS to system performance, in all possible combinations in which it can operate. Based on the above quantification of the contribution of a PSS, an appropriate financial compensation mechanism to pay generators for the services rendered is proposed. Additionally, a set of contingencies is considered as well, and an analysis whether and how the PSS payoffs are affected by changes in system topology is then performed. For a realistic scenario in which a 24-hour load curve and various load types are considered, the proposed method is applied in conjunction with the N-1 security criterion.

Keywords: ancillary services, cooperative game theory, PSS-control service, Shapley value, transfer capability.

5.1 Introduction

In deregulated power systems, the independent system operator (ISO), or a similar entity, is entrusted with ensuring a required degree of security, reliability and stability of the system and perform several other functions. *Ancillary services* are all those activities that are necessary for the ISO to support power transmission, while maintaining reliable and stable operation. Procurement, operation and management of these services are therefore often the responsibility of the ISO. These services include regulation of frequency and tie-line power flow, voltage and reactive power control, system stability, maintenance of generation and transmission reserves, and many others.

According to NERC Operating Policy-10, the following services are recognized as ancillary services [42]:

- for maintaining generation and load balance
  - regulation service
  - load following service
  - contingency reserve service
- for bulk transmission system security
  - reactive power supply from generation sources
  - frequency response service
- for emergency preparedness
  - system black start capability

In a deregulated environment, the ISO is faced with the difficult task of providing security constrained transmission services in a fair and equitable manner, in view of the transmission networks being subjected to heavy stress due to the various trades and transactions taking place amongst parties. It is also to be noted that these networks were originally designed to accommodate transactions based on only certain load/generation patterns at best. In a deregulated environment, the generation and load patterns resulting from market activities may be quite different, in principle, from the ones used in network planning, possibly worsening the security and stability margins.

System security considerations are critical for healthy and efficient market operation, and hence these play an important role in system transfer capability limits. Thus, system transfer capability, and hence the amount of allowable transactions in electricity markets, need to be evaluated based on system security to ensure their operational feasibility. In this context, one important issue that has emerged from deregulation is how the ISO can maintain system security at a desired level, and in order to do so, what system support services (ancillary services) it requires, and how such services are procured and compensated for.

Determining the cost of system security has also been of great interest in power systems [66]-[72]. In most of these works, Lagrange multiplier based methods were used to analyze the different cost components. The idea of pricing security was first advanced in [67] by considering line flow constraints; contingency pricing was studied in [68], and the costs related to outages were analyzed in [69]. In [70] and [71], an OPF based technique was proposed wherein possible ways of costing voltage security was discussed; the effect of minimizing operating cost, reactive power generation and/or maximizing loading margins were compared. In [72], a transaction security cost analysis has been carried out using a risk-taking strategy that provides proper market signals to the participating players in the market. These articles concentrate on discussing the issue of pricing system security from a “power flow” perspective and there is no actual consideration of power system dynamics, in general, and to PSSs in particular, which is the main thrust of this chapter.

5.2 PSS-Control as an Ancillary Service

PSSs have long been accepted and recognized as essential means for stable system operation, particularly small-signal stability phenomena; they render a service to the system by providing damping action on small disturbances – continually occurring even during system normal operation – thus influencing directly system transmission security and reliability. In the absence of this service, the system could become unstable from sustained low frequency oscillations, whilst with a tuned PSS in operation the system will respond better to perturbations. An attempt is being made here to examine in detail the importance of each single PSS in a system and the extent to which it contributes to system stabilization; evidently, a coordinated PSS setting will have a beneficial influence on system performance. While in a centralized system this matter can be solved solely through regulations, in a deregulated and competitive environment, as in the case of voltage control, giving incentives to the providers of this service is a more logical approach. In this context, it is argued that the PSS-control effort being provided by generators be considered part of the system ancillary services, and hence be eligible for financial compensation. Thus, as explained in detail below, the importance of a PSS in enhancing the electricity market clearing capability providing the ISO with a secure operating margin is used to develop possible mechanisms for financial compensation to generators for such services.

The problem of tuning and optimization of PSS parameters in deregulated electricity markets is a challenging issue, which has not been properly addressed yet. The issue of responsibility and coordinated tuning of PSS amongst the most important issues associated with PSS tuning in a deregulated environment. As of now, no definite guidelines have been established by the ISOs or equivalent authorities, with regard to this question. Nevertheless, some operating authorities have outlined certain rules on PSS installation requirements on synchronous generators. For example, Western Electricity Coordinating Council (WECC) requires that PSS be installed on every existing synchronous generators of a given capacity and excitation system type [2].

It is to be emphasized here, however, that this chapter does not propose a "market for PSS-control service" as such, but only a payoff mechanism to generators, to "entice" them to participate in a cooperative environment. A competitive market for such a service is infeasible at this stage because of its specialized nature, often depending on the location of generators in the system, and can give rise to market inefficiencies from gaming and strategic operations. Lastly, it is also emphasized that this chapter does not focus on parameter tuning aspects of the PSS, anymore; a previously reported PSS parameter setting obtained earlier by means of GA is considered, as will be explained later in this chapter.

5.3 A Game Theoretic Based Method to Allocate the Benefit from PSS

Generally, it is not a straight forward exercise to evaluate the worth and contribution of an individual PSS to system welfare. This is because of the complexity and difficulty associated with relating the performance of a PSS to a "dollar figure" that would quantify system welfare (benefit/savings) accrued from a coordinated PSS. Part of the complexity also arises from the way the system performance is measured and "valued". To address these issues, a cooperative game theoretic approach is employed here.

A Shapley value criterion is used to determine the marginal contribution of each PSS in the system, and hence how each PSS should be paid for the control service it provides. In other words, Shapley value is used to allocate payoffs to each player, *i.e.* generator equipped with PSS, in the system, depending on its importance to overall system stability and security.

As previously outlined (see Section 1.4), game theory in a broad sense, has found several applications in power systems, particularly in the context of deregulation. Nevertheless, few research articles employ Shapley value based methodologies to price and allocate various services. In [73], a Shapley value based game theoretic approach has been used to determine the allocation of cost savings and emission trading amongst participating utilities in an energy brokerage system. In [74], the transmission costs are allocated using a similar game theoretic approach, which is further compared to other more conventionally used methods such as, postage-stamp method and MW-miles method, thus emphasizing the fairness of allocation associated to such a method.

5.3.1 Shapley Value Criterion

As mentioned earlier, in most deregulated power systems, it would be the responsibility of the ISO or a similar entity to evolve a coordinated PSS tuning and operation strategy based on certain system-wide objective function.

From a game theoretic perspective, as discussed in Section 1.4 of this thesis, PSSs operation can be modeled as a cooperative game, having as its characteristic function a benefit/savings formulation which is based on the objective function used in the tuning process, and where one or more generators are considered together (in all possible *coalitions*) to obtain a fair revenue allocation.

Thus, this analysis of the worth of the PSS-control ancillary service is based on two important issues: (a) how the coalitions are formed amongst the PSS, and consequently (b) how the benefit from a PSS service is allocated. In these two interrelated issues, the main concern is to obtain the most likely outcome from various game situations. Especially when it comes to distribution

of the savings due to PSS control action, the revenue corresponding to a PSS in a particular coalition is very difficult to evaluate.

An intuitively attractive solution concept for *n*-person cooperative games with transferable utility (payment, in this case) has been proposed by Shapley in 1953 [75] and is called the Shapley value criterion. The Shapley value criterion can be defined by means of the following postulates [76]:

a) *Joint efficiency* – the sum of all players' payoffs equals the value of the grand coalition (*n*-player coalition, which is the highest joint payoff the *n* players can achieve within the game).

   To explain this, the sum of the individual payments to each PSS is what the ISO accrues as benefit or savings by having PSS at all generators (grand coalition).

b) *Zero Payoff to any Dummy Player* – if a player fails to contribute anything to the value of any coalition that he may join, then he is called a *dummy player*. The payoff to a dummy player is zero.

   In a multi-machine power system a generator that is completely isolated from the interconnected power system and from other generators can be called a *dummy player* because it has no role in providing for system stabilization service. Hence it is not eligible to receive any payment from the ISO.

c) *Symmetry* – If all players are identical, they share the total system savings equally.

   This postulate, however, does not play a significant role in this analysis since all generators have different characteristics, which is the typical case in power systems.

d) *Additivity* – The payoff of any given player is equal to the sum of all payoffs it would receive as a member of all possible coalitions.

   This means that the payment actually received by a generator, reflects how each PSS contributes to enhancing the system security, since this payment is the sum of that PSS's contribution in all possible coalitions.

The marginal contribution of a player i in the coalition C ($\forall\ i \in C$) will be given by [76]:

$$\Psi_i(C) = v(C) - v(C \setminus \{i\}) \tag{5.1}$$

The Shapley value ϕ, which is the weighted average of the marginal contributions of a player i in all possible coalitions, is hence given by:

$$\phi_i = \sum_C C_W(C)\ \Psi_i(C) \tag{5.2}$$

where $C_W(C) = \dfrac{(r-1)!(n-r)!}{n!}$

in which r is the size of the coalition C.

Having obtained the contribution of a PSS to system savings, a mechanism for financial compensation to synchronous generators for their PSS-control service can now be devised for the ISO. The payment ρ proposed here has the following structure:

$$\rho_i = \rho_{Fi} + \rho_{Vi}(\phi_i) \tag{5.3}$$

In (5.3), ρ_{Fi} represents the component of payment associated with availability of PSS at generator i. This component is payable to the generator for having the PSS installed and adhering to ISO's instructions on parameter settings. The generator is entitled to this component of payment even if the ISO instructs that the said PSS remain off-line. The second component of ρ denotes the variable payment component, proportional to the "worth" of the PSS in system stabilization, and is determined using the proposed Shapley value based method.

An important aspect in ancillary services is the way in which they are handled and managed by the ISO. Many times, ancillary services, such as spinning reserve, regulation, *etc.*, are part of the market clearing process and the suppliers have to simultaneously bid for energy and these ancillary services [77]. On the other hand, certain services such as reactive power support can be on long-term contracts, as in UK where bi-annual tenders are held to establish the contracts [78]. It is envisaged that PSS-control ancillary service would also be on long-term contracts between generators and ISO, so that short-term price volatility due to emergency system conditions do not significantly affect the payment structure.

5.4 Analysis and Results

In an interconnected and deregulated power system with several generators equipped with PSS, the parameters of the PSS would have been optimally tuned in a coordinated manner by the ISO, or a similar entity. These PSSs render a service to the power system by way of providing stabilization action to small disturbances that occur in the system continually. The stabilization action is through auxiliary corrective signals to the reference of the AVR.

5.4.1 Total Transaction Capability Enhancement due to PSS-Control

In order to be able to accurately allocate payoffs to PSSs, it is important to have a good understanding of their contribution to the system. In the present approach, the contribution is measured in terms of the enhanced transfer capability due to addition of each PSS.

For convenience, Table 5.1 provides the set of tuned PSS parameters obtained in [80], which will be considered in the present analysis, *i.e.* the PSS in actual operation.

Table 5.1 The nominal PSS

	Gen-1	**Gen-2**	**Gen-3**
Gain	45.06	45.52	2.13
Time constant	0.17	0.06	0.44

With all PSSs on-line, the system loading is now increased gradually and uniformly at all buses, using a Load Scaling Factor (LSF) that denotes the load increase with respect to the base load. This load increase scenario is only used to illustrate the effect of PSS on the system transfer capability and damping, which assumed to change throughout the operating day, as illustrated in the Section 5.4.4. The dominant eigenvalue of the system shifts toward instability as the system loading is increased, or, in other words, the damping factor ξ decreases monotonically as the LSF increases. A typical damping factor of ξ = 7% is considered as a cut-off value, *i.e.* beyond which the market shall not be cleared; such a criterion may be imposed by the ISO in order to maintain a "reasonable" margin of system security. This is demonstrated in Figure 5.1.

By setting the PSSs to off-line status in all possible combinations, all the feasible coalitions in which the three PSS may operate are obtained. C-123 denotes the coalition in which all PSSs are in service (the grand coalition); the maximum LSF up to which the market may be cleared if the load would increase uniformly (the point where the damping factor intersects the cut-off damping ξ = 0.07), is 1.64 pu, which corresponds to a total of 516.6 MW (system base loading is 315 MW), which in turn translates to an improvement in system transfer capability of 201.6 MW, with respect to *base loading*.

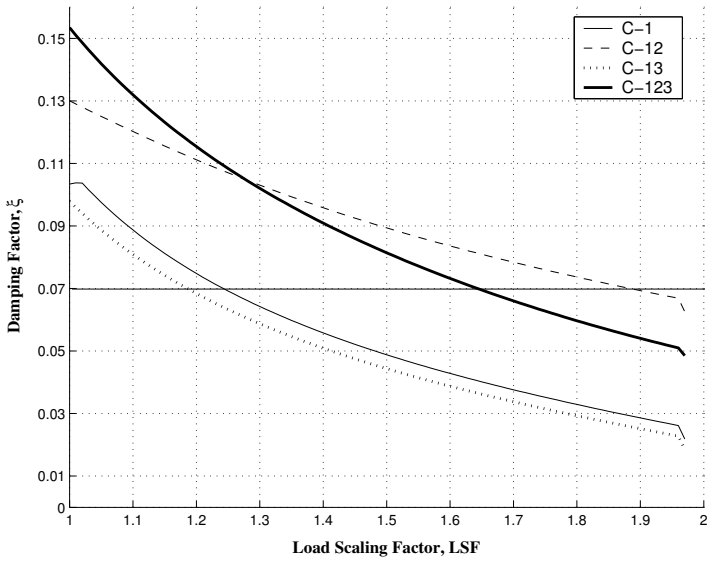

Figure 5.1 P-ξ curves for the feasible coalitions, in normal conditions, *i.e.* no contingencies, for a uniform loading scenario

Observe from Figure 5.1 that, as expected, different coalitions have different effect on the system transfer capability. Consequently, one can also examine their effect on system transfer capability, as explained here for coalition C-123 (Figure 5.1). Thus, assuming that the worth of unit increase in system transfer capability with respect to the *base loading* is \$10/MW, *i.e.* σ_{MW} = \$10/MW, the benefit from a specific PSS coalition (σ_C) can be calculated. It is to be noted that the value of σ_{MW} = \$10/MW used here is only to demonstrate the proposed method; in real systems, the ISO would be required to determine/negotiate the actual value σ_{MW}, *i.e.* the "worth" given to 1 MW increase in system capability, since this value is not actually being utilized and is only being used as a relative measure of how "secure" the system is.

As the market is cleared at these loading conditions, the individual generators would be entitled to an additional payment in return for providing the PSS-control ancillary service and improving the system transfer capability. Consequently, the ISO's problem is to allocate the total worth σ_C achieved from PSS operation in a fair and rational manner. Table 5.2, based on each coalition's benefits σ_C, outlines the application of the Shapley value criterion introduced earlier in this paper, and yields the fair share of payment each PSS would be entitled to, in dollars, for a 315 MW loading level. Note that, for each PSS *i*, the values of ϕ_{PSSi} denote the terms of the Shapley value in equation (5.2). Also note that this analysis would depend on the actual market clearing

conditions, *i.e.* actual generation and load levels, which change throughout the day.

Table 5.2 Shapley value based payment to generators

	C-1	C-2	C-3	C-12	C -13	C-23	C-123	Shapley Value, ϕ
σ_C	756.0	0	0	2,772.0	567.0	0	2,016.0	
C_W	1/3	1/3	1/3	1/6	1/6	1/6	1/3	
PSS-1								
ψ	756.0	–	–	277.2	567.0	–	201.6	**1,480.5**
ϕ_{PSS1}	252.0	–	–	46.2	94.5	–	67.2	**(73.44%)**
PSS-2								
ψ	–	0	–	201.6	–	0	144.9	**819.0**
ϕ_{PSS2}	–	0	–	33.6	–	0	48.3	**(40.63%)**
PSS-3								
ψ	–	–	0	–	- 189.0	0	-756.0	**-283.5**
ϕ_{PSS3}	–	–	0	–	- 31.5	0	-252.0	**(-14.1%)**
Total Payment, ρ								**2,016.0**

It can be observed from Table 5.2, that the Shapley values, and consequently the variable payment components are \$1,480.5, \$819 and -\$283.5 for PSS-1, 2 and 3, respectively. This translates into a 73.44% share of the payoff to PSS-1, 40.63% to PSS-2 and -14.1% to PSS-3 in the variable component. The negative Shapley value associated to PSS-3 denotes that it would receive a negative variable component of payment for introducing an overall detrimental effect on system transfer capability. This is evident from the fact that PSS-3 has a negative marginal contribution in coalition C-13.

5.4.2 System Transfer Capability and Payoffs Considering Contingencies

Once a method of determining the payoffs to participating generators is in place, it would be of interest to investigate if such payoffs obtained for the normal operating condition, at a given instance of time, will still be a fair allocation in a contingency state, when there is a change in system topology. This is important, since typically, an N-1 contingency criterion is used to define system security levels. To this effect, a set of contingencies represented by the outage of one transmission line at a time was considered. Note that outage of line 4-5 was not included, since there was no feasible power flow solution for this contingency, which would lead to a voltage collapse problem that is beyond the scope of this chapter. Hence, the contingencies considered are: 4-6, 5-7, 6-9, 7-8, 8-9, which are denoted by CTG-1 – CTG-5, respectively.

Table 5.3 shows, for all feasible coalitions and considering all contingencies, the amount of power, over and above the nominal load that the system can serve without infringing any operating constraints, whilst $\xi \geq 0.07$, at the previous 315 MW loading level.

Table 5.3 System Transfer Capability Considering Contingencies

		CTG-1	CTG-2	CTG-3	CTG-4	CTG-5
Transfer capability, MW	**C-1**	0	0	0	148.05	88.2
	C-12	72.45	0	0	144.90	220.5
	C-13	0	0	0	97.65	63.0
	C-123	72.45	110.25	179.55	179.55	173.25

Based on the above, one can obtain the total enhancement in worth due to PSS operation σ_C and consequently determine the payoffs to the generators in each contingency case, using the method of Shapley values (see Table 5.4).
As observed in Table 5.4 the payoffs to PSSs vary considerably across contingencies, as expected, given that the contribution and significance of a PSS does not remain the same in all operating conditions or system configurations.

Table 5.4 Payoffs to PSSs Considering Contingency Conditions

		PSS-1	PSS-2	PSS-3
CTG-1 (worst contingency)	σ_C, **\$**	724.5		
	ϕ, **\$**	362.25	362.25	0
	ϕ, **%**	50	50	0
CTG-2	σ_C	1,102.5		
	ϕ, **\$**	367.5	367.5	367.5
	ϕ, **%**	33.33	33.33	33.33
CTG-3	σ_C	1,795.5		
	ϕ, **\$**	598.5	598.5	598.5
	ϕ, **%**	33.33	33.33	33.33
CTG-4	σ_C	1,795.5		
	ϕ, **\$**	1,496.3	267.8	31.5
	ϕ, **%**	83.33	14.91	1.75
CTG-5	σ_C	1,732.5		
	ϕ, **\$**	1,344.0	588.0	-199.5
	ϕ, **%**	77.58	33.94	-11.52

Figure 5.2 depicts the variable payoff shares for the generators in return for the PSS-control service for the normal operating condition and under contingencies CTG-1 to CTG-5. It is evident how the system topology affects the payment allocation, as a direct result of the impact a contingency has on PSS contribution to system security. Hence, the contribution of a PSS in various operating conditions or system configurations can be appropriately recognized and paid for, using the proposed scheme.

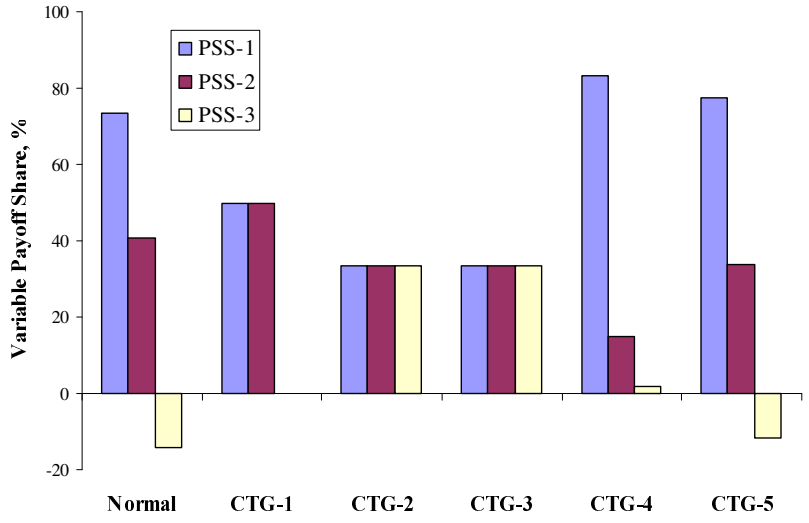

Figure 5.2 Variable payoff shares to generators for PSS-control service in different operating conditions

5.4.3 Practical Application

Using the proposed Shapley value based method, the worth of the PSSs contributions in a more realistic scenario, which also considers the N-1 security criterion, can be determined. Thus, in Figure 5.3, ξ for the dominant system eigenvalue in the grand coalition of PSS is plotted as a function of LSF, for each contingency case. It is shown, for the grand coalition, how the contingencies affect the system from a transfer capability point of view. Evidently, the worst contingency is that in which the system transfer capability is reduced to a minimum. In this example, it occurs when line 4-6 is out of service (CTG-1); hence, CTG-1 is identified as the worst contingency and used here to implement the N-1 criterion. Observe in Table 5.3 that, in this case, the variable payoff is equally distributed between PSS-1 and PSS-2, while no variable payoff is assigned to PSS-3; this is fairly intuitive also, since PSS-3 is

not present in any of the feasible coalitions. However, PSS-3 shall continue to receive the fixed component of payment, ρ_F.

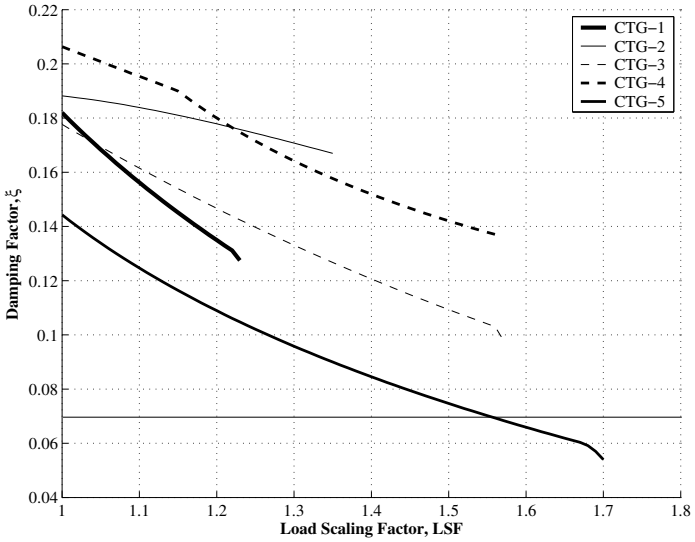

Figure 5.3 Grand coalition's damping factors during contingencies

5.4.4 Payment Allocation over a 24-Hour Period

The total payoff to the generators for their PSS-control service is now determined for a 24-hour period, in 1-hour time intervals. The load curve used in this section represents an "actual" market clearing, considering the N-1 security criterion and a 5% transfer reliability margin; Figure 5.4 shows the daily load curves for each of the load types considered, and the aggregate load curve.

It should be mentioned that the N-1 contingency criterion used assures that the worst contingency for all loading conditions considered is CTG-1, which is reasonable for this system

Based on (5.3), the total payoff to each PSS is given for each hour by:

$$\rho_i^k = \rho_{F_i} + \phi_i \cdot \sigma_{MW} \cdot \Delta P_i^k \tag{5.4}$$

Considering a fixed payoff ρ_F of \$1000, the total payoffs to each generator over a 24-hour period are determined, and the results reported in Figure 5.5. It can be observed that PSS-1 receives the highest payoff, as it contributes more to the system transfer capability as discussed earlier, while PSS-3 receives less than the fixed component of payment as a result of its negative variable payoff component.

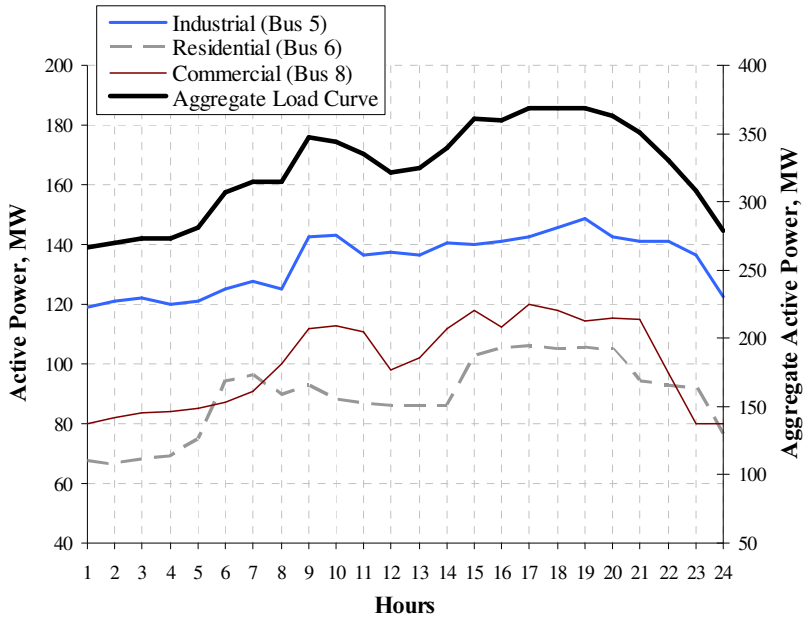

Figure 5.4 System aggregate load curve over a 24-hour period

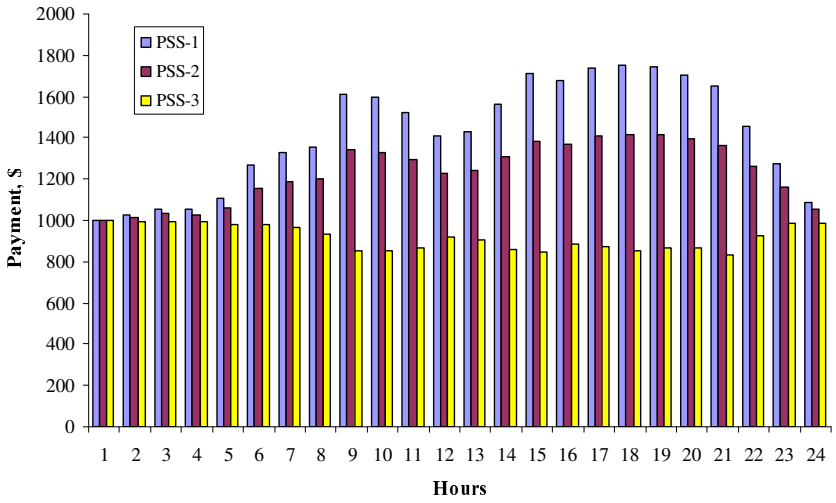

Figure 5.5 Payment allocation for PSS over a 24-hour period

5.4.5 Practical Implementation Consideration

Despite its benefits, Shapley value is not a common allocation method. One of the reasons is that for large systems, the computational costs can be significant, considering the fact that in a system with n generators equipped with PSS, the possible number of coalitions would be 2^n-1. Nevertheless, these costs can be minimized by reducing the number of times the method needs to be applied by dividing the load curves in classes of similar problems, *i.e.* identifying similar load change patterns, and by reducing the number of coalitions by filtering out the infeasible ones. However, more work needs to be done to further establish this concept so that it becomes applicable to large systems.

5.5 Concluding Remarks

In this chapter, it is argued that power system stabilizer control action has an important impact on power system stability and security, and therefore could be regarded as a system ancillary service within the NERC Operating Policy guidelines for Interconnected Operations Services. To this effect, a scheme for allocating payoffs to generators for their PSS-control services is proposed. The payment scheme is based on cooperative game theory, using the concept of Shapley values. The system benefit accrued from a generators providing PSS-control service is allocated in a fair and rational manner, using our proposed approach, which is based on weighted marginal contribution of a PSS in all coalitions it may be part of, thus reflecting better the role and importance of that PSS to the system.

The proposed method concentrate on determining the relative contribution to system security enhancement of the various PSS present in the system, and is not directly dependent on specific "dollar figures," which are assumed to be the result of contractual agreements between the service providers and the ISO.

A realistic scenario represented by a 24-hour load curve, which is obtained considering three different load types and an N-1 contingency criterion, is also considered, revealing that the loading conditions and system topology affect the payments to generators. Therefore, it is important to recognize the need of re-scheduling the payment scheme in accordance to actual load levels and system topology.

Since the method proposed here involves relatively high computational costs, particularly for large-sized systems, there is still a need for developing more appropriate tools to address this issue.

6 PSS-CONTROL ECONOMIC WORTH ALLOCATION BASED ON SYSTEM DYNAMIC PERFORMANCE

In this chapter, the game theoretic payment allocation scheme presented in previous chapter is extended by making use of the dynamic performance assessment tools developed in the first part of this thesis. The optimal PSS is obtained using the GA based method for all coalitions, and a composite performance index is adopted. The method is applied for different system topologies (under a set of contingency operation conditions). The importance of each PSS with respect to system dynamic performance is evaluated and, based on that, an ISO constrained operating requirement on a PSS is suggested and investigated.

Keywords: ancillary services, game theory, Shapley value, power system dynamics, PSS-control service, performance indices, ISE, settling time, peak angle deviation, savings to system

6.1 Introduction

The importance of the PSS to the system has been clearly understood and appreciated by power system engineers and operators. However, their worth and their contribution to system savings have never been investigated and outlined in an analytical manner. This is because of the complexity and difficulty associated with relating the system dynamic performance of a PSS to a "dollar figure" which would quantify savings accrued from a properly tuned PSS. Once the system savings to the ISO from a PSS are appropriately attributed, it would be possible to develop proper pricing mechanisms to compensate the generators for these ancillary services.

In the present chapter, as in the previous chapter, PSS-control is regarded as an ancillary service and the financial compensation mechanism for the generators is now modified by employing various performance indices which comprise system dynamic performance information. By means of the Shapley value criterion, the ways system savings are accrued through PSS control action and how to assign a quantitative "dollar-figure" to the quality of system

dynamics in the presence of PSS are examined. Subsequently, the marginal contribution of each PSS in the system, and hence how each PSS should be paid for the control service it provides, are determined. In other words, Shapley value criterion is used to allocate payments to each player (*i.e.* generator equipped with PSS) in the system, depending on how important the PSS is to overall system dynamic performance.

Further, one should also recognize that each PSS would have different impact on the system in terms of stabilization action. For example, PSS on Gen-1 could possibly be more vital to system stability than a PSS on Gen-3, and so on. This discriminatory behavior is highly dependent on the current operating context defined by the operating condition, type of event and the specific PSSs that are in service.

6.2 Optimal PSS, Minimum PSS, Goodness Index & Savings

6.2.1 Optimal and Minimum PSS

The quadratic performance index J as defined by (2.13), which is a measure of the system performance, is used here to evaluate the goodness of a PSS, and to subsequently determine its fair share of payment. The performance index associated with the MPSS[2] is termed as *Reference Performance Index* (RPI) and shall be denoted by J_{ref}.

Table 6.1 provides the optimal PSS parameters, the *Minimum PSS*, and the corresponding performance indices. Notice that $J_{ref} = 2{,}941.2\times10^{-6}$ p.u.

Table 6.1 Minimum PSS and Optimal PSS in the grand coalition

		PSS Parameters	
		MPSS	**Optimal PSS**
Gain, pu	**Gen-1**	41.8	45.06
	Gen-2	–	45.52
	Gen-3	1.0	2.13
Time constant, sec	**Gen-1**	0.1	0.17
	Gen-2	–	0.06
	Gen-3	0.01	0.44
Perf. Index, p.u.	$\boldsymbol{J}\times10^{-6}$	2,941.20	3.1524

[2] The concept of MPSS has been introduced in Section 2.4.3

6.2.2 Goodness Index

A new index, referred to as the *Goodness Index (GI)*, which is a measure of damping and settling time of the rotor angle oscillation of the perturbed system, with an optimally tuned PSS, as compared to MPSS, is defined as follows:

$$GI = (RPI - J) \qquad \text{for all feasible coalitions} \tag{6.1}$$

The objective here is to evaluate the contribution of a PSS to system dynamic performance and its worth in bringing about cost savings. All possible coalitions in which a PSS may participate are determined, and hence obtained the set of optimal PSS parameters for each coalition, using the GA based PSS tuning method reported in Chapter 3. Table 6.2 shows the various coalitions which can be formed by generators – all equipped with PSS –, and the corresponding optimal PSS parameters, the performance and goodness indices (*J* and *GI*, respectively). It is to be noted that for coalitions C-2, C-3 and C-23, the system is not stable and hence these coalitions are not feasible.

Table 6.2 Coalitions, Optimal PSS, and Performance and Goodness Indices

Coalition *C*	Optimal PSS		*J* $\times 10^{-6}$	*GI*
	Gain (Kc_1 , Kc_2 , Kc_3)	Time constant (T_{1_1}, T_{1_2}, T_{1_3})		
C-1	(62.658, – , –)	(0.1215, – , –)	6.3079	2,934.89
C-2	Infeasible	Infeasible	–	–
C-3	Infeasible	Infeasible	–	–
C-12	(43.167, 47.513, –)	(0.176, 0.098, –)	3.4068	2,937.79
C-13	(65.74, – , 1.0)	(0.1192, – , 0.01)	6.3468	2,934.85
C-23	Infeasible	Infeasible	–	–
C-123	(45.06, 45.52, 2.13)	(0.17, 0.06, 0.44)	3.1524	2,938.05

Coalition C-13 has a low *GI* and, for PSS-3, both the gain K_C and time constant T_1 tend to their lower bounds (which are set in the genetic search algorithm at 1.0 p.u. and 0.01 seconds, respectively). Thus, it can be said that coalition C-13 converges to coalition C-1, PSS-3 being naturally minimized through the optimization process.

However, in spite of that, PSS-3 is a very important player in coalition C-123, as reflected by the corresponding performance indices.

6.2.3 Savings to System

In this sub-section, an attempt is being made to correlate the dynamic performance index of the PSS to an economic index, in dollar terms, that represents the benefit to the system by having the PSS. In order to do so, the following approach is taken:

a) Let us consider the system without PSS at any machine. In such a case, the system is unstable and is in a blackout condition. This understandably has immense cost on the system, which is though very difficult to ascertain, and is beyond the scope of discussion in this thesis. For our system considered, the total load of 315 MW remains unserved when there is no PSS and the system is unstable.

b) Now, let us consider the MPSS – a sub-optimal PSS which barely stabilizes the system – having a rather high performance index ($J = 2{,}941.2\times10^{-6}$, see Table 6.1). However, by virtue of this PSS the system is able to serve all the customer loads. Hence it brings about savings to the system (referred to as *base savings,* S_{Base}), as compared to (a). Assuming the *cost of unserved energy* of \$100/MWh, S_{base} from MPSS equals \$31,500.

c) Next, let us consider an optimally tuned PSS, *e.g.* the grand coalition C-123. The system performance index is now significantly improved ($J = 3.1524\times10^{-6}$, see Table 6.1), because of reduced oscillations and power swings in the system. This brings about further savings to the system as compared to base savings, and shall be referred to as *incremental savings* (ΔS) from coalition C-123.

d) A *savings rate (SR)* can now be defined as the savings brought about by the MPSS, per unit of its performance index (*RPI*), as given by:

$$SR = S_{Base} / RPI \tag{6.2}$$

Without any loss of generality, it can be assumed that *SR* remains constant over all coalitions and hence can be used to determine the incremental savings and the total savings. For the system considered *SR* is obtained as follows:

$SR = 31{,}500/(2{,}941.2\times10^{-6}) = 10.7099\times10^{6}$ \$/p.u. *RPI*

e) Finally the incremental savings from a coalition (of optimal PSSs) can be determined as follows:

$$\Delta S_C = SR \cdot GI_C \tag{6.3}$$

f) Thus the total savings (S_C) from a coalition can be obtained as follows:

$$S_C = S_{Base} + \Delta S_C \tag{6.4}$$

For the system considered, the incremental and total savings corresponding to each coalition is given in Table 6.3. Observe that the system achieves the highest savings with the grand coalition (coalition C-123), which

is worth $62,966.24. This is the savings incurred by the ISO from having the PSS installed, optimally tuned and operating at all generators.

Table 6.3 Calculation of savings from PSS operation

Coalition	*GI*, p.u.	Incremental Savings (ΔS), $	Total Savings (S), $
No PSS	Infeasible	–	–
MPSS	0	31,500.00	31,500.00
C-1	2,934.89	26,024.00	62,932.44
C-12	2,937.79	27,771.38	62,963.51
C-13	2,934.85	25,979.38	62,932.03
C-123	2,938.05	27,933.84	62,966.24

6.3 Rational Allocation of Savings using Shapley Value Criterion

As argued here earlier, the individual generators would be entitled to a payment in return for providing the PSS-Control ancillary service. Consequently the ISO's problem is to allocate the savings achieved from PSS operation ($62,966.24 in this example) in a fair and rational manner.

It has also been discussed previously in this thesis the theoretical background of cooperative game theory and assessment of contribution of individual players in a game. The method to calculate Shapley values for each player in the game was also outlined. Using the approach described therein, the Shapley values for each generator PSS of the example system are obtained as depicted in Table 6.4. It can be observed that PSS-1 receives the highest payoff ($62,948.82), PSS-2 receives $16.58, while PSS-3 receives the least payoff of $0.84.

The highest revenue allocation to PSS-1 can be explained as follows:

- From Table 6.2 it is evident that all feasible coalitions always include PSS-1. Moreover, none of the coalitions that do not include PSS-1 is stable.
- The *GI* of all coalitions does not differ significantly as compared to *GI* of coalition C-1 (Table 6.2).

Table 6.4 Shapley value calculations

	C-1	C-2	C-3	C-12	C-13	C-23	C-123	ϕ
GI	2,934.89	0	0	2,937.79	2,934.85	0	2,938.05	
C_W	1/3	1/3	1/3	1/6	1/6	1/6	1/3	
S	62,932.44	0	0	62,963.51	62,932.03	0	62,966.24	
PSS-1								
ψ	62,932.44	–	–	62,963.51	62,932.03	–	62,966.24	**62,948.82**
ϕ_{PSS1}	20,977.48	–	–	10,493.92	10,488.67	–	20,988.74	
PSS-2								
ψ	–	0	–	31.07	–	0	34.211	**16.58**
ϕ_{PSS2}	–	0	–	5.18	–	0	11.404	
PSS-3								
ψ	–	–	0	–	-0.4170	0	2.7250	**0.84**
ϕ_{PSS3}	–	–	0	–	-0.0694	0	0.9082	
System Savings, *S*								**62,966.24**

Therefore, it can be concluded that PSS-1 has a dominant effect in terms of providing PSS-Control ancillary service and is hence entitled to such a large payment. Similarly, since PSS-2 and PSS-3 are contributing less to system stabilization service, naturally they would receive payments that are in proportion to their role in providing PSS-Control service. Moreover, PSS-3 even appears to have a detrimental effect to system dynamic performance, if it would be involved in coalition C-13.

It is also to be noted in Table 6.4 that the sum of the total payoffs made by the ISO is the total savings accrued by it from optimal PSS operation.

6.3.1 Effect of Bias Induced by Perturbation

As argued minutely in Chapter 2 of this thesis, linear analysis techniques have been commonly used in order to obtain linear system models suitable for small-signal stability analysis and PSS tuning. The linearized models of power systems are obtained by small perturbation analysis. Note that in this example too, the system was modeled by applying a 0.01 per unit perturbation in the mechanical torque of Gen-1.

From the evaluation of Shapley values in previous section, it was evident that PSS-1 is dominant in providing system stabilization service. This leads us to question whether this is an inherent characteristic of the system – that it requires the maximum PSS control action from Gen-1 – or rather a feature that has been carried through by the way the system is perturbed, and hence the tuning methodology (in which Gen-1 only was perturbed).

To examine this issue, a case where all generator mechanical torques are perturbed simultaneously by 0.01 pu is now considered. Subsequently, the PSS parameters are retuned for the new perturbation scenario, using the same GA based approach. The new set of optimal PSS parameters corresponding to all possible coalitions, and the associated *J* and *GI* values are given in Table 6.5.

Table 6.5 Coalitions, Optimal PSS and Goodness Index with all machines perturbed

Coalition ***C***	**Optimal PSS**		***J*** $\times 10^{-6}$	***GI***
	Gain (Kc_1 , Kc_2 , Kc_3)	**Time constant** ($T1_1$, $T1_2$, $T1_3$)		
C-1	(70.784, – , –)	(0.1092, – , –)	12.29	2,928.91
C-2	Infeasible	Infeasible	–	–
C-3	Infeasible	Infeasible	–	–
C-12	(71.15, 48.7, –)	(0.1602, 0.1275, –)	1.924	2,939.28
C-13	(18.93, – , 1.0)	(0.145, – , 0.407)	195.21	2,745.99
C-23	Infeasible	Infeasible	–	–
C-123	(64.93, 59.88, 40.8)	(0.28, 0.195, 0.214)	0.636	2,940.56

From Table 6.5 the following observations can be made:

- Comparing PSS parameters in the grand coalition C-123 obtained by perturbing Gen-1 only (Table 6.2), with those obtained by simultaneously perturbing all generators (Table 6.5), it can be observed that these are now more evenly weighed.
- The observed detrimental behavior of PSS-3 is even more pronounced in this case.

Table 6.6 shows the calculations of Shapley values for the case of simultaneous perturbation of all generators, and it can be noted that:

- As in the previous case shown in Table 6.4, PSS-1 retains its dominant character and receives the highest payment ($62,601.96), while PSS-2 now receives a significantly higher amount ($713.13).
- PSS-3 has a negative Shapley value, that is, it would receive a negative component of payment for introducing an overall detrimental effect on system dynamic performance. This implies that in the payment function, as given in equation (5.3), the variable component ρ_{Vi} is negative, and the generator's overall payment is therefore negatively affected.
- This is evident from the fact that PSS-3 has a negative marginal contribution in coalition C-13. Although the grand coalitionC-123 returns with the highest system savings, if say, due to a contingency, PSS-2 is out of service,

the coalition C-13 will provide a highly inferior performance even as compared to coalition C-1.

- It should also be observed that the figure of total savings made by the ISO in this case ($62,993.19) is slightly higher than that made in the previous case ($62,966.24), and this can only be explained as dynamic interactions between machines during the small-signal stability event.

Table 6.6 Shapley value calculations when all machines perturbed

C_i	C-1	C-2	C-3	C-12	C-13	C-23	C-123	ϕ
GI	2,928.91	0	0	2,939.28	2,745.99	0	2,940.56	
C_W	1/3	1/3	1/3	1/6	1/6	1/6	1/3	
S	62,868.36	0	0	62,979.39	60,909.32	0	62,993.19	
PSS-1								
ψ	62,868.36	–	–	62,979.39	60909.32	–	62,993.19	**62,601.96**
ϕ_{PSS1}	20,956.12	–	–	10,496.56	10151.55	–	20,997.73	
PSS-2								
ψ	–	0	–	111.028	–	0	2,083.87	**713.13**
ϕ_{PSS2}	–	0	–	18.505	–	0	694.62	
PSS-3								
ψ	–	–	0	–	-1,959.05	0	13.795	**-321.91**
ϕ_{PSS3}	–	–	0	–	- 326.508	0	4.598	
System Savings, *S*								**62,993.19**

6.3.2 ISO Imposed Non-Operating Constraint on a PSS

As observed from Table 6.4 and Table 6.6, PSS-3 has little or even negative contribution to overall system dynamic performance. Therefore, it is reasonable to investigate the system behavior without a PSS at Gen-3. Table 6.7 shows in a similar manner as before, the Shapley value calculations for the system with PSS-1 and PSS-2 only, for (a) a small perturbation of 0.01 per unit at Gen-1 only (referred to as case Case-1) and (b) small perturbation of 0.01 per unit at all generators (referred to as case Case-2).

Table 6.7 Shapley value calculations without PSS at Gen-3

C_i	C-1		C-2		C-12		ϕ	
	Case-1	**Case-2**	**Case-1**	**Case-2**	**Case-1**	**Case-2**	**Case-1**	**Case-2**
GI	2,934.89	2,928.91	0	0	2,937.79	2,939.28		
C_W	1/2	1/2	1/2	1/2	1/2	1/2		
S	62,932.44	62,868.36	0	0	62,963.51	62,979.39		
PSS-1								
ψ	62,932.44	62,868.36	–	–	62,963.51	62,979.39	**62,947.9**	**62,923.9**
ϕ_{PSS1}	31,466.22	31,434.18	–	–	31,434.18	31,489.69		
PSS-2								
ψ	–	–	0	0	31.07	111.03	**15.54**	**55.51**
ϕ_{PSS2}	–	–	0	0	15.54	55.51		
System savings, *S*							**62,963.5**	**62,979.4**

From Table 6.7 the following inferences can be drawn:

- The system savings of $62,979.4 is now distributed between PSS-1 and PSS-2. It can be observed that PSS-1 receives a major share of the savings.
- The system savings does not change considerably when PSS-3 is removed from the system (for both cases). This will also be verified later by comparing the system dynamic performance of coalitions C-12 and C-123.
- Hence PSS-3 can be removed from the system, without significantly compromising on system savings. Moreover, the risk of having PSS-3 involved in certain coalition (such as C-13) in which it exhibits an overall detrimental effect on system stability is eliminated.

Figures 6.1 and 6.2 show the angular speed variations recorded at the rotor of Gen-1 in both cases considered (Case-1 and Case-2), for coalitions C-12 and C-123, respectively.

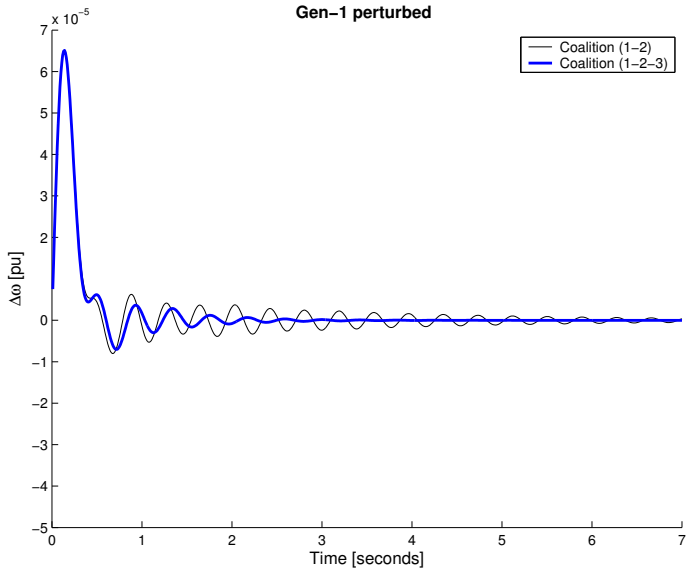

Figure 6.1 Gen-1 rotor oscillations when Gen-1 perturbed, for coalitions C-12 and C-123

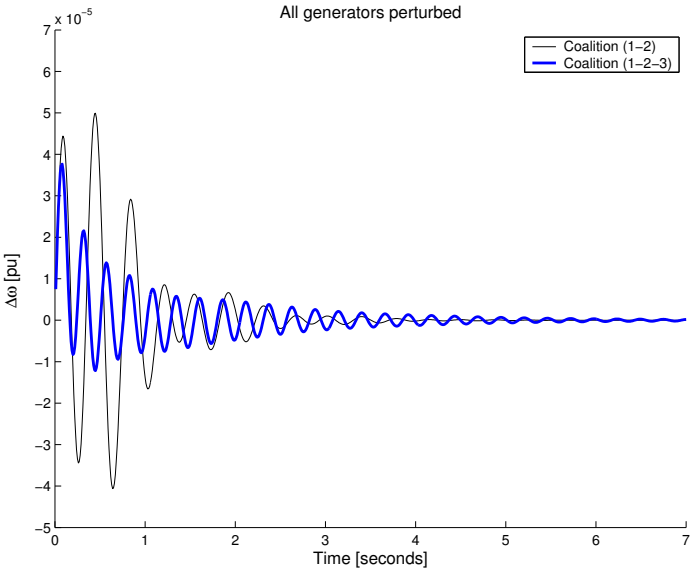

Figure 6.2 Gen-1 rotor oscillations when all generators are perturbed simultaneously, for coalitions C-12 and C-123

As indicated by the performance indices as well, the system exhibits a fairly well damped dynamic oscillation when system is operated with all PSSs in

service and with PSS-3 out of service, as well. Therefore, since the system can be operated with rather similar performance with or without PSS-3 in service, and also considering the risk posed by PSS-3 in certain operating situations, the ISO can constrain Gen-3 to operate with its PSS offline.

6.4 Comprehensive Dynamic Performance Criteria

In this section, the importance of the choice of performance criteria to assess the dynamic performance of each PSS in the system, in order to achieve a more fair and accurate payment allocation to PSSs is investigated. In this respect, a composite performance index is suggested and tested for contingency situations as well.

In order to proceed with the analysis of how to allocate the system savings to individual PSS, it is important to establish a mechanism to assess their impact on system stability after a disturbance. To this effect, based on system dynamics, three different criteria which will constitute the basis for obtaining valuable indices of performance, and ultimately a *goodness of the system* in various configurations.

6.4.1 Integral of Squared Error (ISE)

By means of an ISE criterion, a performance index expressed as the square of deviation in rotor angle variation from the steady-state value (J_{ISE}), is calculated. Mathematically, it is stated as in (6.5), where the above mentioned deviation is integrated from time $t = 0$ to the time when $\Delta\delta$ reaches steady-state value, $t = \infty$.

$$J_{ISE} = \int_0^{\infty} (\Delta\delta - \Delta\delta_{SS})^2 \cdot dt \tag{6.5}$$

6.4.2 Settling Time (TS) after a Small Perturbation

A performance index based on the settling time of the dynamic response after a perturbation is defined as follows:

$$\begin{aligned} J_{TS} &= \left|\Delta\delta_k - \Delta\delta_{k-1}\right| \le 0.03 \cdot \Delta\delta_{SS} \\ &\text{for at least 20 consecutive samples of } \Delta\delta \\ &\text{with a sampling interval of 10 ms} \end{aligned} \tag{6.6}$$

From (6.6) it is evident that oscillation of rotor angle deviation is considered to have reached its steady state value if it remains within a band of ±3% of $\Delta\delta_{SS}$ for at least 200 ms.

6.4.3 Peak Rotor-Angle Deviation (Peak $\Delta\delta$)

It is the highest rotor angle deviation from the steady-state; in other words it measures the highest amplitude of the rotor angle variation oscillation, usually at the first swing. Mathematically, the peak $\Delta\delta$ performance index is given as follows:

$$J_{Peak} = \max\left(\Delta\delta - \Delta\delta_{SS}\right) \tag{6.7}$$

6.4.4 Performance and Goodness Indices

In order to make use of the above three criteria, a formulation of a performance index which can be used as a base for comparison is needed. In a similar manner as outlined earlier, a minimum PSS is determined. In Table 6.8, the parameters of the optimal PSS and MPSS, are provided with the corresponding values of the three different performance indices. This time, the RPI (corresponding to MPSS) will have different values for each of the above criteria ($J_{ISE,ref}$, $J_{TS,ref}$ and $J_{Peak,ref}$ respectively). The current PSS in this table is same with the optimal PSS from previous chapter, and for the purpose of this analysis it is considered to be the given PSS, *i.e.* the actual PSS parameter settings in operation.

Notice that the value of the ISE performance index for the optimal PSS is different from the one reported in Table 6.1 – and that is because it is calculated only for the nominal operating point, and not for an operating domain.

Table 6.8 Minimum PSS, Optimal PSS and corresponding performance indices

		PSS	
		MPSS	**Current PSS**
Gain, pu	**Gen-1**	30	45.06
	Gen-2	–	45.52
	Gen-3	–	2.13
Time constant, sec	**Gen-1**	0.081	0.17
	Gen-2	–	0.06
	Gen-3	–	0.44
ISE Preformance Index, pu	J_{ISE}	146.93×10^{-6}	3.3422×10^{-6}
TS Performance Index, sec	J_{TS}	11.3	2.86
Peak $\Delta\delta$ Perf. Index, rad	J_{Peak}	0.005999	0.004662

Finally, for each of the three performance criteria described earlier, a new index, referred to as the *Goodness Index (GI)*, is defined below in a general form:

$$GI_{criterion} = (RPI_{criterion} - J_{criterion}) \tag{6.8}$$

In (6.8), the index *criterion* stands for each of the three earlier mentioned criteria (ISE, TS, Peak $\Delta\delta$).

The objective is to evaluate the contribution of a PSS to system dynamic performance and its worth in bringing about cost savings. All possible coalitions in which a PSS may participate are determined, and the set of optimal PSS parameters for each coalition, is obtained using the GA based PSS tuning method discussed in Chapter 3. Table 6.2 shows the various coalitions which can be formed by the generators and the corresponding optimal PSS parameters. It is to be noted that for coalitions C-2, C-3 and C-23, the system is not stable and hence these coalitions are not feasible.

In Table 6.9, the performance indices and their corresponding GIs are provided for feasible coalitions when the system is in a *normal operating state*, *i.e.* there are no contingencies and the generators are optimally dispatched.

Table 6.9 Performance index and GI for feasible coalitions with optimal PSS in normal operating state

	ISE		**Settling Time**		**Peak Rotor-Angle Deviation**	
Coalition *C*	J_{ISE}, **pu** $\times 10^{-6}$	***GI*, pu**	$J_{TS,}$ **sec**	***GI*, sec**	J_{Peak}, **rad**	***GI*, rad**
C-1	4.7623	142.1677	3.80	7.50	0.0046364	0.0013632
C-12	3.2329	143.6971	2.67	8.63	0.0045372	0.0014624
C-13	4.8068	142.1232	3.80	7.50	0.0046193	0.0013803
C-123	3.1116	143.8184	1.55	9.75	0.0044143	0.0015853

For all the performance criteria considered, the coalition C-13 exhibits the lowest *GI*, while the highest *GI* is in the grand coalition C-123.

6.5 System Savings as Affected by Choice of Performance Criteria

6.5.1 Savings to System

In this sub-section, for the performance indices described in the previous section, the savings concept, as outlined in Section 6.2.3, is obtained as follows:

a) Base savings – assuming a *cost of unserved energy* of \$100/MWh,

S_{base} = \$31,500

b) Savings rate

$$SR_{criterion} = S_{Base} / J_{REF,\,criterion} \tag{6.9}$$

For the system considered, *SR* for each criterion is as follows:

SR_{ISE} = 31,500/(146.93×10^{-6}) = 214.39×10^{6} \$/p.u. *RPI*

SR_{TS} = 31,500/11.3 = 2,787.61 \$/s

SR_{Peak} = 31,500/0.0059996 = 5,250,350 \$/rad

c) Incremental savings

$$\Delta S_{C,criterion} = SR \cdot GI_{C,criterion} \tag{6.10}$$

d) Total savings

$$S_{C,\,criterion} = S_{Base} + \Delta S_{C,\,criterion} \tag{6.11}$$

The total savings corresponding to all feasible coalitions are given in Table 6.10. The system exhibits the best performance – therefore achieves the highest savings – when in the grand coalition (C-123). These are the savings incurred by the ISO from having the PSS installed, optimally tuned and operating at all generators. As different criteria of performance assessment are being used, the savings quantum also varies accordingly, which is reasonably understood, since, in this specific work, the concept of savings relies on a subjective perception.

Table 6.10 Calculation of Savings from PSS operation

Coalition	ISE		Settling Time		Peak Rotor-Angle Deviation	
	***GI*, pu**	**Savings, \$**	***GI*, sec**	**Savings, \$**	***GI*, rad**	**Savings, &**
No PSS	Infeas.	–	Infeas.	–	Infeasible	–
MPSS	0.0	31,500.00	0.0	31,500.00	0.0	31,500.00
C-1	142.168	61,979.02	3.80	52,407.08	0.0046364	38,657.28
C-12	143.697	62,306.91	2.67	55,557.08	0.0045372	39,178.11
C-13	142.123	61,969.48	3.80	52,407.08	0.0046193	38,747.06
C-123	143.818	62,332.91	1.55	58,679.20	0.0044143	39,823.38

6.5.2 Shapley Value Calculation

As argued earlier, the individual generators would be entitled to a payment in return for providing the PSS-Control ancillary service. Consequently, the ISO's problem is to allocate the savings achieved from PSS operation in a fair and rational manner.

In Section 5.3, the theoretical background of cooperative game theory and assessment of contribution of individual players in a game is discussed. The method to calculate Shapley values for each player in the game was also outlined. Using the approach described therein, the Shapley values for each PSS of our example system, are obtained as described in Table 6.11, 6.12 and 6.13 for the ISE, TS and peak $\Delta\delta$ performance criteria, respectively. From these tables, it can be observed that PSS-1 consistently receives the highest payoff, while PSS-3 receives the least payoff. The highest revenue allocation to PSS-1 can be explained as follows:

- As before, it is evident that all feasible coalitions always include PSS-1.
- None of the coalitions that do not include PSS-1 is stable.
- PSS-1 is the only PSS which by itself can stabilize the system, *i.e.* it is the only one-player feasible coalition

Hence, PSS-1 is the most critical of all the PSSs in the system, and therefore is entitled to such a large payment.

Table 6.11 Shapley value calculations for ISE performance index

C_i	C-1	C-2	C-3	C-12	C-13	C-23	C-123	ϕ_{ISE}
GI	142.1677	0	0	143.6971	142.1232	0	143.8184	
C_W	1/3	1/3	1/3	1/6	1/6	1/6	1/3	
S	61,979.02	0	0	62,306.91	61,969.48	0	62,332.91	
PSS-1								
ψ	61,979.02	–	–	62,306.91	61,969.48	–	62,332.91	**62,150.04**
ϕ_{PSS1}	20,659.67	–	–	10,384.48	10,328.25	–	20,777.64	
PSS-2								
ψ	–	0	–	327.8847	–	0	363.4302	**175.79**
ϕ_{PSS2}	–	0	–	54.647	–	0	121.1434	
PSS-3								
ψ	–	–	0	–	-9.54	0	26.005	**7.078**
ϕ_{PSS3}	–	–	0	–	-1.59	0	8.668	
System Savings, *S*								**62,332.91**

Table 6.12 Shapley value calculations for Settling-Time performance index

C_i	C-1	C-2	C-3	C-12	C-13	C-23	C-123	ϕ_{TS}
GI	7.5	0	0	8.63	7.5	0	9.75	
C_W	1/3	1/3	1/3	1/6	1/6	1/6	1/3	
S	52,407.08	0	0	55,557.08	52,407.08	0	58,679.2	
PSS-1								
ψ	52,407.08	–	–	55,557.08	52,407.08	–	58,679.2	**55,022.79**
$\phi_{PSS\,1}$	17,469.03	–	–	9,259.513	8,734.513	–	19,559.73	
PSS-2								
ψ	–	0	–	3,150	–	0	6,272.124	**2,615.708**
$\phi_{PSS\,2}$	–	0	–	525	–	0	2,090.708	
PSS-3								
ψ	–	–	0	–	0	0	3,122.124	**1,040.708**
$\phi_{PSS\,3}$	–	–	0	–	0	0	1,040.708	
System Savings, *S*								**58,679.2**

Table 6.13 Shapley value calculation for Peak $\Delta\delta$ performance index

C_i	C-1	C-2	C-3	C-12	C-13	C-23	C-123	ϕ_{Peak}
GI	0.001363	0	0	0.001462	0.00138	0	0.001585	
C_W	1/3	1/3	1/3	1/6	1/6	1/6	1/3	
S	38,657.28	0	0	39,178.11	38,747.06	0	39,823.38	
PSS-1								
ψ	38,657.28	–	–	39,178.11	38,747.06	–	39,823.38	**39,147.75**
$\phi_{PSS\,1}$	12,885.76	–	–	6,529.69	6,457.84	–	13,274.46	
PSS-2								
ψ	–	0	–	520.83	–	0	1,076.322	**445.58**
$\phi_{PSS\,2}$	–	0	–	86.806	–	0	358.77	
PSS-3								
ψ	–	–	0	–	89.78	0	645.268	**230.05**
$\phi_{PSS\,3}$	–	–	0	–	14.9635	0	215.089	
System Savings, *S*								**39,823.38**

It may also be noted from Table 6.10 that the sum of the total payoffs made by the ISO equals total savings accrued by it in the grand coalition.

Table 6.14 shows, for each criterion, the total savings of the system and their allocation to generators, both in absolute terms ($) and per cent. As observed earlier, PSS-1 receives the highest share of the payments. However, the payment distribution differs slightly with the assessment criteria.

In order to even out those differences and obtain a more relevant indication of a generator's contribution, a *composite savings share* (CSS) is proposed as follows:

$$CSS = b_1 \cdot \phi_{ISE} + b_2 \cdot \phi_{TS} + b_3 \cdot \phi_{Peak} \tag{6.12}$$

where b_1, b_2 and b_3 are weights attached to each criterion and $b_1 + b_2 + b_3 = 1$. In this work, each criterion was given an equal weight, *i.e.* $b_1 = b_2 = b_3 = 1/3$. This is envisaged to lead to a more balanced distribution of savings, which also quantifies more accurately the contribution of all PSSs to system stability.

Table 6.14 Shapley values for different criteria and Average Savings Share for a generator under normal operation

	ISE Criterion	**Settling Time Criterion**	**Peak $\Delta\delta$ Criterion**	$J_{COMPOSITE}$
Total Savings, $	**62,332.91**	**58,679.204**	**39,823.38**	–
Gen-1	$62,150.04	$55,022.79	$39,147.75	52,106.86
	99.71%	93.77%	98.3%	97.16%
Gen-2	$175.79	$2,615.71	$445.58	1,079.03
	0.28%	4.46%	1.12%	1.95%
Gen-3	$7.08	$1,040.71	$230.05	425.95
	0.01%	1.77%	0.58%	0.79%

It is to be noted that while equal weights for each component have been used in (6.12), this need not necessarily be always the case. The ISO may choose to prioritize the criteria, depending on system conditions.

6.6 Savings Allocation under Contingency States

Once a method of allocating the savings is in place, it would be interesting to investigate whether the allocation thus obtained in a normal operating state, will still be a fair allocation in a contingency state when there is a change in system topology.

To this effect, a set of contingencies represented by outages of transmission lines, one at a time, is considered. Since there is no power flow solution in the case of line 4-5 outage, the contingency states with outage of the other lines are analyzed.

The *composite savings share*, in per cent, obtained in a similar manner as the one outlined in Table 6.14, for the normal and contingency states (lines on outage are given within the brackets) are also reported in Table 6.15.

Table 6.15 Average savings share (in %) allocated to a generator under normal operation and under contingencies

	Gen-1	**Gen-2**	**Gen-3**
Normal	97.259	1.953	0.788
CTG-1 (4-6)	93.761	6.737	-0.4979
CTG-2 (5-7)	97.191	2.095	0.7137
CTG-3 (6-9)	97.480	2.128	0.3912
CTG-4 (7-8)	94.413	4.180	1.4068
CTG-5 (8-9)	97.749	1.822	0.429

It can be observed, particularly in case of CTG-1 and CTG-4, that distribution of savings is considerably affected (see Table 6.15). In both cases, the share of Gen-1 is reduced by a few per cent points from the normal operating condition in favor of Gen-2. This implies that during these contingency states, Gen-2 plays a more important role in stabilizing the system and should be accordingly paid.

At the same time, in case of CTG-1, Gen-3 receives a negative share. This is because during this particular contingency the PSS on Gen-3 is acting in a detrimental manner for the system. This implies that in the payment function (5.3), ρ_{Vi} (for i = 3) is negative, and the generator's overall payment is negatively affected.

6.7 Concluding Remarks

In this chapter, the work of Chapter 5 is extended to the application of the game theoretic allocation of economic worth of PSS-control to a performance criterion based on the system dynamics.

It is demonstrated that the criteria used to assess a player's performance do influence the savings quantum and share allocation. Our results show that the *Integral of Squared Error* criterion yields the maximum savings to the system while the *Peak* $\Delta\delta$ criterion yields the minimum, among the three considered.

It should however be noted that this does not necessarily mean to rank the criteria. The objective here is to provide the system operator with a flexible choice of possibilities for calculation of system savings and hence its allocation; it is, ultimately, the system operator's decision as to which criterion is more relevant for the system. In this chapter, a composite criterion, which is

an average of all criteria considered, has been used in order to obtain a more accurate allocation of savings.

For the example system considered, it has been demonstrated how the total system savings from the grand coalition are allocated to the three PSSs. It was observed that PSS-1 received the highest payoff, thereby reflecting its importance to system stability. On the other hand, PSS-3 was detrimental to system savings as well as system stability in certain contingency situations. Hence it received the least payoff, or even a negative payoff. Given its dynamic behavior apparently detrimental to system, the case in which the PSS-3 is instructed to remain off-line is investigated, and the simulations show that the system dynamic behavior is not significantly affected.

The savings share allocation method is applied for the same system under contingencies, and it was revealed that the PSSs contribution to system dynamic performance changes, and consequently, their savings shares. Therefore it is important to recognize the need of re-scheduling the payment scheme in certain system operating conditions.

7 SUMMARY AND CONCLUSIONS

The work presented in this thesis focuses on aspects related to PSSs tuning and evaluation of their contribution to system stability and security from an economic perspective in the context of ancillary services. Thus, a GA based method to simultaneously tune PSSs is developed in the first part of this thesis, while the second is dedicated to a game theory based method to financially compensate the PSSs for the control effort they provide for the power system.

The GA based parameter optimization method developed in this thesis is applied to tune the lead-lag, derivative and PID types of PSS. A Lyapunov method based parameter optimization incorporating an ISE criterion has been used within the GA process of tuning the lead-lag and derivative types. On the other hand, in case of PID PSS, the ISE criterion was modified to fit the discrete-time representation of the power system.

One of the primary requirements of a good tuning method is that the resulting PSS be robust enough to wide variations in system parameters, while also being computationally manageable. In this respect, the proposed GA based tuning method provides highly satisfactory results. Conventional approaches, which consider one nominal operating condition, have been applied to tuning of lead-lag and derivative PSS. Investigations reveal that the classical approach does provide satisfactory performances for operating conditions up to the nominal, but deteriorated responses as the load increases further. Moreover, the classically tuned PSS fails to stabilize the system at certain operating conditions. The proposed GA based method, on the other hand, provides the option of including any operating point within its tuning domain, thus ensuring system stability over a large domain – even larger than the tuning domain.

Although the design method is meant to merely cope with small-signal stability phenomena, when tested for transients (*e.g.* three-phase short-circuits) and contingencies (*e.g.* transmission line outages) the system performed satisfactory, as well.

The second broad topic this thesis dwells upon is concerned with PSSs operation in the new deregulated environment. It is argued that, as the power systems of today move from a monopolistic to a decentralized operating environment, and as PSS control action has a significant impact on power system security, it should be regarded as a system ancillary service within the NERC Operating Policy guidelines for Interconnected Operations Services. To this effect, a scheme for allocating payoffs to generators for their PSS-control services based on cooperative game theory, using the concept of Shapley values, is proposed. By virtue of this approach, the system benefit accrued from a generator providing PSS-control service is allocated in a rational and equitable manner. The payoff scheme is based on weighted marginal contribution of a PSS in all coalitions (not only the actual contribution it has in its nominal operating status) it may be part of, thus reflecting better the role and importance of that PSS to the system.

The proposed method concentrates on determining the relative contribution to system security enhancement of the various PSSs present in the system, and not directly dependent on specific "dollar figures," which are assumed to be the result of contractual agreements between the service providers and the ISO. A realistic scenario represented by a 24-hour load curve obtained with three different load types and by considering an N-1 contingency criterion, reveals that the loading conditions and system topology affect the payments to generators. Therefore, it is important to recognize the need of re-scheduling the payment scheme in accordance to actual load levels and system topology.

Application of the proposed game theoretic allocation method is further extended to design a performance criterion based on the system dynamics. It is demonstrated how various criteria used to assess a player's performance do influence the savings quantum and share allocation. The results, among the three criteria considered, show that the ISE criterion yields the maximum savings to the system while the *Peak* $\Delta\delta$ criterion yields the least savings. However, the ISO is ultimately responsible to choose the most appropriate criteria that are relevant to the system.

In order to obtain a more accurate allocation of savings, a composite criterion has also been used. The savings share allocation method is applied for the same system under contingencies, and it was revealed that the PSSs savings shares change, consistently with their contribution to system dynamic performance.

It is important to note that although this thesis discusses the issue of payments to generators within a deregulated market environment, it does not propose a "market for PSS-control service" as such, but only a payoff mechanism, to "entice" generators to participate in a cooperative and coherent environment, under the jurisdiction of an ISO, or a similar entity.

7.1 Salient Features of this Work

- The thesis provides a detailed description of the development of the system mathematical models, both for single-machine infinite bus, as well as the multi-machine system under small perturbations. These models are generic enough and can be applied to large-sized power systems.
- An exhaustive analysis of classical tuning methods applicable to lead-lag and derivative PSS is provided and a comparison of performances achieved by systems having PSS designed using these methods is presented.
- The thesis proposes a novel approach to tune lead-lag PSS using a GA with a Lyapunov method of parameter optimization incorporated within its objective function. The main feature of this method is that it is a time-domain approach and uses a performance criterion which accurately quantifies the dynamic performance of the system under perturbation. The genetic process further uses this in the individuals' fitness assignment stage as a measure of one's quality, thereafter creating a sound basis to finding the best individual in the population.
- The GA based optimization approach is also applied for tuning of PID PSS. The main feature of this approach is that, since the PID PSS acts in discrete mode, the system model has been developed in discrete-time domain. An optimal sampling period has been determined considering the conflicting requirements of computation time versus accuracy of information on system dynamics due to discretization.
- In the context of the new deregulated environment, the thesis introduces the concept of *PSS-control* as an ancillary service. A game theoretic approach which uses the Shapley value criterion is developed and used to allocate payoffs to PSSs, in return for the system welfare they bring about by providing this service.
- The payoff allocation scheme takes into consideration not only the actual contribution a PSS has in its nominal operative status, but the weighted marginal contribution that PSS would have in all coalitions it may be part of, thus establishing the basis to attain an equitable solution for all participants.
- In order to obtain a fair allocation of payoffs, the way the performance of the PSSs is evaluated is very important. This thesis analyses two different types of approaches: one that measures the enhancement in system transfer capability due to PSS-control action, and another one that quantifies the contribution of PSSs in power system oscillations damping when the system is subjected to small perturbations.

7.2 Scope for Future Work in this Area

Tuning of PSS has been a challenging problem for power engineers and although a lot of work has been reported in this area, several issues remain unresolved, particularly in the context of a deregulated environment. Based on the work reported in this thesis, some of the issues that need to be further addressed within the same framework are briefly outlined.

- The system investigated has been limited up to a three generator, nine bus system. It would be desirable to examine GA based PSS tuning for larger and more realistic systems.
- As mentioned in one of the earlier chapters, siting of PSS is an important issue, more so, when the system size increases considerably. It is thus important to examine the GA based PSS tuning method while incorporating the PSS siting issues.
- The systems considered in the thesis assume that the loads are constant impedance loads. It would be of interest to the designer to understand how the dynamics of the system will be affected by the load dependence on voltage and consequently, how the optimal PSS parameters will be affected.
- The powerful properties of GA based optimization can be further exploited to examine various other controller structures and determine their globally optimal settings.
- Test and implement different genetic algorithm strategies (*e.g.* multi-population, multi-objective) in an attempt to achieve a less time consuming process and gain better understanding of genetic algorithms applicability to various power system phenomena.

As argued in the second part of the thesis, operation of PSS could qualify for financial compensation from the ISO as an ancillary service. However, before such a payoff scheme is implemented in deregulated systems, several issues need to be resolved therein as well. Some of the pertinent ones are brought out here.

- There is a need to properly identify and come into an agreement between participating entities of the deregulated system, as to how to quantify the "benefit" accrued from a PSS in the system. This thesis has attempted to address this issue to some extent. However, more detailed analysis is called for, before such schemes can be implemented in practice.
- Since the game theoretic allocation of payoffs method proposed in this thesis involves determining each possible coalition in which a PSS may participate, it would lead to high a computational burden for large systems

with many PSS. There is a need to develop appropriate computational tools to address this issue.

8 REFERENCES

[1] P. Kundur, ”A Course on Power Stability and Control,” ABB T&D University, Ludvika, Sweden, April 2000.

[2] “Western Electricity Coordinating Council Policy Statement on Power System Stabilizers” [Online]. Available: http://www.wecc.biz

[3] “General Transmission System Design Requirements for the Interconnection of New Generators (Resources) to The NEPOOL System” [Online]. Available: http://www.iso-ne.com

[4] B.E. Eliasson, “Damping of Power Oscillations in Large Power Systems”, PhD thesis TFRT-1032, Department of Automatic Control, Lund University of Technology, Lund, Sweden, May 1990.

[5] B.E. Eliasson and D.J. Hill, “Damping Structure and Sensitivity in the Nordel Power System”, IEEE Transactions on Power Systems, Vol. 7, No. 1, February 1992, pp. 97-105.

[6] F.P. DeMello and C. Concordia, “Concepts of synchronous machines stability as affected by excitation control,” IEEE Trans. on Power Apparatus and Systems, Vol. PAS-88, April 1969, pp. 316-329.

[7] W.G. Heffron, R.A. Phillips, “Effect of modern amplidyne voltage regulator on under-excited operation of large turbine generators,” AIEE Transactions on Power Apparatus and Systems, Vol. PAS-71, August 1952, pp. 692-697.

[8] E.V. Larsen and D.A. Swann, “Applying power system stabilizers. Part I: General concepts; Part II: Performance objectives and tuning concepts; Part III: Practical considerations,” IEEE Transactions on Power Apparatus and Systems, Vol. PAS-100, June 1981, pp. 3017-3046.

[9] P. Kundur, M. Klein, G.J. Rogers and M.S. Zywno, “Application of power system stabilizers for enhancement of overall system stability,” IEEE Transactions on Power Systems, Vol. 4, May 1989, pp. 614-626.

[10] Y.N. Yu and C. Siggers, "Stabilization and optimal control signals for a power system," IEEE Transactions on Power Apparatus and Systems, Vol. PAS-90, July/August 1971, pp. 1469-1481.

[11] H.A.M. Moussa and Y.N. Yu, "Optimal power system stabilization through excitation and/or governor control," IEEE Transactions on Power Apparatus and Systems, Vol.PAS-91, May/June 1972, pp. 1166-1174.

[12] F.P. DeMello, P.J. Nolan, T.F. Laskowski and J.M. Undrill, "Co-ordinated application of stabilizers in multi-machine power systems", IEEE Transactions on Power Apparatus and Systems, Vol. PAS-99, May/June 1980, pp. 892-901.

[13] R.J. Fleming, M.A. Mohan and K. Parvatisam, "Selection of parameters of stabilizers in multi-machine power systems," IEEE Transactions on Power Apparatus and Systems, Vol.PAS-100, May 1981, pp. 2329-2333.

[14] O.H. Abdalla, S.A. Hassan and N.T. Tweig, "Co-ordinated stabilization of a multi-machine power system," IEEE Transactions on Power Apparatus and Systems, Vol. PAS-103, Mar. 1984, pp. 483-494.

[15] A. Doi and S. Abe, "Coordinated synthesis of power system stabilizers in multimachine power systems," IEEE Transactions on Power Apparatus and Systems, Vol. PAS-103, June 1984, pp.1473-1479.

[16] C.M. Lim and S. Elangovan, "Design of stabilizers in multi-machine power systems", Proceedings of IEE, Part-C, Vol.132, May 1985, pp. 146-153.

[17] C.M. Lim and S. Elangovan, "New approach to power system stabilizer design," Electric Power Systems Research, Vol.8, 1985, pp. 285-292.

[18] S. Elangovan and C.M. Lim, "Efficient pole-assignment method for designing stabilizers in multi-machine power systems," Proceedings of IEE, Part-C, Vol. 134, November 1987, pp.383-384.

[19] A. Ghosh, G. Ledwich, O.P. Malik and G.S. Hope, "Power system stabilizer based on adaptive control techniques," IEEE Transactions on Power Apparatus and Systems, Vol. PAS-103, August 1984, pp. 1983-1989.

[20] S.J. Cheng, Y.S. Chow, O.P. Malik and G.S. Hope, "An adaptive synchronous machine stabilizer," IEEE Transactions on Power Systems, Vol. PWRS-1, August 1986, pp.101-109.

[21] S.J. Cheng, O.P. Malik and G.S. Hope, "Damping of multi-modal oscillations in power systems using a dual-rate adaptive stabilizer," IEEE Transactions on Power Systems, Vol. PWRS-3, February 1988, pp. 101-108.

[22] C.M. Lim, "A self-tuning stabilizer for excitation or governor control of power systems," IEEE Trans. on Energy Conversion, Vol. 4, June 1989, pp. 152-159.

[23] C.M. Lim and T. Hiyama, "Self-tuning control scheme for stability enhancement of multi-machine power systems," Proceedings of IEE, Part-C, Vol.137, July 1990, pp.269-275.

[24] C.M. Lim and T. Hiyama, "Application of a self-tuning control scheme to a power system with multi-mode oscillations," Electric Power Systems Research, Vol.24, 1992, pp.91-98.

[25] T. Hiyama, "Application of rule-based stabilizing controller to electric power system," Proceedings of IEE, Part-C, Vol.136, May 1989, pp. 175-181.

[26] T. Hiyama, "Rule-based stabilizer for multi-machine power system," IEEE Transactions on Power Systems, Vol. PWRS-5, May 1990, pp. 403-411.

[27] W.C. Chan and Y.Y. Hsu, "An optimal variable structure stabilizer for power system stabilization," IEEE Transactions on Power Apparatus and Systems, Vol. PAS-102, June 1983, pp. 1738-1746.

[28] M.L. Kothari, J. Nanda, K. Bhattacharya, “Design of variable structure power system stabilizers with desired eigenvalues in the sliding mode,” IEE Proceedings-C (Generation, Transmission and Distribution), Vol. 140, No. 4, July 1993, pp. 263-268.

[29] K. Bhattacharya, M.L. Kothari, J. Nanda, "Design of discrete-mode variable structure power system stabilizers," Electrical Power & Energy Systems, Vol. 17, No. 16, 1995, pp. 399-406.

[30] Y.Y. Hsu and C.H. Cheng, "Design of fuzzy power system stabilisers for multimachine power systems," IEE Proceedings, Vol. 137, Part C, No. 3, May 1990.

[31] P. Hoang and K. Tomsovic, "Design and analysis of an adaptive fuzzy power system stabilizer," IEEE Transactions on Energy Conversion, Vol. 11, Dec. 1996, pp. 455 - 461.

[32] Y. Zhang, G.P. Chen, O.P. Malik, G.S. Hope, "An artificial neural network based adaptive power system stabilizer," IEEE Transactions on Energy Conversion, Vol. 8, No. 1, March 1993.

[33] R. Segal, M.L. Kothari and S. Madnani, "Radial basis function (RBF) network adaptive power system stabilizer," IEEE Transactions on Power Systems, Vol. 15, May 2000, pp. 722-727.

[34] M.A. Abido and Y.L. Abdel-Magid, "A hybrid neuro-fuzzy power system stabilizer for multimachine power systems," IEEE Transaction on Power Systems, Vol. 13, No. 4, November 1998.

[35] N. Mithulananthan, C.A. Cañizares, J. Reeve, G.J. Rogers, "Comparison of PSS, SVC and STATCOM Controllers for Damping Power System Oscillations", IEEE Transactions on Power Systems, Vol. 18, No. 2, May 2003, pp. 786-792.

[36] J.H. Holland, *Adaptation in Natural and Artificial Systems*, University of Michigan Press, Ann Arbor, Michigan, 1975.

[37] M.A. Abido and Y.L. Abdel-Magid, "Hybridizing rule-based power system stabilizers with genetic algorithms," IEEE Transactions on Power Systems, Vol.14, May 1999, pp. 600-607.

[38] Y.L. Abdel-Magid, M.A. Abido, S. Al-Baiyat and A.H. Mantawy, "Simultaneous stabilization of multi-machine power systems via genetic algorithms," IEEE Transactions on Power Systems, Vol. 14, November 1999, pp. 1428-1439.

[39] Y.L Abdel-Magid, M.A. Abido, "Optimal multiobjective design of robust power system stabilizers using genetic algorithms," IEEE Transactions on Power Systems, Vol. 18, No. 3 , August 2003, pp.1125-1132

[40] P. Zhang and A.H. Coonick, "Coordinated Synthesis of PSS Parameters in Multi-Machine Power Systems Using the Method of Inequalities Applied to Genetic Algorithms," IEEE Transactions on Power Systems, Vol. 15, No. 2, May 2000, pp. 811-816.

[41] A.L.B. Do Bomfim, G.N. Taranto, D.M. Falcao, "Simultaneous tuning of power system damping controllers using genetic algorithms," IEEE Transactions on Power Systems, Vol. 15, No. 1, February 2000, pp. 163-169

[42] "NERC Operating Policy-10 on Interconnected Operation Services," North Amer. Elect. Reliability Council, Draft-3.1, 2000.

[43] K. Bhattacharya, M.H.J. Bollen and J.E. Daalder, *Operation of restructured power systems*, Kluwer Academic Publishers, USA, 2001.

[44] F. Forgó, J. Szép and F. Szidarovszky, *Introduction to the Theory of Games – Concepts, Methods, Applications*, Kluwer Academic Publishers 1999.

[45] Y. Tsukamoto and I. Iyoda, "Allocation of fixed transmission cost to wheeling transactions by cooperative game theory," IEEE Trans on Power Systems, Vol. 11, May 1996, pp. 620-629.
[46] J. Contreras and F. Wu, "Coalition formation in transmission expansion planning," IEEE Trans. Power Syst., Vol. 14, pp. 1144–1152, Aug. 1999.
[47] J. Contreras and F. Wu, "A kernel-oriented coalition algorithm for transmission expansion planning," IEEE Trans. on Power Systems, Vol. 15, November 2000, pp. 919-925.
[48] J.M. Zolezzi and Hugh Rudnick, "Transmission Cost Allocation by Cooperative Games and Coalition Formation," IEEE Transactions on Power Systems, Vol. 17, No. 4, November 2002, pp. 1008-1015.
[49] X.H. Tan and T.T. Lie, "Allocation of transmission loss cost using cooperative game theory in the context of open transmission access," IEEE-PES Winter Meeting 2001, Vol. 3, January 2001, pp. 1215-1219.
[50] M. Fahrioglu and F.L. Alvarado, "Designing incentive compatible contracts for effective demand management," IEEE Trans. on Power Systems, Vol. 15, No. 4, November 2000, pp. 1255-1260.
[51] H. Song, C.C. Liu and J. Lawarree, "Nash equilibrium bidding strategies in a bilateral electricity market," IEEE Trans. on Power Systems, Vol. 17, No. 1, February 2003, pp. 73-79.
[52] C. Yeung, A. Poon, and F.Wu, "Game theoretical multi-agent modeling of coalition formation for multilateral trades," IEEE Trans. on Power Systems, Vol. 14, August 1999, pp. 929–934.
[53] X. Bai, S. M. Shahidehpour, V. C. Ramesh, Y. Erkeng, "Transmission analysis by Nash game method," IEEE Transactions on Power Systems, Vol. 12, August 1997, pp.1046-1052.
[54] R.W. Ferrero, S.M. Shahidehpour, V.C. Ramesh, "Transaction analysis in deregulated power systems using game theory," IEEE Transactions on Power Systems, Vol. 12, August 1997, pp.1340-1347.
[55] P.M. Anderson and A.A. Fouad, *Power system control and stability*, Iowa State University Press 1977.
[56] P. Kundur, *Power System Stability and Control*, McGraw-Hill Inc. 1994.
[57] Yao-Nan Yu, *Electric Power System Dynamics*, Academic Press 1983.
[58] Y.N. Yu and Q.H. Li, "Pole-placement power system stabilizers design of an unstable nine-machine system", IEEE Transactions on Power Systems, Vol. PWRS-5, May 1990, pp. 353-358.
[59] D.E. Goldberg, *Genetic Algorithms in Search, Optimization and Machine Learning*, Addison-Wesley Publishing Company Inc., January 1989.
[60] K. Bhattacharya, J. Nanda and M.L. Kothari, "Optimization and performance analysis of conventional power system stabilizers", International Journal of Electrical Power & Energy Systems, Vol. 19, 1997, pp. 449-458.
[61] Y.L. Abdel-Magid, M. Bettayeb, M.M. Dawoud, "Simultaneous stabilization of power systems using genetic algorithm," IEE Proceedings- Generation, Transmission and Distribution, Vol. 144, No. 1, January 1997.
[62] K. Bhattacharya, M.L. Kothari, J. Nanda, M. Aldeen and A. Kalam, "Tuning of power system stabilizers in multi-machine systems using ISE technique", Electric Power Systems Research, Vol. 46, 1998, pp. 119-131.

[63] C.J. Wu and Y.Y. Hsu, "Design of self-tuning PID power system stabilizer for multi-machine power systems", IEEE Transactions on Power Systems, August 1988, pp. 1059-1064.

[64] P.K. Dash, A.C. Liew and B.R. Mishra, "An adaptive PID stabilizer for power systems using fuzzy logic", Electric Power Systems Research, Volume 44, March 1998, pp. 213-222.

[65] Y.P. Wang, N.R. Watson and H. H. Chong, "Modified genetic algorithm approach to design of an optimal PID controller for AC-DC transmission systems", International Journal of Electrical Power & Energy Systems, Volume 24, Jan 2002, pp. 59-69.

[66] G. Strbac, S. Ahmed, D. Kirschen and R. Allan, "A method for computing the value of corrective security," IEEE Trans. on Power Systems, Vol. 13, No. 3, pp. 1096–1102, August 1998.

[67] F. C. Schweppe, W. C. Caramanis, R. D. Tabors, and R. E. Bohn, *Spot Pricing of Electricity*, Kluwer Academic Publisher, 1988.

[68] R. J. Kaye, F. F. Wu and P. Varaiya, "Pricing for System Security," *IEEE Transactions on Power Systems*, Vol. 10, No. 2, pp. 575–583, May 1995.

[69] F. Alvarado, Y. Hu, D. Ray, R. Stevenson and E. Cashman, "Engineering foundations for the determination of security costs," IEEE Transactions on Power Systems, Vol. 6, No. 3, pp. 1175–1182, August 1991.

[70] W. D. Rosehart, C. A. Cañizares, and V. Quintana, "Multi-objective optimal power flows to evaluate voltage security costs in power networks," IEEE Transactions on Power Systems, Vol. 18, No. 2, May 2003, pp. 578-587.

[71] F. Milano, C.A. Cañizares, and M. Ivernizzi, "Multi-objective optimization for pricing system security in electricity markets," IEEE Transactions on Power Systems, Vol. 18, No. 2, May 2003, pp. 596-604.

[72] H. Chen, C. A. Cañizares, and A. Singh, "Transaction security cost analysis by take-risk strategy," Proceedings of the Power Systems Computation Conference (PSCC), Spain, June 2002.

[73] D. Chattopadhyay, "An energy brokerage system with emission trading and allocation of cost savings," IEEE Transactions on Power Systems, Vol. 10, No. 4, November 1995.

[74] X. Tan, T.T. Lie, "Application of the Shapley value on transmission cost allocation in the competitive power market environment," IEE Proc.-Gener. Transm. Distrib., Vol. 149, No. 1, January 2002, pp. 15-20.

[75] L. Shapley,"Contributions to the theory of games," *Annals of Math Studies*, Princeton University Press 1953, Vol. II, No. 28, pp. 307-317.

[76] J. C. Harsanyi, *Rational behavior and bargaining equilibrium in games and social situations*, Cambridge University Press 1977.

[77] T. Alvey, D. Goodwin, X. Ma, D. Streiffert and D. Sun, "A security constrained bid clearing system for the New Zealand wholesale electricity market," IEEE Transactions on Power Systems, May 1998, pp.340-346.

[78] The National Grid Company plc., NGC Reactive Market Report: Fifth Tender Round for Obligatory and Enhanced Reactive Power Services, May 2000.

[79] P. Gomes, N. Martins, F.P. DeMello and X. Vieira Filho, "Assuring system reliability in a competitive environment" Proc. CIGRE, 1998, Paper No.38-104.

[80] A. Andreoiu, K. Bhattacharya, "Robust tuning of power system stabilisers using a Lyapunov method based genetic algorithm," IEE Proceedings – Generation, Transmission and Distribution, Vol. 149, No. 5, September 2002, pp. 585-592.

[81] A.A.P. Perm, C.A. Cañizares, N. Mithulananthan, "Effects of Limits in Small Signal Stability Analysis of Power Systems", IEEE Power Engineering Society Summer Meeting 2001, Vol. 3, pp. 1805-1810.

LIST OF PUBLICATIONS

I. **A. Andreoiu**, K. Bhattacharya, "Robust Tuning of Power System Stabilizers Using Lyapunov Method Based Genetic Algorithm", IEE Proceedings on Generation, Transmission and Distribution, Vol. 149, No. 5, September 2002, pp. 585-592.

II. **A. Andreoiu**, K. Bhattacharya, "Lyapunov's Method Based Genetic Algorithm for Multi-Machine PSS Tuning," Proceedings of IEEE PES Winter Meeting, New York, USA, January 27-31, 2002.

III. **A. Andreoiu**, K. Bhattacharya, "Genetic Algorithm Based Tuning of PID Power System Stabilizers," Proceedings of the 14th Power System Computation Conference, Seville, Spain, June 24-28, 2002.

IV. **A. Andreoiu**, K. Bhattacharya, "A Lyapunov Method Based Genetic Algorithm for a Robust PSS Tuning," Euro Conference on Risk Management in Power Systems and Operation in Market Environment, Porto, Portugal, September 8-11, 2001.

V. **A. Andreoiu**, K. Bhattacharya, C. Cañizares, "Pricing Power System Stabilizers Using Game Theory," IEEE Transactions on Power Systems (under review).

VI. **A. Andreoiu**, K. Bhattacharya, "Game Theory Based Evaluation of PSS-Control Effort," IEE Proceedings on Generation, Transmission and Distribution (under review).

VII. **A. Andreoiu**, K. Bhattacharya, "PSS-Control as an Ancillary Service," International Journal of Electric Power System Research (under review).

LIST OF SYMBOLS AND ACRONYMS

Notation

Throughout this work, following conventions were adopted:

- a bar on top of a symbol denotes a phasor or a complex number (*e.g.* $\overline{V}, \overline{S}$)
- a dot on top of a symbol denotes the first derivative of a variable (*e.g.* $\dot{x}$)
- bold face symbols denote matrices (*e.g.* **A**, **Y**)
- underlined symbols denote vectors (*e.g.* $\underline{V}, \underline{I}$)
- upper case symbols denote rms values

Symbols

A	state (plant) matrix of the system
B	control matrix
D	damping coefficient
Γ	perturbation matrix
P	active power
Q	reactive power
Q	weighing matrix
H	inertia constant
I_d, I_q	direct- and quadrature-axis components of armature current
M	inertia coefficient
δ	rotor angle
Δ	denotes small perturbation or deviation of a variable from its steady-state value
x_d, x_q	synchronous reactances in *d*- and *q*-axis, respectively
x_d'	direct-axis transient reactance
x_q	quadrature-axis reactance
E_{fd}	equivalent excitation voltage (field circuit voltage)
E_q'	*q*-axis component of the transient emf proportional to the field winding flux linkages
f	frequency
J	performance index

K_A , T_A	AVR gain and time constant, respectively
K_C	lead-lag PSS gain
K_d	derivative PSS gain
K_P, K_D, K_I	proportional, derivative and integral gains of a PID-PSS
T_W	PSS wash-out time constant
T_m, T_e	mechanical and electrical torque, respectively
T_{do}'	time constant of excitation circuit
T_S	sampling time
V_d, V_q	direct and quadrature components of terminal voltage
$\mathbf{Y}$	admittance matrix
$T_1, \ldots T_4$	lead/lag PSS time constants
$\underline{X}$	state vector
b	weights attached to considered criteria
$\underline{p}$	perturbation vector
s	Laplace operator
t	time
u	stabilizing signal
C	set of coalitions
GI	goodness index
i	index for players in the game
ρ_V	PSS-control variable payment component
ρ_F	PSS-control fixed payment component
C_W	weight on a coalition
$\psi(C)$	marginal contribution of a player in a coalition
GI	goodness index
J_{ref}	reference performance index
K_c	PSS gain
n	total number of players
N	set of all n players/generators
r	size of a coalition
S	savings
SR	savings rate
ΔS	incremental savings
T_w	PSS wash-out filter time constant
u_i	control signal from i^{th} PSS
$v(C)$	payoff from a coalition (or savings)
$\Delta\delta$	rotor-angle deviation
$\Delta\delta_{SS}$	steady-state value of $\Delta\delta$
ω	angular velocity of generator
ρ	payment function
ϕ	weighted average of the marginal contributions of a player in all possible coalitions (Shapley value)

Acronyms

ac	alternating current
ANN	Artificial Neural Networks
AVR	Automatic Voltage Regulator
CTG	contingency
CSS	composite savings share
d	direct axis of a generator
dc	direct current
FACTS	Flexible AC Transmission System
GA	Genetic Algorithm
GEP	Generator Exciter Power system
ISE	Integral of Squared Error
ISO	Independent System Operator
MIMO	Multi Input Multi Output
MPSS	Minimum PSS
NEPOOL	New England Pool
OLS	Orthogonal Least Squares
PSS	Power System Stabilizer
PID	Proportional-Integral-Derivative
q	quadrature axis of a generator
RBF	Radial Basis Function
RLS	Recursive Least Squares
SMIB	Single Machine to Infinite Bus
SISO	Single Input Single Output
STATCOM	Static Synchronous Compensators
TGR	Transient Gain Reduction
VSC	Variable Structure Control
VSCPSS	Variable Structure PSS
WECC	Western Electricity Coordinating Council

9 APPENDICES

9.1 Appendix I

9.1.1 Network Reduction

The size of the network model can be reduced by matrix operation, since all nodes have zero injection currents except for the internal generator nodes. This is shown below.

Let $\bar{\mathrm{I}} = \overline{\mathbf{Y}} \cdot \overline{\mathrm{V}}$ (9.1)

where $\overline{\mathrm{V}}$ is the bus voltage vector, $\overline{\mathbf{Y}}$ is the admittance matrix of the system and $\bar{\mathbf{I}}$ is the bus current vector. Therefore,

$$\bar{\mathbf{I}} = \begin{bmatrix} \bar{\mathbf{I}}_n \\ \bar{\mathbf{0}} \end{bmatrix} \tag{9.2}$$

Now the matrices $\overline{\mathbf{Y}}$ and $\overline{\mathbf{V}}$ are partitioned accordingly to get

$$\begin{bmatrix} \bar{\mathbf{I}}_n \\ \bar{\mathbf{0}} \end{bmatrix} = \begin{bmatrix} \overline{\mathbf{Y}}_{nn} & \overline{\mathbf{Y}}_{nr} \\ \overline{\mathbf{Y}}_{rn} & \overline{\mathbf{Y}}_{rr} \end{bmatrix} \begin{bmatrix} \overline{\mathbf{V}}_n \\ \overline{\mathbf{V}}_r \end{bmatrix} \tag{9.3}$$

where the subscript n is used to denote generator nodes and the subscript r is used for the remaining nodes (Figure 9.1). Thus for the analyzed system $\overline{\mathbf{V}}_n$, which now is the generator terminal voltage vector, has $(n \times 1)$ dimension and $\overline{\mathbf{V}}_r$ has $(r \times 1)$ dimension.

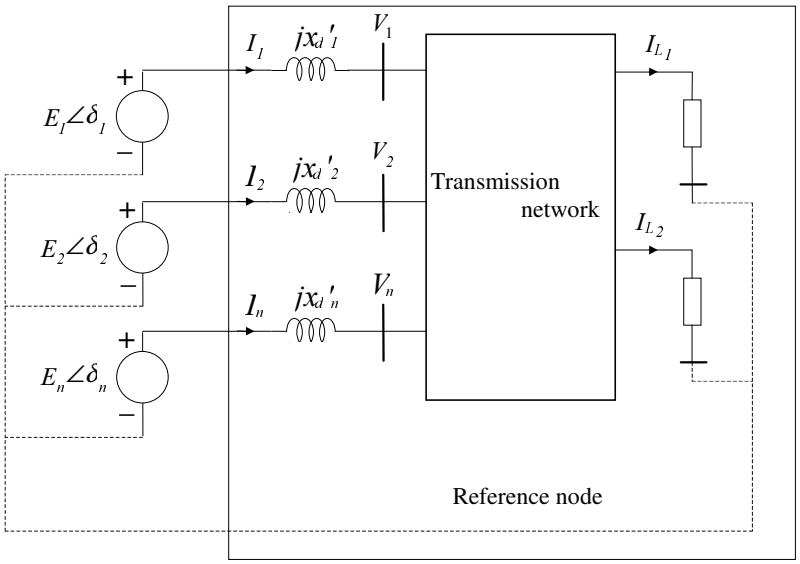

Figure 9.1 Multi-machine system representation

Expanding equation (9.3),

$$\begin{aligned} \bar{\mathrm{I}}_n &= \overline{\mathbf{Y}}_{nn} \cdot \overline{\mathrm{V}}_n + \overline{\mathbf{Y}}_{nr} \cdot \overline{\mathrm{V}}_r \\ \overline{0} &= \overline{\mathbf{Y}}_{rn} \cdot \overline{\mathrm{V}}_n + \overline{\mathbf{Y}}_{rr} \cdot \overline{\mathrm{V}}_r \end{aligned} \tag{9.4}$$

from which we eliminate $\overline{\mathrm{V}}$, to find

$$\bar{\mathrm{I}}_n = (\overline{\mathbf{Y}}_{nn} - \overline{\mathbf{Y}}_{nr} \cdot \overline{\mathbf{Y}}_{rr}^{-1} \cdot \overline{\mathbf{Y}}_{rn}) \cdot \overline{\mathrm{V}}_n \tag{9.5}$$

If $(\overline{\mathbf{Y}}_{nn} - \overline{\mathbf{Y}}_{nr} \cdot \overline{\mathbf{Y}}_{rr}^{-1} \cdot \overline{\mathbf{Y}}_{rn}) = \overline{\mathbf{Y}}_{\mathrm{m}}$ then (9.5) becomes: $\bar{\mathrm{I}}_n = \overline{\mathbf{Y}}_{\mathrm{m}} \cdot \overline{\mathrm{V}}_n$ (9.6)

The matrix $\overline{\mathbf{Y}}_{\mathrm{m}}$ is the desired reduced matrix of $\overline{\mathbf{Y}}$. It has the dimensions ($n \times n$), where n is the number of generators.

9.1.2 Small-signal Stability Models of Power Systems

The phasor diagram of the i^{th} machine of a multi-machine system may be shown as in Figure 9.2. While d_i and q_i are the system coordinate axes for the i^{th} machine alone, D and Q are the axes of the common system coordinates for all machines in the system. The phase-angle difference between d_i and D, or

q_i and Q, is denoted by δ_i, which is constantly changing and could be positive or negative.

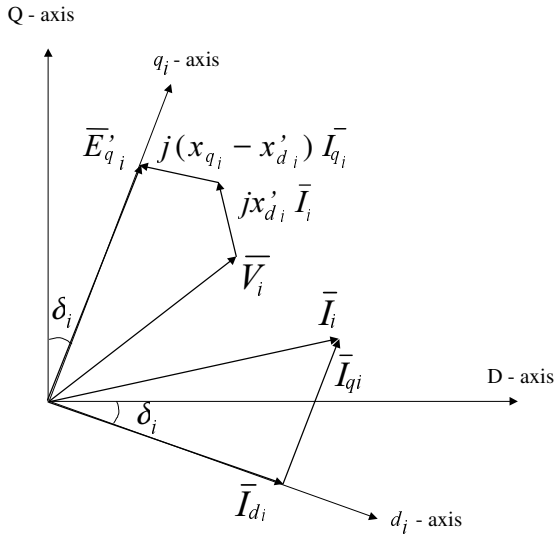

Figure 9.2 Phasor diagram of the i^{th} machine

Note: The upper bar stands for complex values. Since we look only into the reduced network (having only the generator nodes), we leave out the subscript *n* standing for generator nodes. Therefore, the terminal voltage $\overline{V}_i$ of the i^{th} machine of the system in common coordinates becomes:

$$\overline{V}_i = E'_{q_i} e^{j(90-\delta_i)} - j\,x'_{d_i}\bar{I}_i + (x_{q_i} - x'_{d_i})I_{q_i}e^{-j\delta_i} \quad (9.7)$$

Also note that

$$\overline{E}'_{q_i} = E'_{q_i} e^{j(90-\delta_i)}, \qquad \bar{I}_{q_i} = j\,I_{q_i} e^{-j\delta_i} \quad (9.8)$$

For the *n* machines of an multi-machine system, equation (9.7) becomes a system of *n* equations and may be written in matrix form as:

$$\overline{\mathbf{V}} = \left[e^{j(90-\delta)}\right]\cdot \mathbf{E}'_{\mathrm{q}} - j\cdot\left[x_d{}'\right]\cdot\bar{\mathbf{I}} + \left[x_q - x'_q\right]\cdot\left[e^{-j\delta}\right]\cdot\mathbf{I}_{\mathrm{q}} \quad (9.9)$$

where the coefficients $[e^{j(90-\delta)}]$, $[x_d']$, $[x_q - x_d']$, and $[e^{-j\delta}]$ should be read as diagonal matrices and $\overline{\mathbf{V}}$, $\mathbf{E}'_{\mathbf{q}}$, $\bar{\mathbf{I}}$, and $\bar{\mathbf{I}}_{\mathbf{q}}$ are column vectors of size *n*.

9.1.3 Armature Current Components

Substituting the solution of $\overline{\mathbf{V}}$ of (9.9) in (9.6) and solving for $\bar{\mathbf{I}}$ gives

$$\bar{\mathbf{I}} = \overline{\mathbf{Y}} \cdot ([e^{j(90-\delta)}] \cdot \mathbf{E}_{\mathbf{q}}^{'} - j \cdot [x_d'] \cdot \bar{\mathbf{I}} + [x_q - x_d'] \cdot [e^{-j\delta}] \cdot \bar{\mathbf{I}}_{\mathbf{q}}) \tag{9.10}$$

where

$$\overline{\mathbf{Y}} = (\overline{\mathbf{Y}}_{\mathrm{m}}{}^{-1} + j \cdot [x_d'])^{-1} \tag{9.11}$$

Note that the admittance matrix $\overline{\mathbf{Y}}$ in equation (9.11) refers to the reduced network, therefore differs from $\mathbf{Y}$ matrix from (9.1).

For the i^{th} machine of an n-machine system in D-Q coordinates, the current has n terms

$$\bar{I}_i = \sum_{j=1}^{n} \overline{Y}_{ij} [e^{j(90-\delta_j)} \cdot E_{q_j}^{'} + (x_{q_j} - x_{d_j}^{'}) \cdot e^{-j\delta_j} \cdot I_{q_j}] \tag{9.12}$$

including the term of $j = i$.

In d_i - q_i coordinates,

$$\begin{aligned} \bar{i}_i &= \overline{I}_i e^{j\delta_i} = \\ &= \sum_{j=1}^{n} Y_{ij} \cdot [e^{j(\beta_{ij}+\delta_{ij}+90)} E_{q_j}^{'} + (x_{q_j} - x_{d_j}^{'}) \cdot e^{-j(\beta_{ij}+\delta_{ij})} \cdot I_{q_j}] \end{aligned} \tag{9.13}$$

where $\overline{Y}_{ij} = Y_{ij} \cdot e^{j\beta_{ij}}$, $\qquad \delta_{ij} = \delta_i - \delta_j$ (9.14)

Therefore

$$\begin{aligned} i_{d_i} &= \mathrm{Re}(\bar{i}_i) = \sum_{j=1}^{n} Y_{ij} [-S_{ij} E_{q_j}^{'} + (x_{q_j} - x_{d_j}^{'}) C_{ij} I_{q_j}] \\ i_{q_i} &= \mathrm{Im}(\bar{i}_i) = \sum_{j=1}^{n} Y_{ij} [C_{ij} E_{q_j}^{'} + (x_{q_j} - x_{d_j}^{'}) S_{ij} I_{q_j}] \end{aligned} \tag{9.15}$$

where

$$C_{ij} = \cos(\beta_{ij} + \delta_{ij}), \qquad S_{ij} = \sin(\beta_{ij} + \delta_{ij}) \tag{9.16}$$

Let the deviation of $\bar{i}_i$ be defined by

$$\Delta(i_{d_i} + ji_{q_i}) = \Delta I_{d_i} + j\Delta I_{q_i} \tag{9.17}$$

Here *I* stands for currents in individual machine coordinates. Same rule will be applied for *V*.

From (9.15), for *n* machines, we will have

$$\begin{aligned} \Delta \underline{\mathrm{I}}_{\mathrm{d}} &= \mathbf{P}_{\mathrm{d}} \Delta \underline{\delta} + \mathbf{Q}_{\mathrm{d}} \Delta \underline{\mathrm{E}}_{\mathrm{q}}^{'} + \mathbf{M}_{\mathrm{d}} \Delta \underline{\mathrm{I}}_{\mathrm{q}} \\ \mathbf{L}_{\mathrm{q}} \Delta \underline{\mathrm{I}}_{\mathrm{q}} &= \mathbf{P}_{\mathrm{q}} \Delta \underline{\delta} + \mathbf{Q}_{\mathrm{q}} \Delta \underline{\mathrm{E}}_{\mathrm{q}}^{'} \end{aligned} \tag{9.18}$$

where

$$\begin{aligned} &P_{d_{ij}} = Y_{ij} \cdot [\, C_{ij} E_{q_j}^{'} + (x_{q_j} - x_{d_j}^{'})\, S_{ij} I_{q_j}\,] \\ &P_{q_{ij}} = Y_{ij} \cdot [\, S_{ij} E_{q_j}^{'} - (x_{q_j} - x_{d_j}^{'})\, C_{ij} I_{q_j}\,] \\ &P_{d_{ij}} = -\sum_{j \neq i} P_{d_{ij}}, \qquad P_{q_{ij}} = -\sum_{j \neq i} P_{q_{ij}} \\ &Q_{d_{ij}} = -Y_{ij} S_{ij}, \qquad Q_{q_{ij}} = Y_{ij} C_{ij}, \qquad j = 1,...,n \\ &L_{q_{ij}} = -Y_{ij}\, (x_{q_j} - x_{d_j}^{'})\, S_{ij} \qquad j \neq i \\ &L_{q_{ii}} = 1 - Y_{ii} (x_{q_i} - x_{d_i}^{'})\, S_{ii} \\ &M_{q_{ij}} = Y_{ij} (x_{q_j} - x_{d_j}^{'})\, C_{ij} \qquad j = 1,...,n \end{aligned} \tag{9.19}$$

The solutions for $\Delta \underline{\mathrm{I}}_{\mathrm{d}}$ and $\Delta \underline{\mathrm{I}}_{\mathrm{q}}$ of (9.18) become

$$\begin{aligned} \Delta \underline{\mathrm{I}}_{\mathrm{d}} &= \mathbf{Y}_{\mathrm{d}}\, \Delta \underline{\mathrm{E}}_{\mathrm{q}}^{'} + \mathbf{F}_{\mathrm{d}}\, \Delta \underline{\delta} \\ \Delta \underline{\mathrm{I}}_{\mathrm{q}} &= \mathbf{Y}_{\mathrm{q}}\, \Delta \underline{\mathrm{E}}_{\mathrm{q}}^{'} + \mathbf{F}_{\mathrm{q}}\, \Delta \underline{\delta} \end{aligned} \tag{9.20}$$

where

$$\begin{aligned} &\mathbf{Y}_{\mathrm{d}} = \mathbf{Q}_{\mathrm{d}} + \mathbf{M}_{\mathrm{d}} \mathbf{Y}_{\mathrm{q}}, \qquad \mathbf{F}_{\mathrm{d}} = \mathbf{P}_{\mathrm{d}} + \mathbf{M}_{\mathrm{d}} \mathbf{F}_{\mathrm{q}} \\ &\mathbf{Y}_{\mathrm{q}} = \mathbf{L}_{\mathrm{q}}^{-1}\, \mathbf{Q}_{\mathrm{q}}, \qquad \mathbf{F}_{\mathrm{q}} = \mathbf{L}_{\mathrm{q}}^{-1}\, \mathbf{P}_{\mathrm{q}} \end{aligned} \tag{9.21}$$

9.1.4 K-Constant Derivation

Having found the *d* and *q* current components including the transmission relation, K_1, ..., K_6 will be expressed using the electrical torque relation, internal voltage equation, and from the terminal voltage relation, as shown below.

An electric torque approximately equals an electric power when the synchronous speed is chosen as the base speed. Thus, for the i^{th} machine,

$$T_{e_i} \cong \mathrm{Re}(\bar{I}_{n_i}^{*} \cdot \bar{V}_{n_i}) = I_{q_i} E_{q_i}^{'} + I_{q_i} (x_{q_i} - x_{d_i}^{'})\, I_{d_i} \tag{9.22}$$

After linearization and for *n* machines, (9.22) becomes:

$$\Delta \underline{\mathrm{T}}_{\mathrm{e}} = \mathbf{K}_1 \cdot \Delta \underline{\delta} + \mathbf{K}_2 \cdot \Delta \underline{\mathrm{E}}_{\mathrm{q}}^{'} \tag{9.23}$$

where

$$\begin{aligned} \mathbf{K}_1 &= \mathbf{Q}_{\mathrm{t}} \cdot \mathbf{F}_{\mathrm{q}} + \mathbf{D}_{\mathrm{t}} \cdot \mathbf{F}_{\mathrm{d}} \\ \mathbf{K}_2 &= \mathbf{Q}_{\mathrm{t}} \cdot \mathbf{Y}_{\mathrm{q}} + \mathbf{D}_{\mathrm{t}} \cdot \mathbf{Y}_{\mathrm{d}} + \mathbf{I}_{\mathrm{q0}} \end{aligned} \tag{9.24}$$

in which $\mathbf{D_t}$, $\mathbf{Q_t}$ and $\mathbf{I_{q0}}$ are diagonal matrices with the elements as follows

$$\begin{aligned} D_{t_{ii}} &= (x_{q_i} - x_{d_i}^{'})\, I_{q0_i} \\ Q_{t_{ii}} &= (x_{q_i} - x_{d_i}^{'})\, I_{d0_i} + E_{q0_i}^{'} \\ I_{q0_{ii}} &= I_{q0_i} \end{aligned} \tag{9.25}$$

The component of torque given by $\mathbf{K_1}$ is in phase with $\Delta\delta$ hence representing a synchronizing torque component. The second term of ( ) represents the component of torque resulting from variations in field flux linkage.
The internal voltage equation for *n* machines may be written

$$(\mathbf{1} + s \cdot \mathbf{T}_{\mathrm{do}}{}') \cdot \Delta \underline{\mathrm{E}}_{\mathrm{q}}{}' = \Delta \underline{\mathrm{E}}_{\mathrm{fd}} - [x_d - x_d{}'] \cdot \Delta \underline{\mathrm{I}}_{\mathrm{d}} \tag{9.26}$$

where **1** is the unity matrix and $\mathbf{T_{do}'}$ a diagonal matrix. Substituting $\Delta\underline{\mathrm{I}}_{\mathrm{d}}$ of (9.20) in (9.26) and shifting terms gives

$$(1 + sT_{do_i}^{'} K_{3_{ii}})\, \Delta E_{q_i}^{'} = K_{3_{ii}} \left(\Delta E_{fd_i} - \sum_{j \neq i}^{n} \frac{1}{K_{3_{ij}}} \Delta E_{q_j}^{'} - \sum_{j=1}^{n} K_{3_{ij}} \Delta \delta_j\right) \tag{9.27}$$

where

$$\begin{aligned} K_{3_{ii}} &= (1 + (x_{d_i} - x_{d_i}^{'}) \cdot Y_{d_{ii}})^{-1} \\ K_{3_{ij}} &= ((x_{d_i} - x_{d_i}^{'}) \cdot Y_{d_{ij}})^{-1} \\ K_{4_{ij}} &= ((x_{d_i} - x_{d_i}^{'}) \cdot F_{d_{ij}}) \end{aligned} \tag{9.28}$$

The terminal voltage relation could be written as

$$\begin{aligned} \Delta \underline{V}_d &= [x_q] \cdot \Delta \underline{I}_q \\ \Delta \underline{V}_q &= \Delta \underline{E}_q^{'} - [x_d'] \cdot \Delta \underline{I}_d \end{aligned} \tag{9.29}$$

Furthermore

$$\Delta \underline{V} = \mathbf{V}_0^{-1} \cdot \mathbf{V}_{d0} \cdot \Delta \underline{V}_d + \mathbf{V}_0^{-1} \cdot \mathbf{V}_{q0} \cdot \Delta \underline{V}_q \tag{9.30}$$

which can be written as

$$\Delta \underline{V} = \mathbf{K}_5 \cdot \Delta \underline{\delta} + \mathbf{K}_6 \cdot \Delta \underline{E}_q^{'} \tag{9.31}$$

where

$$\begin{aligned} \mathbf{K}_5 &= \mathbf{D}_v \cdot [x_q] \cdot \mathbf{F}_q - \mathbf{Q}_v \cdot [x_d'] \cdot \mathbf{F}_d \\ \mathbf{K}_6 &= \mathbf{D}_v \cdot [x_q] \cdot \mathbf{Y}_q - \mathbf{Q}_v \cdot [x_d'] \cdot \mathbf{Y}_d + \mathbf{Q}_v \end{aligned} \tag{9.32}$$

and

$$\mathbf{D}_v = \mathbf{V}_0^{-1} \cdot \mathbf{V}_{d0}, \qquad \mathbf{Q}_v = \mathbf{V}_0^{-1} \cdot \mathbf{V}_{q0}$$

In these equations, $\mathbf{V_0}$, $\mathbf{V_{d0}}$, $\mathbf{V_{q0}}$, $\mathbf{D_V}$, $\mathbf{Q_V}$, $[x_q]$ and $[x_d']$ should be read as diagonal matrices.

9.2 Appendix II – System Data

9.2.1 System data for SMIB[3]

P = 0.8
Q = 0.6
V = 1.0
r = 0.0
x = 0.2
B = 0.0
G = 0.0
x_d = 1.60
x_q = 1.55
x_d' = 0.32
M = 10.0 s
T_{do}' = 6.0 s
f = 50 Hz
K_A = 50
T_A = 0.05 s
dT_M = 0.01
T_2 = 0.05 s
T_4 = 0.05 s
T_W = 10.0 s

[3] All data are in per unit, except when specified

9.2.2 System data for 3-machine system (WSCC 3-machine, 9-bus)

Table 9.1 Generator data

Generator	1	2	3
Rated MVA	247.5	192.0	128.0
Voltage, kV	16.5	18.0	13.8
Power factor	1.0	0.85	0.85
Type	hydro	steam	steam
Speed, r/min	180	3600	3600
x_d, pu	0.1460	0.8958	1.3125
x_d', pu	0.0608	0.1198	0.1813
x_q pu	0.0969	0.8645	1.2578
x_q' pu	0.0969	0.1969	0.250
x_l pu	0.0336	0.0521	0.0742
T_{do}', sec	8.96	6.00	5.89
T_{qo}', sec	0.0	0.535	0.60
H, sec	23.64	6.40	3.01

Table 9.2 Network data

Bus	Type	Impedance [pu]	Admittance [pu]	Tap ratio [kV/kV]
1-4	Traf.	0.0 + *j*0.0576	0.0 + *j*0.0	16.5/230
2-7	Traf.	0.0 + *j*0.0625	0.0 + *j*0.0	18/230
3-9	Traf.	0.0 + *j*0.0586	0.0 + *j*0.0	13.8/230
4-5	line	0.010 + *j*0.085	0.0 + *j*0.088	-
4-6	line	0.017 + *j*0.092	0.0 + *j*0.079	-
5-7	line	0.032 + *j*0.161	0.0 + *j*0.153	-
6-9	line	0.039 + *j*0.170	0.0 + *j*0.179	-
7-8	line	0.0085 + *j*0.0720	0.0 + *j*0.0745	-
8-9	line	0.0119 + *j*0.1008	0.0 + *j*0.1045	-

9.3 Appendix III

9.3.1 Matrices of Multi-machine System without PSS

$$\mathbf{A}=\begin{bmatrix}
-\frac{D_1}{M_1} & -\frac{K_{1\,11}}{M_1} & -\frac{K_{2\,11}}{M_1} & 0 & 0 & -\frac{K_{1\,12}}{M_1} & -\frac{K_{2\,12}}{M_1} & 0 & 0 & -\frac{K_{1\,13}}{M_1} & -\frac{K_{2\,13}}{M_1} & 0\\
2\pi f & 0 & 0 & 0 & 0 & 0 & 0 & 0 & 0 & 0 & 0 & 0\\
0 & -\frac{K_{4\,11}}{T'_{do_1}} & -\frac{1}{T'_{do_1}K_{3\,11}} & \frac{1}{T'_{do_1}} & 0 & -\frac{K_{4\,12}}{T'_{do_1}} & -\frac{1}{T'_{do_1}K_{3\,12}} & 0 & 0 & -\frac{K_{4\,13}}{T'_{do_1}} & -\frac{1}{T'_{do_1}K_{3\,13}} & 0\\
0 & -\frac{K_{A_1}K_{5\,11}}{T_{A_1}} & -\frac{K_{A_1}K_{6\,11}}{T_{A_1}} & -\frac{1}{T_{A_1}} & 0 & -\frac{K_{A_1}K_{5\,12}}{T_{A_1}} & -\frac{K_{A_1}K_{6\,12}}{T_{A_1}} & 0 & 0 & -\frac{K_{A_1}K_{5\,13}}{T_{A_1}} & -\frac{K_{A_1}K_{6\,13}}{T_{A_1}} & 0\\
0 & -\frac{K_{1\,21}}{M_2} & -\frac{K_{2\,21}}{M_2} & 0 & -\frac{D_2}{M_2} & -\frac{K_{1\,22}}{M_2} & -\frac{K_{2\,22}}{M_2} & 0 & 0 & -\frac{K_{1\,23}}{M_2} & -\frac{K_{2\,23}}{M_2} & 0\\
0 & 0 & 0 & 0 & 2\pi f & 0 & 0 & 0 & 0 & 0 & 0 & 0\\
0 & -\frac{K_{4\,21}}{T'_{do_2}} & -\frac{1}{T'_{do_2}K_{3\,21}} & 0 & 0 & -\frac{K_{4\,22}}{T'_{do_2}} & -\frac{1}{T'_{do_2}K_{3\,22}} & \frac{1}{T'_{do_2}} & 0 & -\frac{K_{4\,23}}{T'_{do_2}} & -\frac{1}{T'_{do_2}K_{3\,23}} & 0\\
0 & -\frac{K_{A_2}K_{5\,21}}{T_{A_2}} & -\frac{K_{A_2}K_{6\,21}}{T_{A_2}} & 0 & 0 & -\frac{K_{A_2}K_{5\,22}}{T_{A_2}} & -\frac{K_{A_2}K_{6\,22}}{T_{A_2}} & -\frac{1}{T_{A_2}} & 0 & -\frac{K_{A_2}K_{5\,23}}{T_{A_2}} & -\frac{K_{A_2}K_{6\,23}}{T_{A_2}} & 0\\
0 & -\frac{K_{1\,31}}{M_3} & -\frac{K_{2\,31}}{M_3} & 0 & 0 & -\frac{K_{1\,32}}{M_3} & -\frac{K_{2\,32}}{M_3} & 0 & -\frac{D_3}{M_3} & -\frac{K_{1\,33}}{M_3} & -\frac{K_{2\,33}}{M_3} & 0\\
0 & 0 & 0 & 0 & 0 & 0 & 0 & 0 & 2\pi f & 0 & 0 & 0\\
0 & -\frac{K_{4\,31}}{T'_{do_3}} & -\frac{1}{T'_{do_3}K_{3\,31}} & 0 & 0 & -\frac{K_{4\,32}}{T'_{do_3}} & -\frac{1}{T'_{do_3}K_{3\,32}} & 0 & 0 & -\frac{K_{4\,33}}{T'_{do_3}} & -\frac{1}{T'_{do_3}K_{3\,33}} & \frac{1}{T'_{do_3}}\\
0 & -\frac{K_{A_3}K_{5\,31}}{T_{A_3}} & -\frac{K_{A_3}K_{6\,31}}{T_{A_3}} & 0 & 0 & -\frac{K_{A_3}K_{5\,32}}{T_{A_3}} & -\frac{K_{A_3}K_{6\,32}}{T_{A_3}} & 0 & 0 & -\frac{K_{A_3}K_{5\,33}}{T_{A_3}} & -\frac{K_{A_3}K_{5\,33}}{T_{A_3}} & -\frac{1}{T_{A_3}}
\end{bmatrix}$$

$$\mathbf{B}=\begin{bmatrix}
0 & 0 & 0 & \frac{K_{A_1}}{T_{A_1}} & 0 & 0 & 0 & 0 & 0 & 0 & 0 & 0\\
0 & 0 & 0 & 0 & 0 & 0 & 0 & \frac{K_{A_2}}{T_{A_2}} & 0 & 0 & 0 & 0\\
0 & 0 & 0 & 0 & 0 & 0 & 0 & 0 & 0 & 0 & 0 & \frac{K_{A_3}}{T_{A_3}}
\end{bmatrix}^T$$

$$\mathbf{\Gamma}=\begin{bmatrix}
\frac{1}{2H_1} & 0 & 0 & 0 & 0 & 0 & 0 & 0 & 0 & 0 & 0 & 0\\
0 & 0 & 0 & 0 & \frac{1}{2H_2} & 0 & 0 & 0 & 0 & 0 & 0 & 0\\
0 & 0 & 0 & 0 & 0 & 0 & 0 & 0 & \frac{1}{2H_3} & 0 & 0 & 0
\end{bmatrix}^T$$

9.3.2 Matrices Multi-machine System with PSS

Let us consider the following notations:

$$r_1 = \frac{K_{C_1} \cdot T_{11}}{T_{21}}; \quad m_1 = \frac{r_1 \cdot T_{31}}{T_{41}}$$
$$r_2 = \frac{K_{C_2} \cdot T_{12}}{T_{22}}; \quad m_2 = \frac{r_2 \cdot T_{32}}{T_{42}}$$
$$r_3 = \frac{K_{C_3} \cdot T_{13}}{T_{23}}; \quad m_3 = \frac{r_3 \cdot T_{33}}{T_{43}}$$

Thus, the matrices of the multi-machine power system introduced in Chapter 2 become:

$$\mathbf{C} = \begin{bmatrix}
A_{1,1} & A_{1,2} & A_{1,3} & A_{1,4} & A_{1,5} & A_{1,6} & A_{1,7} & A_{1,8} & A_{1,9} & A_{1,10} & A_{1,11} & A_{1,12} \\
r_1 A_{1,1} & r_1 A_{1,2} & r_1 A_{1,3} & r_1 A_{1,4} & r_1 A_{1,5} & r_1 A_{1,6} & r_1 A_{1,7} & r_1 A_{1,8} & r_1 A_{1,9} & r_1 A_{1,10} & r_1 A_{1,11} & r_1 A_{1,12} \\
m_1 A_{1,1} & m_1 A_{1,2} & m_1 A_{1,3} & m_1 A_{1,4} & m_1 A_{1,5} & m_1 A_{1,6} & m_1 A_{1,7} & m_1 A_{1,8} & m_1 A_{1,9} & m_1 A_{1,10} & m_1 A_{1,11} & m_1 A_{1,12} \\
A_{5,1} & A_{5,2} & A_{5,3} & A_{5,4} & A_{5,5} & A_{5,6} & A_{5,7} & A_{5,8} & A_{5,9} & A_{5,10} & A_{5,11} & A_{5,12} \\
r_2 A_{5,1} & r_2 A_{5,2} & r_2 A_{5,3} & r_2 A_{5,4} & r_2 A_{5,5} & r_2 A_{5,6} & r_2 A_{5,7} & r_2 A_{5,8} & r_2 A_{5,9} & r_2 A_{5,10} & r_2 A_{5,11} & r_2 A_{5,12} \\
m_2 A_{5,1} & m_2 A_{5,2} & m_2 A_{5,3} & m_2 A_{5,4} & m_2 A_{5,5} & m_2 A_{5,6} & m_2 A_{5,7} & m_2 A_{5,8} & m_2 A_{5,9} & m_2 A_{5,10} & m_2 A_{5,11} & m_2 A_{5,12} \\
A_{9,1} & A_{9,2} & A_{9,3} & A_{9,4} & A_{9,5} & A_{9,6} & A_{9,7} & A_{9,8} & A_{9,9} & A_{9,10} & A_{9,11} & A_{9,12} \\
r_3 A_{9,1} & r_3 A_{9,2} & r_3 A_{9,3} & r_3 A_{9,4} & r_3 A_{9,5} & r_3 A_{9,6} & r_3 A_{9,7} & r_3 A_{9,8} & r_3 A_{9,9} & r_3 A_{9,10} & r_3 A_{9,11} & r_3 A_{9,12} \\
m_3 A_{9,1} & m_3 A_{9,2} & m_3 A_{9,3} & m_3 A_{9,4} & m_3 A_{9,5} & m_3 A_{9,6} & m_3 A_{9,7} & m_3 A_{9,8} & m_3 A_{9,9} & m_3 A_{9,10} & m_3 A_{9,11} & m_3 A_{9,12}
\end{bmatrix}$$

where A_{ij} are the elements of the **A** matrix of the multi-machine system described in Section 9.3.1.

$$\mathbf{\Gamma}_1 = \begin{bmatrix}
\frac{1}{2H_1} & \frac{K_{C_1}T_{11}}{2H_1T_{21}} & \frac{K_{C_1}T_{11}T_{31}}{2H_1T_{21}T_{41}} & 0 & 0 & 0 & 0 & 0 & 0 \\
0 & 0 & 0 & \frac{1}{2H_2} & \frac{K_{C_2}T_{12}}{2H_2T_{22}} & \frac{K_{C_2}T_{12}T_{32}}{2H_2T_{22}T_{42}} & 0 & 0 & 0 \\
0 & 0 & 0 & 0 & 0 & 0 & \frac{1}{2H_3} & \frac{K_{C_3}T_{13}}{2H_3T_{23}} & \frac{K_{C_3}T_{13}T_{33}}{2H_3T_{23}T_{43}}
\end{bmatrix}^T$$

$$\mathbf{D}=\begin{bmatrix}
-\frac{1}{T_{W1}} & 0 & 0 & 0 & 0 & 0 & 0 & 0 & 0 \\
\frac{K_{C1}}{T_{21}}\left(1-\frac{T_{11}}{T_{W1}}\right) & -\frac{1}{T_{21}} & 0 & 0 & 0 & 0 & 0 & 0 & 0 \\
\frac{T_{31}}{T_{41}}\frac{K_{C1}}{T_{21}}\left(1-\frac{T_{11}}{T_{W1}}\right) & \frac{1}{T_{41}}\left(1-\frac{T_{31}}{T_{21}}\right) & -\frac{1}{T_{41}} & 0 & 0 & 0 & 0 & 0 & 0 \\
0 & 0 & 0 & -\frac{1}{T_{W2}} & 0 & 0 & 0 & 0 & 0 \\
0 & 0 & 0 & \frac{K_{C2}}{T_{22}}\left(1-\frac{T_{12}}{T_{W2}}\right) & -\frac{1}{T_{22}} & 0 & 0 & 0 & 0 \\
0 & 0 & 0 & \frac{T_{32}}{T_{42}}\frac{K_{C2}}{T_{22}}\left(1-\frac{T_{12}}{T_{W2}}\right) & \frac{1}{T_{42}}\left(1-\frac{T_{32}}{T_{22}}\right) & -\frac{1}{T_{42}} & 0 & 0 & 0 \\
0 & 0 & 0 & 0 & 0 & 0 & -\frac{1}{T_{W3}} & 0 & 0 \\
0 & 0 & 0 & 0 & 0 & 0 & \frac{K_{C3}}{T_{23}}\left(1-\frac{T_{13}}{T_{W3}}\right) & -\frac{1}{T_{23}} & 0 \\
0 & 0 & 0 & 0 & 0 & 0 & \frac{T_{33}}{T_{43}}\frac{K_{C3}}{T_{23}}\left(1-\frac{T_{13}}{T_{W3}}\right) & \frac{1}{T_{43}}\left(1-\frac{T_{33}}{T_{23}}\right) & -\frac{1}{T_{43}}
\end{bmatrix}$$